高エネルギー加速器研究機構 KEK
HIGH ENERGY ACCELERATOR RESEARCH ORGANIZATION
www.kek.jp

KEK – つくば - 27-2-2006

Companions of the PAMELA experiment for cosmic ray research in space

M. Casolino, Wizard collaboration

INFN & University of Roma Tor Vergata

Tor Vergata

INFN Istituto Nazionale di Fisica Nucleare

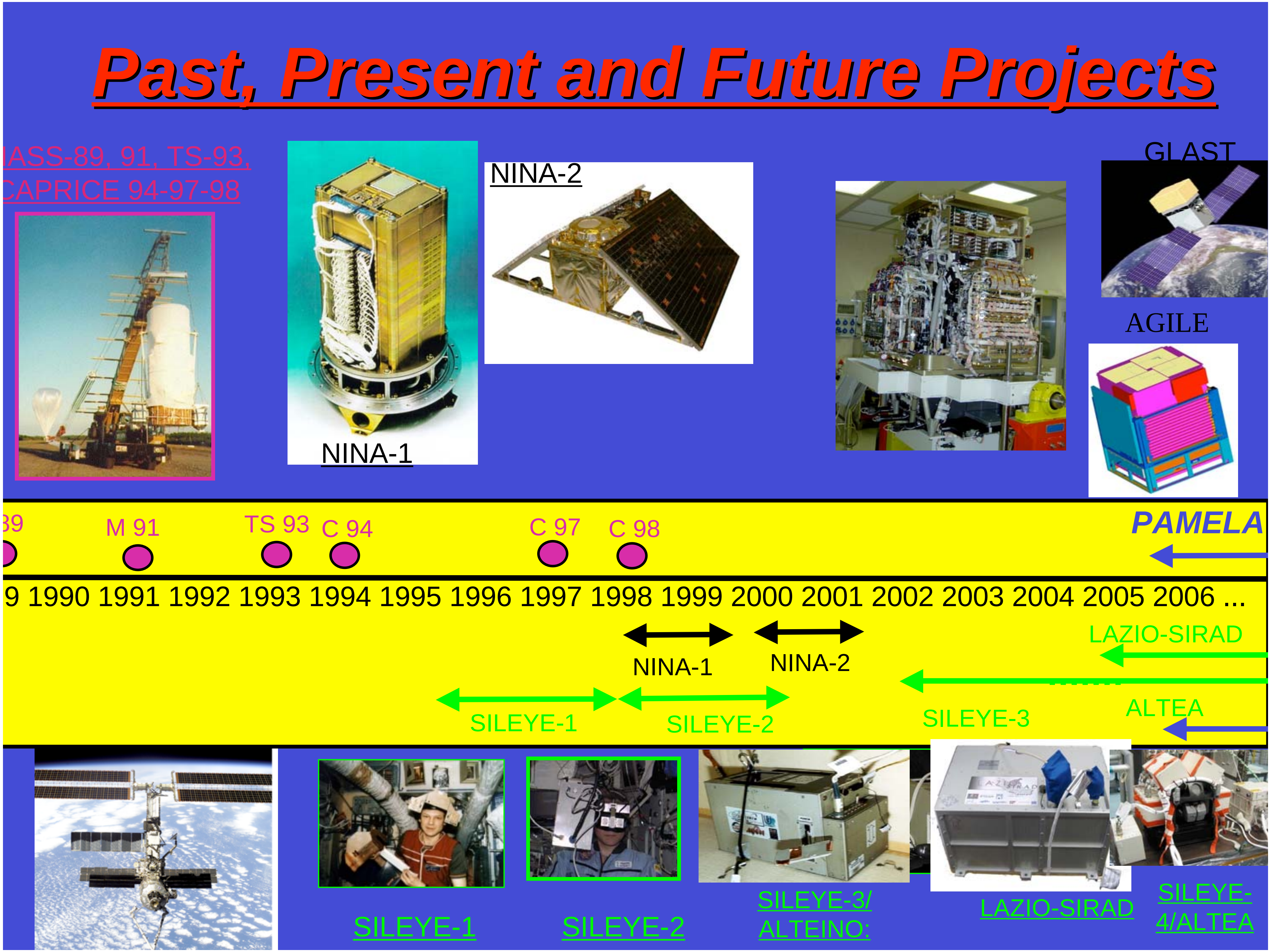
Past, Present and Future Projects
MASS-89, 91, TS-93,
CAPRICE 94-97-98
NINA-1
NINA-2
GLAST
AGILE
89
M 91
TS 93
C 94
C 97
C 98
PAMELA
9 1990 1991 1992 1993 1994 1995 1996 1997 1998 1999 2000 2001 2002 2003 2004 2005 2006 ...
NINA-1
NINA-2
LAZIO-SIRAD
SILEYE-1
SILEYE-2
SILEYE-3
ALTEA
SILEYE-1
SILEYE-2
SILEYE-3/
ALTEINO:
LAZIO-SIRAD
SILEYE-
4/ALTEA

Sileye - NINA institutions

V. Bidoli[1], M. Casolino[1], M. P. De Pascale[1], M. Minori[1], A., L. Narici[1], P. Picozza[1], E. Reali[1], R. Sparvoli[1], V. Zaconte, A. Galper[2], A. Popov[2], S. Avdeev[3], M. Boezio[4], W. Bonvicini[4], A. Vacchi[4], G. Zampa[4,] N. Zampa[4], G. Mazzenga[5], M. Ricci[5], P. Spillantini[6],G. Castellini[7], P. Carlson[8], C. Fuglesang[8], V. Benghin[9], V. P. Salnitskii[9], O. I. Shevchenko[9], V. Shurshakov[9], V. P. Petrov[9], K.A.Trukhanov[9]

[1] Dept. of Physics, Univ. of Rome "Tor Vergata" and INFN Sez. Rome2 , Italy; [2] Moscow State Engineering Physics Institute, Moscow, Russia;[3] Russian Space Corporation "Energia" by name Korolev, Korolev, Moscow region, Russia [4] Dept. of Physics of Univ. and Sez. INFN of Trieste, Italy; [8] Dept. of Physics of Univ. and Sez. INFN of Perugia, Italy; [5] L.N.F. - INFN, Frascati (Rome), Italy; [6] Dept. of Physics of Univ. and Sez. INFN of Florence, Italy; [7] IROE of CNR, Florence, Italy; [8] Royal Institute of Technology, Stockholm, Sweden;
[9]IMBP, Institute of BioMedical Problems,Moscow, Russia

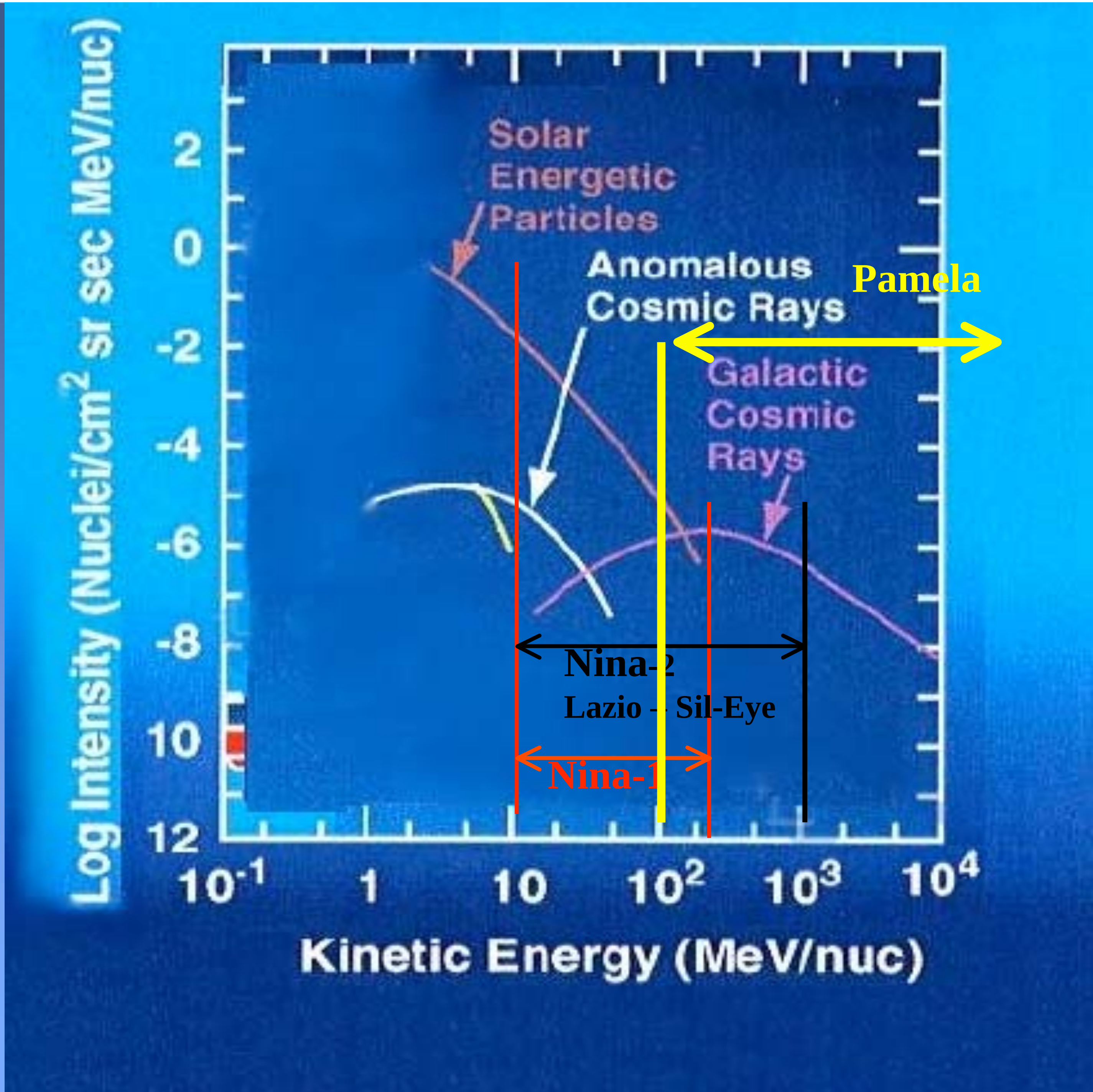

Log Intensity (Nuclei/cm2 sr sec MeV/nuc)
2
0
-2
-4
-6
-8
10
12
10-1
1
10
102
103
104
Kinetic Energy (MeV/nuc)
Solar Energetic Particles
Anomalous Cosmic Rays
Galactic Cosmic Rays
Pamela
Nina-2
Lazio -- Sil-Eye
Nina-1

Observations at the minimum of 23^o solar cycle

Satellite

Mir

ISS

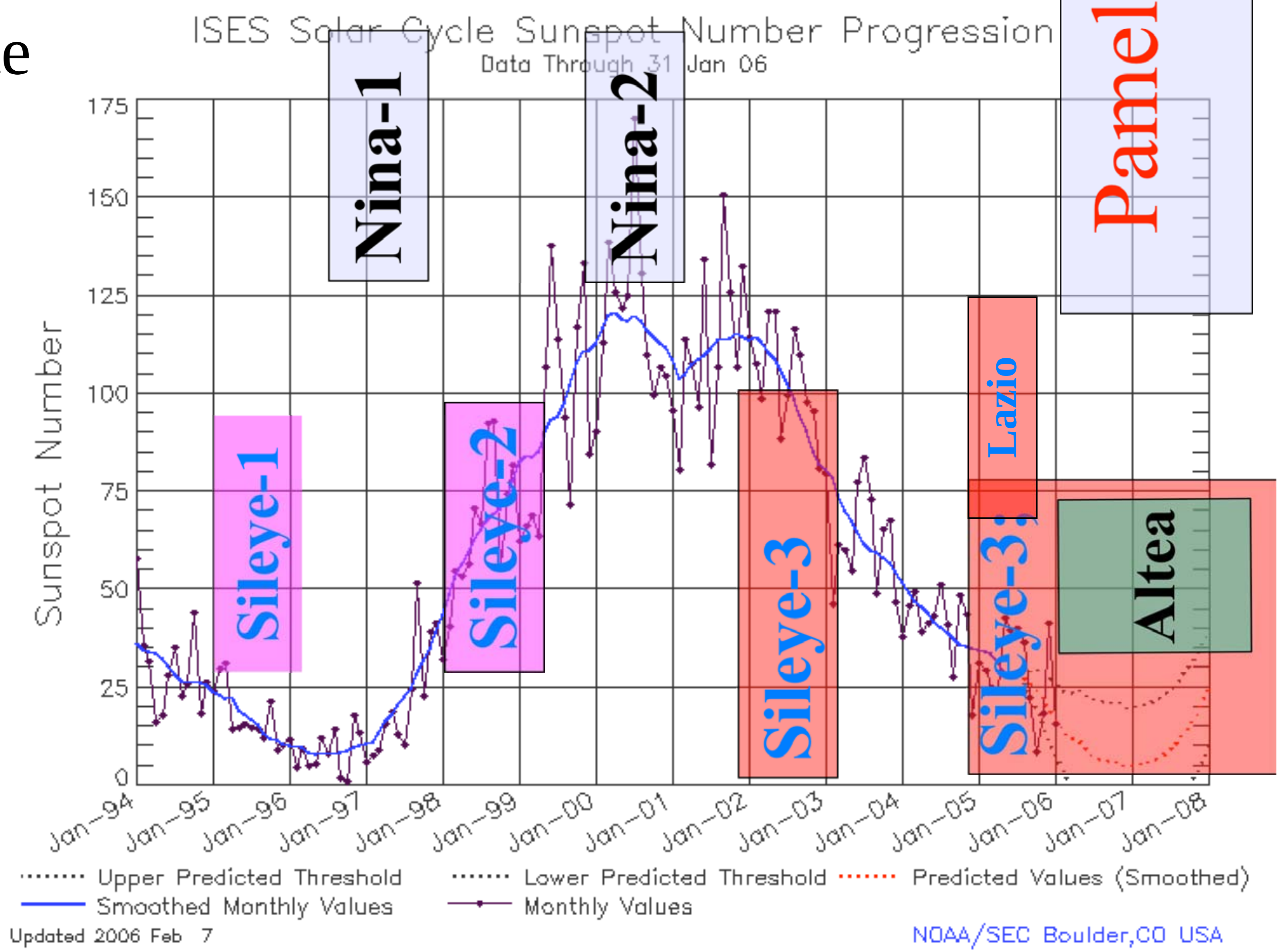

NINA

- 32 silicon detector planes
- 8*8 cm^2, 16 strips
- GF 10 cm^2 sr
- 20 kg detector

RESURS-01 - NINA-1: 1998

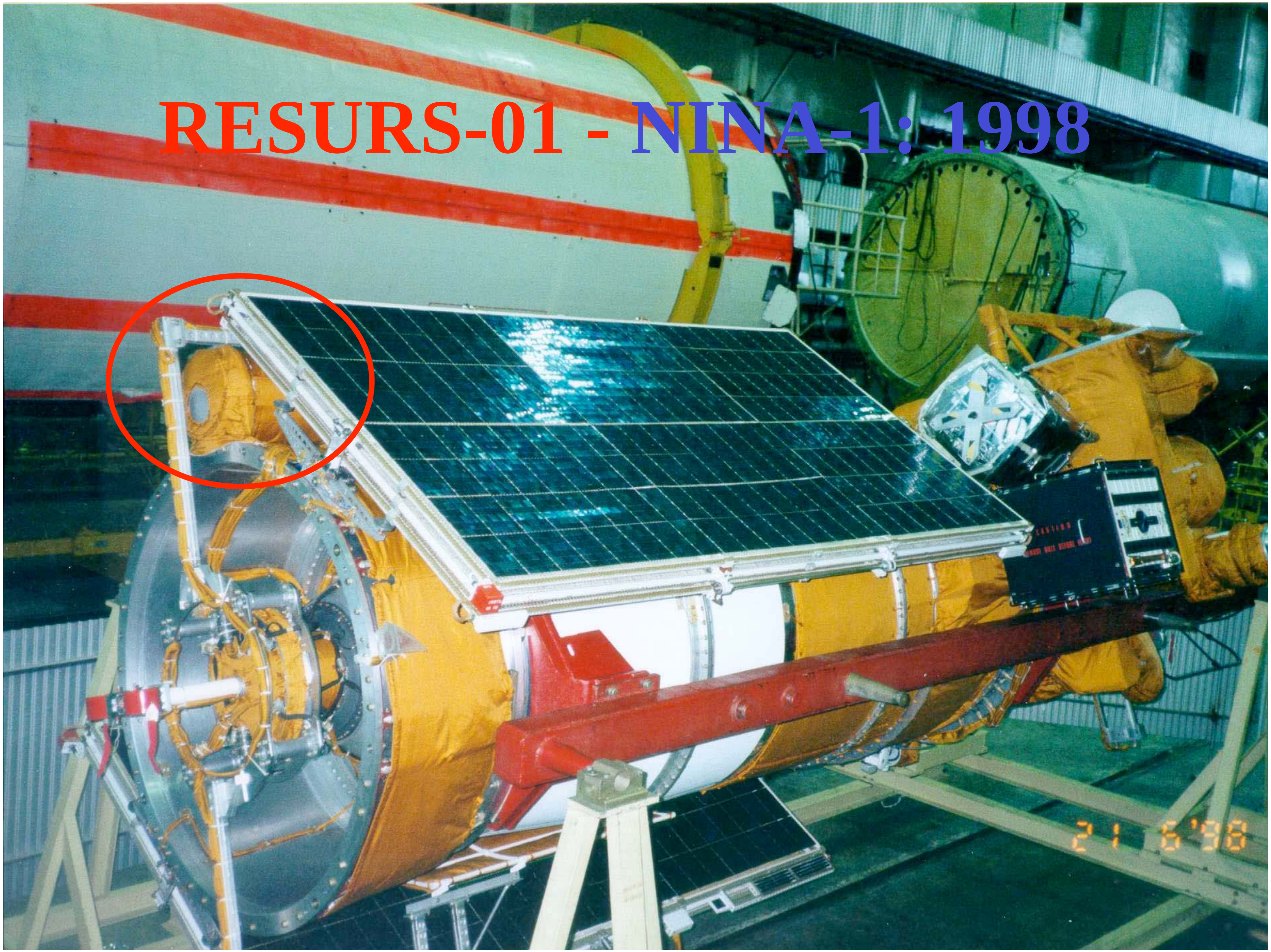

Resurs-O1 n. 4 satellite

Zenit Launcher: 10/7/1998 from the cosmodrome of Baikonur

MITA (ASI) Satellite – NINA-2 (2000)

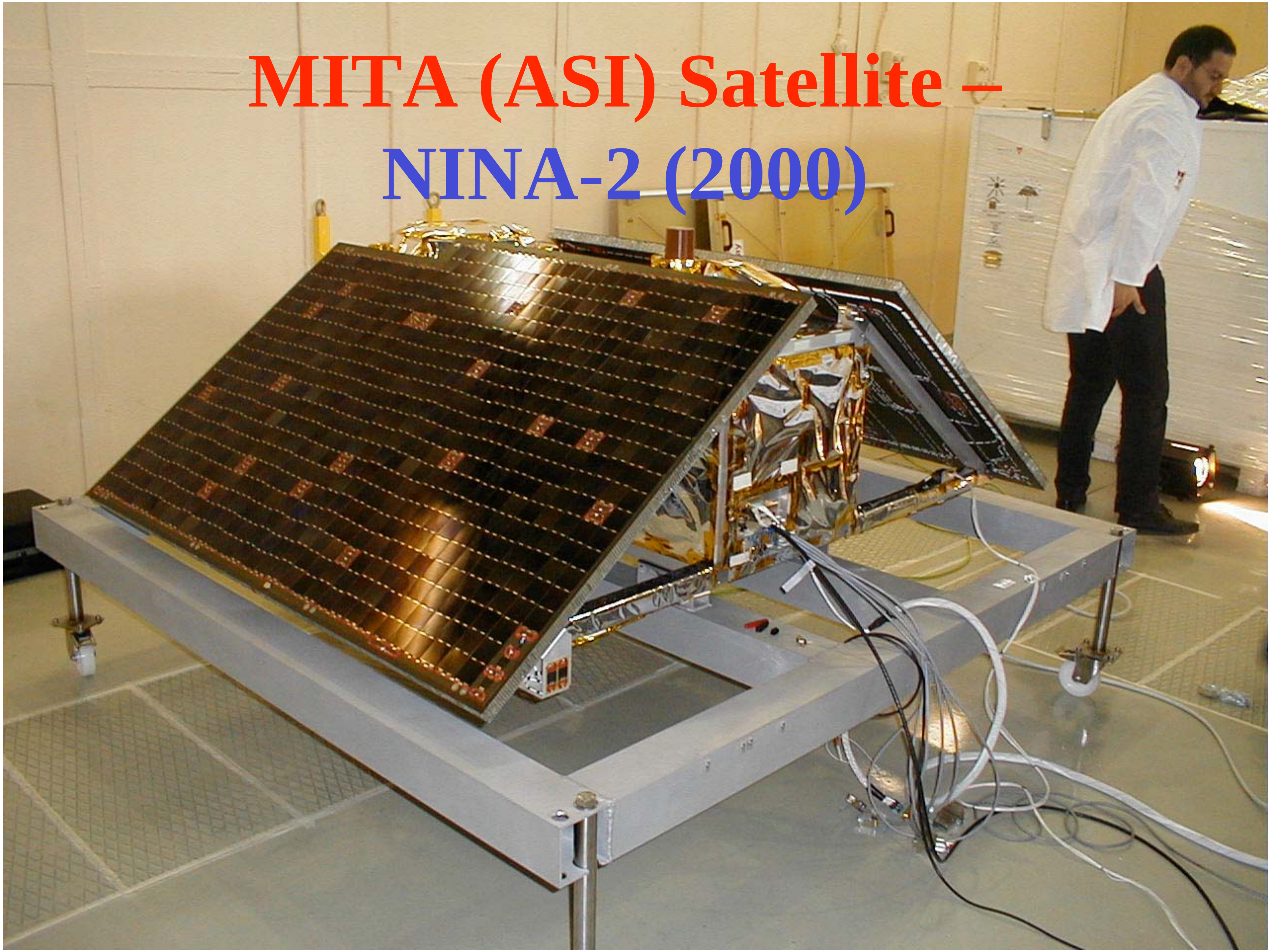

NINA-2 top cover

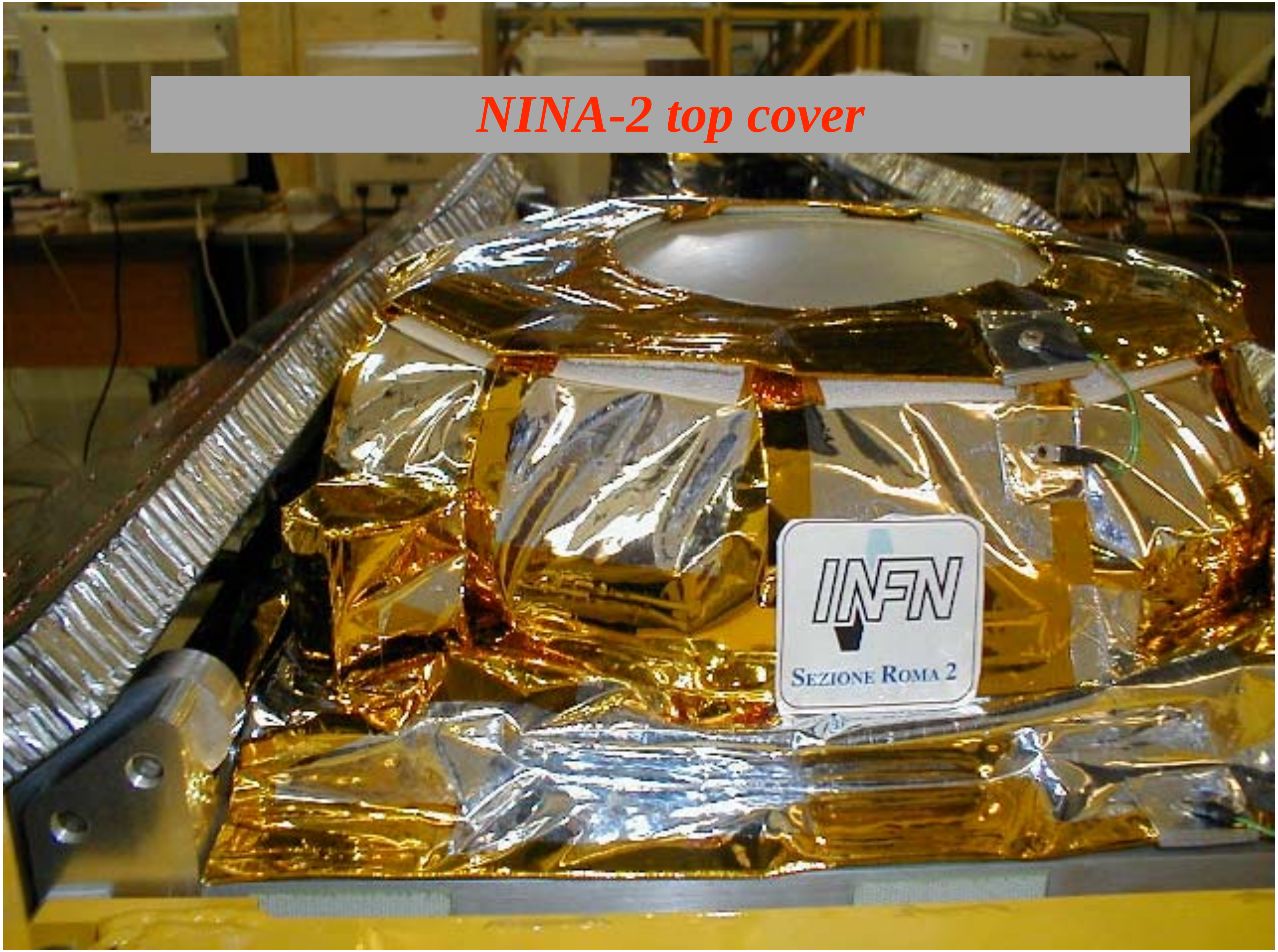


"MITA"
"MITA"


NINA-2: Launched on 15/7/2000 from the cosmodrome of Plesetsk, on Cosmos Rocket

Physics Objectives

- Galactic cosmic rays
- Solar Energetic Part.
- Anomalous Cosmic Ra

- Trapped particle population in the SAA

- Geomagnetic cutoff sh due to solar events
- Albedo particles
- Secondary particles produced in the atmosphere
- Geosismic correlations

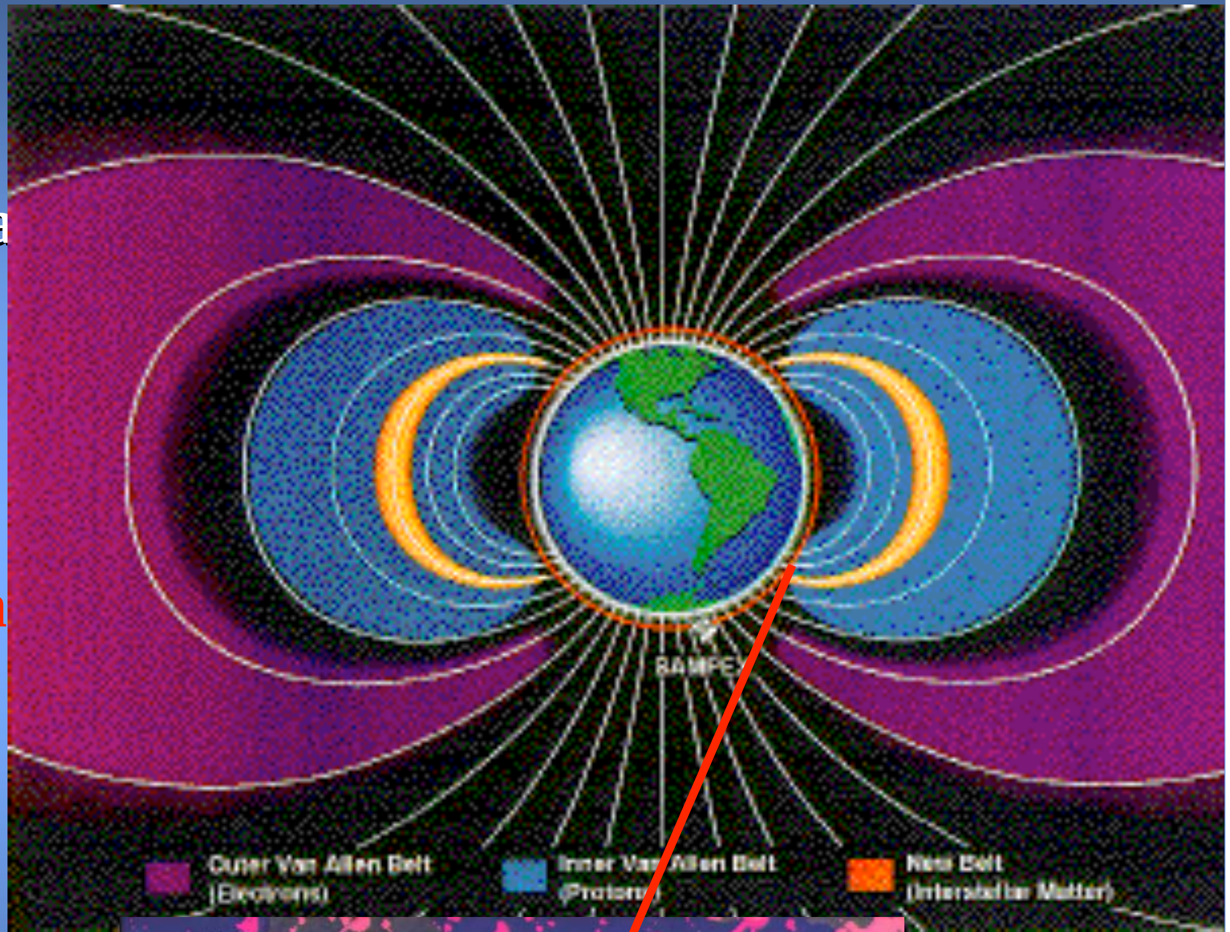

Solar quiet abundances

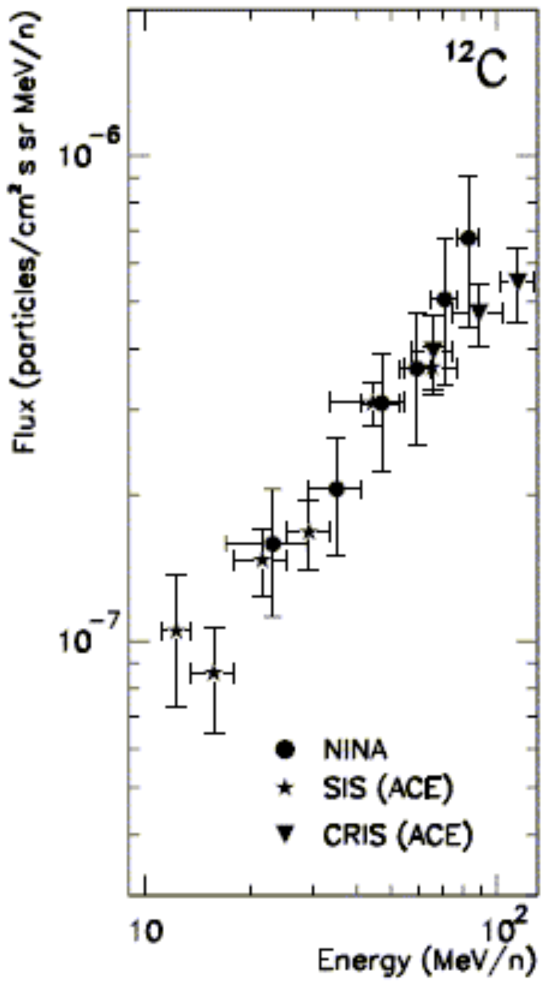

FIG. 9.—Differential energy spectrum for ^{12}C in the solar quiet period December 1998–March 1999 measured by NINA, together with data of SIS and CRIS on board ACE.

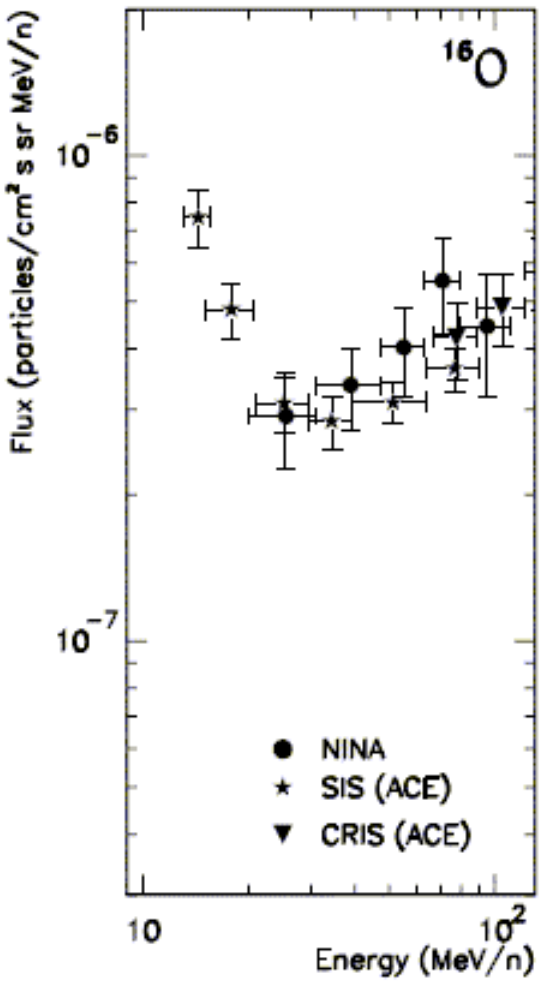

FIG. 10.—Differential energy spectrum for ^{16}O in the solar quiet period 1998 December–1999 March measured by NINA, together with data of SIS and CRIS on board ACE.

ApJ supp. 132, 365, 2001

Ap. Phys. 8 109, 1997

Solar Energetic particles

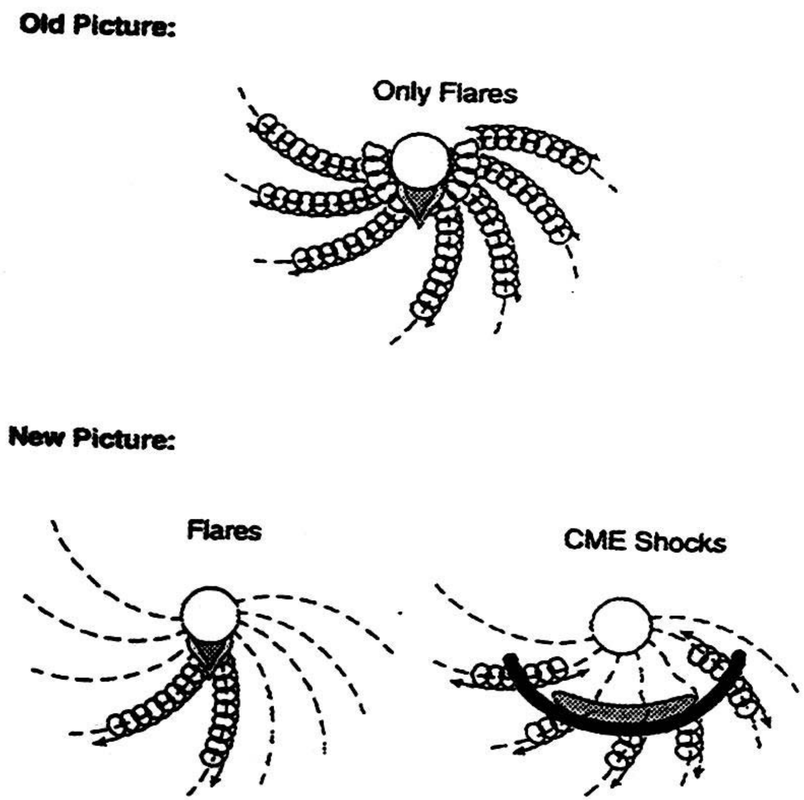

Fig. 2.1. A paradigm shift.

Powered by solar activity:

•Solar flares
(small, local acceleration, ^{3}He rich)

•Coronal mass ejection
(large, shock acceleration)

Reames, 1999

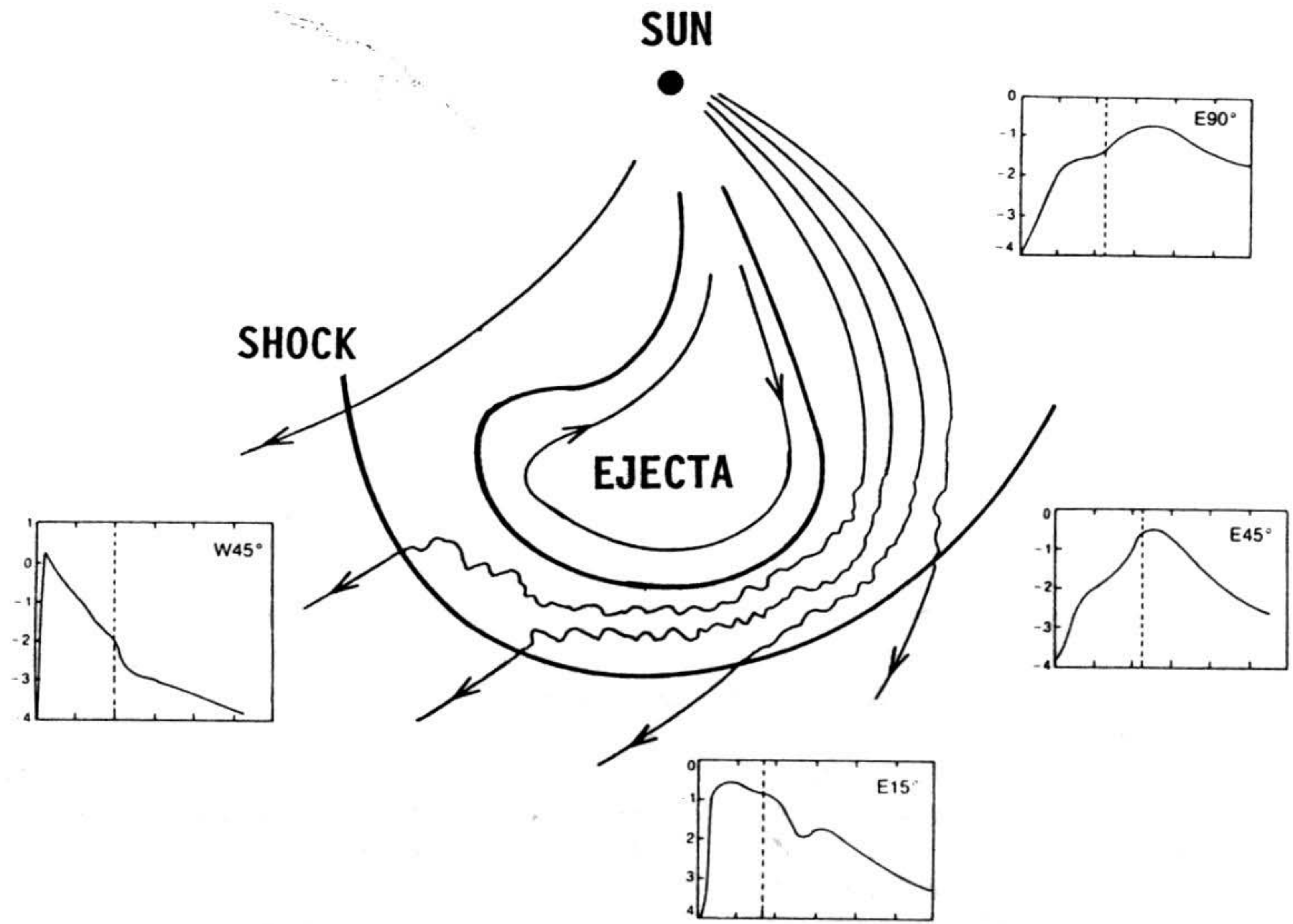

Figure 3. Representative profiles for actual events at 20 MeV for observers at different locations relatve to an interplanetary shock. The differing intensity profiles can be understood in terms of shock acceleration and the large scale structure of shocks. See *Cane et al.* [1988].

On various SEP events…

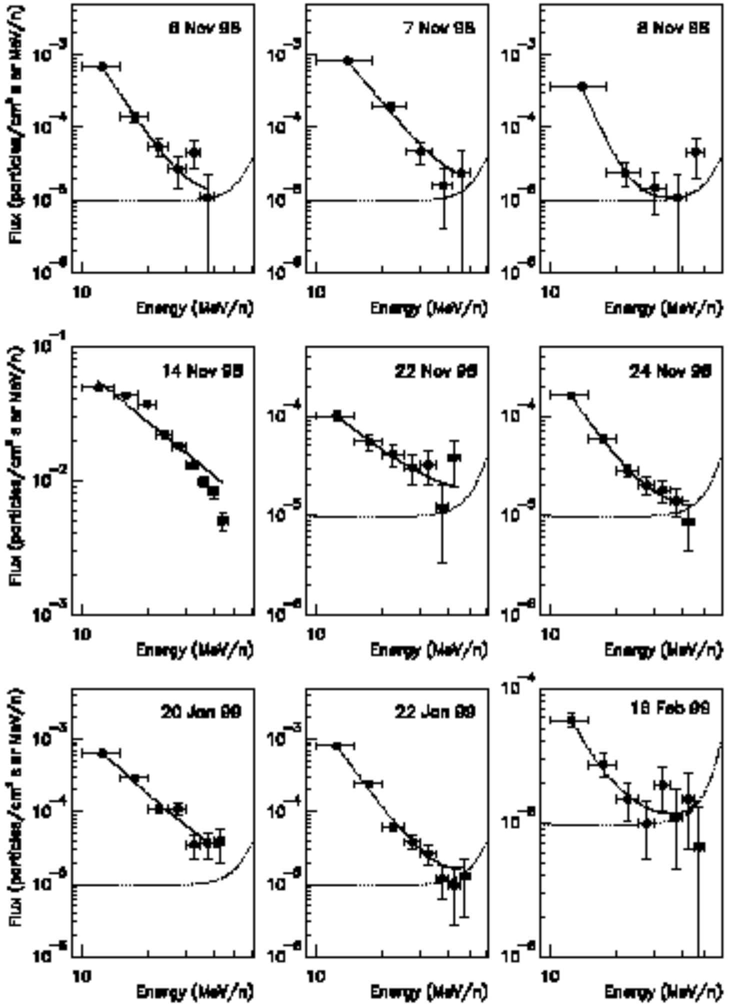

Fig. 5.— Differential energy spectrum for ^{4}He for the 9 different SEPs detected by NINA. The dashed line (see eq. 1) represents the background B(E) of galactic ^{4}He; a power-law spectrum S(E) (see eq. 2) has been super-imposed to the data.

Table 4. ^{3}He/^{4}He ratio

SEP date	$(^3He_{SEP}$ - $^3He_{BG})/^4He$ [15–45 MeV n^{-1}]	$^1H/^4He$ [12–14 MeV n^{-1}]	R $(^3He/^4He)$
6 Nov. 1998	$(6.5 \pm 4.3) \times 10^{-2}$	171 ± 16	3×10^{-3}
7 Nov. 1998	$(3.3 \pm 0.6) \times 10^{-1}$	24 ± 2	6×10^{-4}
8 Nov. 1998	$(2.3 \pm 1.0) \times 10^{-1}$	18 ± 2	5×10^{-4}
14 Nov. 1998	$(1.1 \pm 0.3) \times 10^{-2}$ -	21.9 ± 0.5	5×10^{-4}
22 Nov. 1998	_ 2.8×10^{-2}	22 ± 4	5×10^{-4}
24 Nov. 1998	$(4.1 \pm 3.2) \times 10^{-2}$	17 ± 1	5×10^{-4}
20 Jan. 1999	$(3.1 \pm 6.3) \times 10^{-3}$	182 ± 14	3×10^{-3}
22 Jan. 1999	$(-0.1 \pm 0.6) \times 10^{-2}$	166 ± 8	3×10^{-3}
16 Feb. 1999	$(-0.1 \pm 8.0) \times 10^{-2}$	12.2 ± 2.5	4×10^{-4}

- Energy _ 25 MeV n^{-1}.

Table 5. $^2H/^1H$ ratio and upper limits $^3H/^1H$ ratio

SEP date	$^2H/^1H$ flux [9–12 MeV n^{-1}]	$^3H/^1H$
6 Nov. 1998	_ 5×10^{-5}	_ 7.2×10^{-5}
7 Nov. 1998	$(3.4 \pm 6.1) \times 10^{-5}$	_ 2.0×10^{-4}
8 Nov. 1998	$(5.3 \pm 11.1) \times 10^{-5}$	_ 1.4×10^{-3}
14 Nov. 1998	$(1.7 \pm 2.3) \times 10^{-5}$	_ 5.0×10^{-3}
22 Nov. 1998	$(5.1 \pm 9.0) \times 10^{-5}$	_ 8.5×10^{-4}
24 Nov. 1998	$(3.5 \pm 1.4) \times 10^{-4}$	_ 6.7×10^{-4}
20 Jan. 1999	$(3.5 \pm 2.8) \times 10^{-5}$	_ 5.9×10^{-4}
22 Jan. 1999	$(6.7 \pm 11.2) \times 10^{-6}$	_ 2.5×10^{-4}
16 Feb. 1999	$(3.7 \pm 8.0) \times 10^{-4}$	_ 8.8×10^{-3}

SEP isotopic Composition…

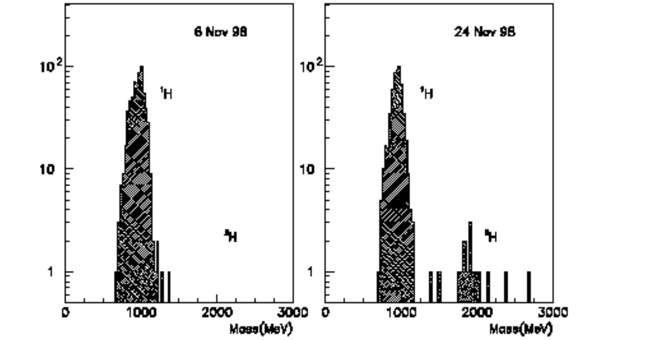

Fig. 12.— Mass reconstruction (Energy $\simeq$ 9 MeV n^{-1}) for the hydrogen isotopes for the 1998 November 6 and 1998 November 24 SEP.

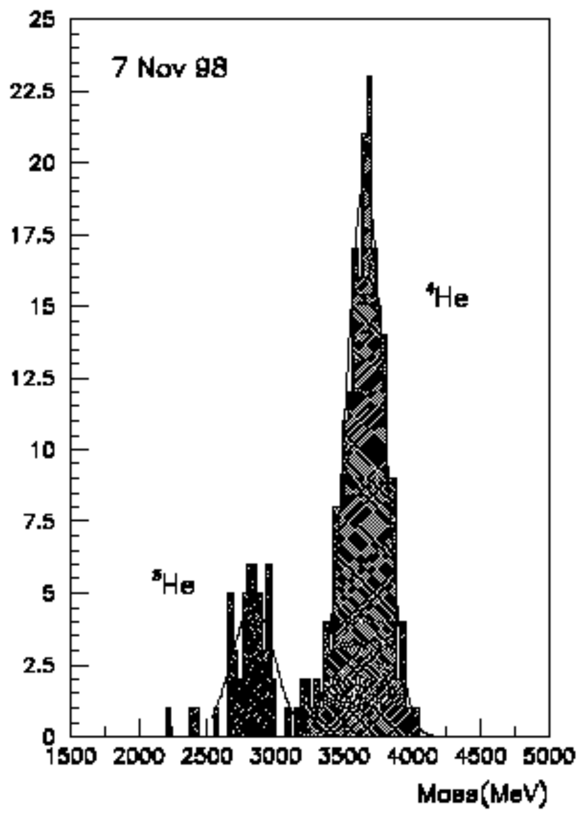

Fig. 6.— 1998 November 7 SEP event: mass reconstructions for ^{3}He and ^{4}He.

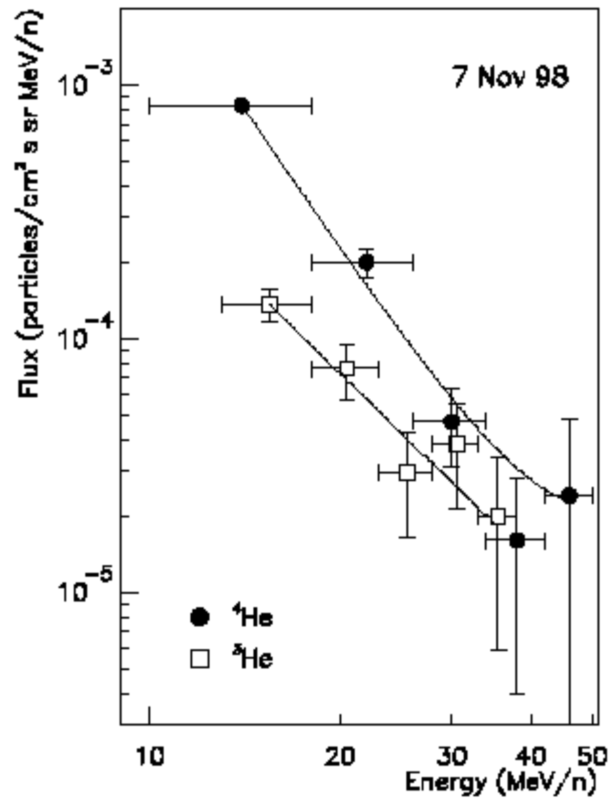

Fig. 7.— 1998 November 7 SEP event: differential energy spectrum for ^{3}He and ^{4}He.

***ApJ* 577, 513, 2002**

Isotope composition of secondary…

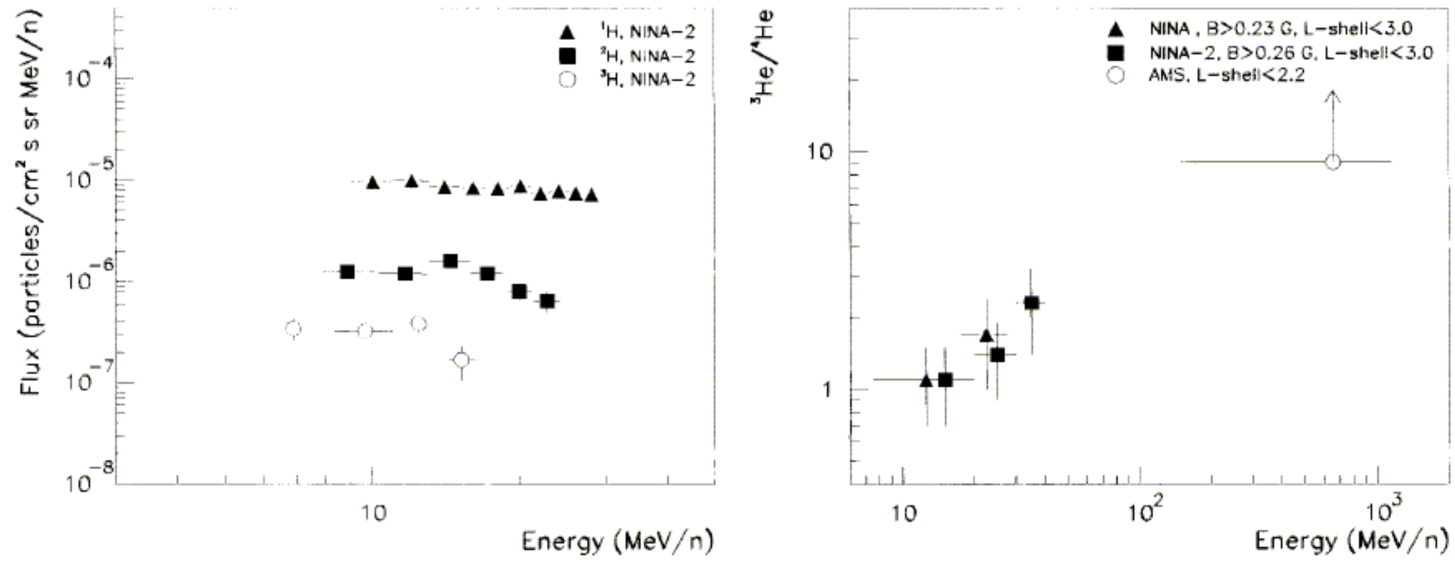

Figure 3. Differential energy spectra of secondary proton, deuterium and tritium at L-shell < 3 and B > 0.26 G, as measured by NINA-2.

Figure 5. Albedo ^{3}He/^{4}He ratio, as measured by NINA and NINA-2. AMS lower limit for L-shell < 2.2 is also shown.

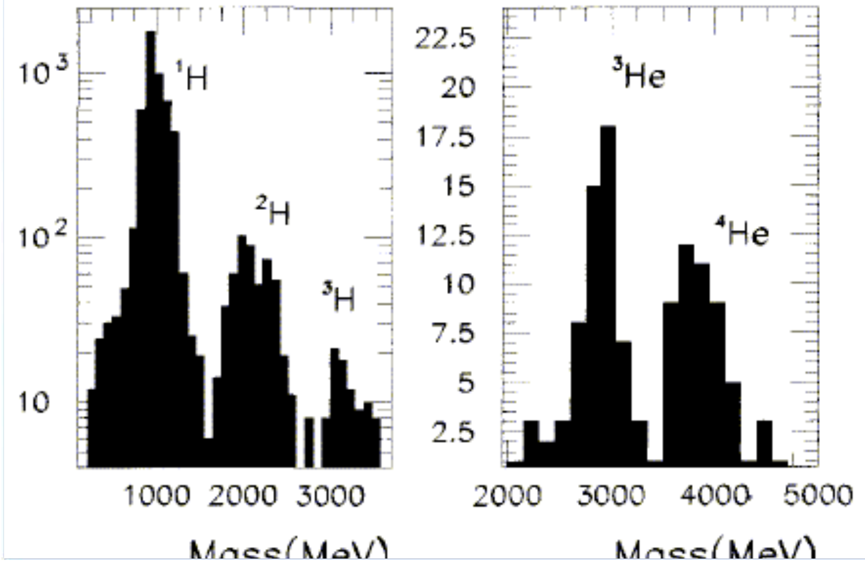

JGR 108 A5 1211, 2003
Ann. Geoph. 20, 1693, 2002

…and trapped particles

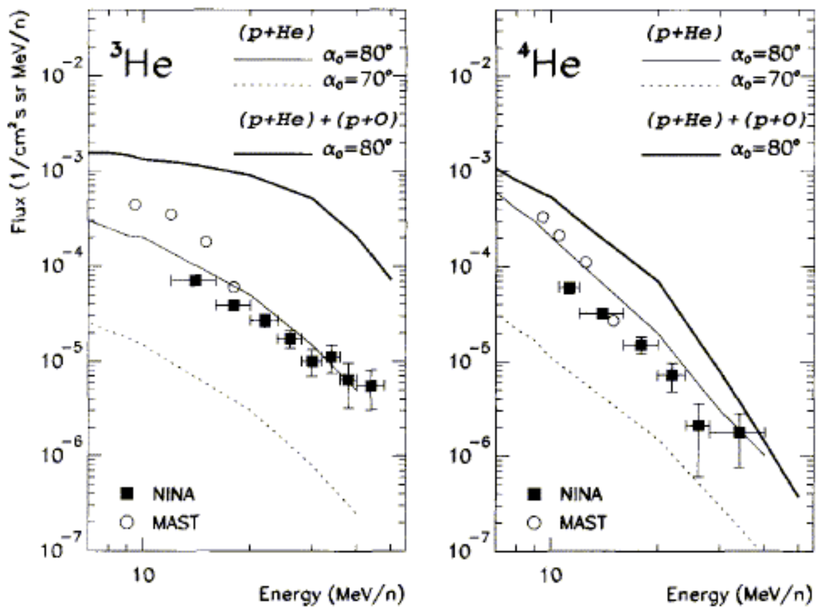

Figure 4. The (left) ^{3}He and (right) ^{4}He differential energy spectra measured inside the SAA by NINA (squares) and MAST (circles). The solid and dotted lines represent the calculated helium flux at equatorial pitch angles $\alpha_0 = 80°$ and $\alpha_0 = 70°$, respectively, assuming atmospheric helium as the source of secondary production [*Selesnick and Mewaldt*, 1996]. The thick line is the sum of the p + He and p + O contributions at $\alpha_0 = 80°$.

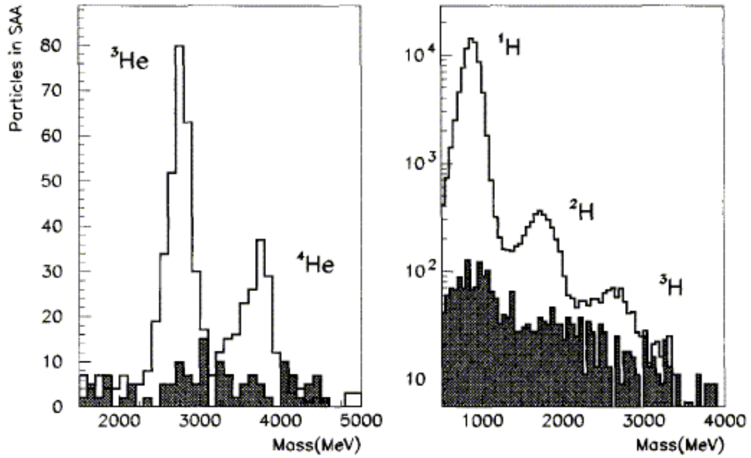

Figure 3. Mass distributions for geomagnetically trapped (left) He and (right) H isotopes measured at L shell < 1.2 and B < 0.22 G. The shaded area represents the estimated background.

JGR 107 A8 10.1029, 2002

SEP event: 9-15 Nov 2000 - NINA-2 Observations

Lowering of Geomagnetic Cutoff

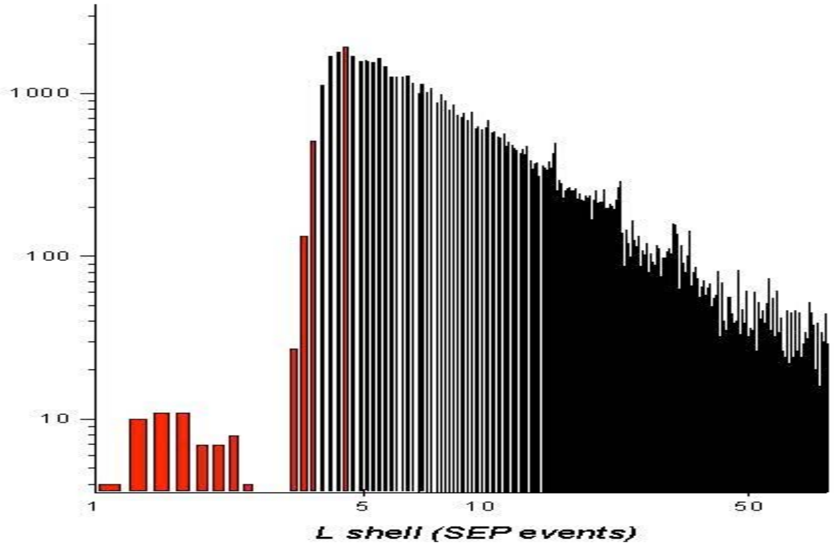

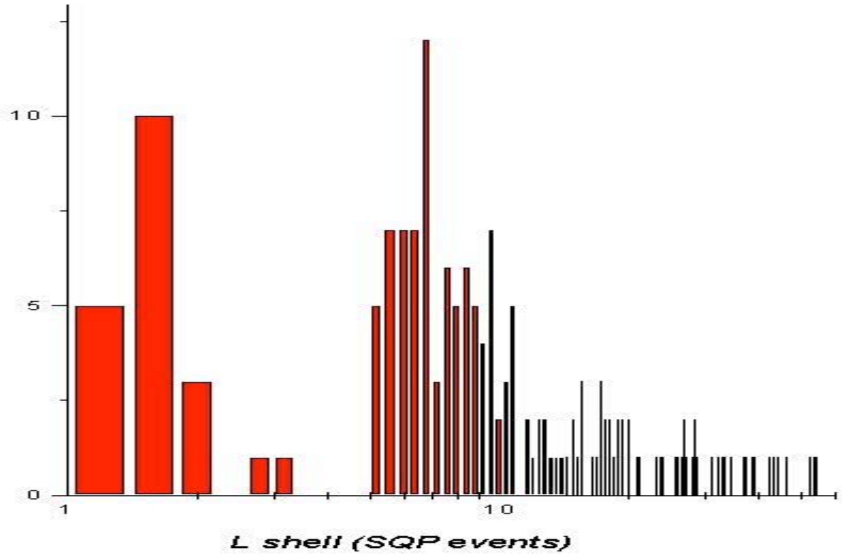

Experiments on Space stations

SilEye-1: **placed on the Space Station MIR in October 1995.**

Years 1996-97: 25 LF measurement sessions
6 cosmonauts
90 Light Flashes recorded

•**SilEye-2:** **placed on the Space Station MIR in 1997**

Years 1998-2000: 24 LF Sessions
4 cosmonauts
130 Light Flashes recorded

•**SilEye-3/Alteino (cr + EEG):**

placed on the International Space Station
on 27th April 2002
9 LF sessions
10 days continuous monitoring of cosmic rays

•Lazio-Sirad (2005)

Altcriss – Sileye3 (2005-2008)

Long term measurements of cosmic ray environment and shielding effects on radiation (in response to ESA-AO2004)

MIR: Sileye-1
(1995-1998)

MIR: Sileye-2 (1998-2000)

- 6 silicon detectors
- Each detector is divided in 16 strips
- Total of 96 independent channels
- 2 iron passive absorbers
- Joystick

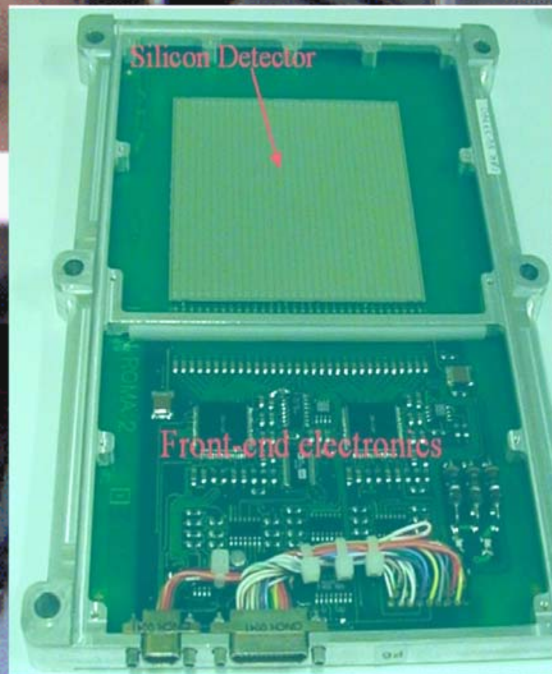

Sileye-2:

Nuclear Identification Capabilities

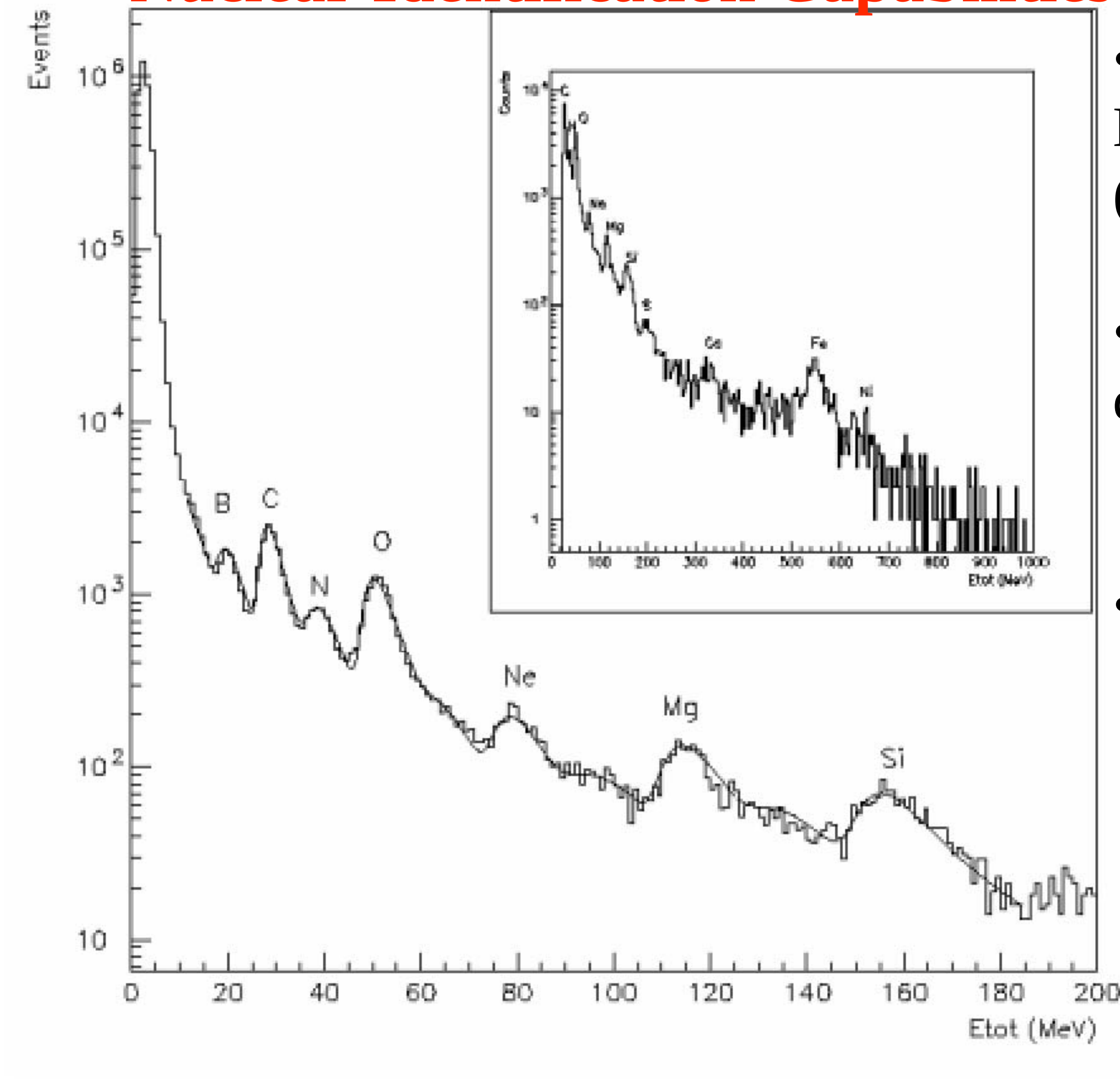

- Selection of E>100MeV/n events (below cutoff)
- Landau Fit (10 distributions)
- Nuclear abundances

Linearity

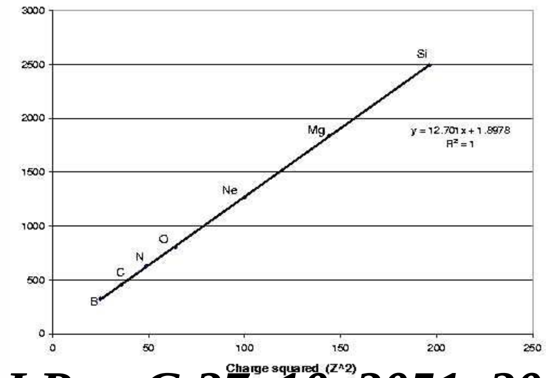

J.Pys. G 27, 10, 2051, 2001

ASR 31 1 135, 2003

Light Flashes: Interaction Between Cosmic Rays and Human Visual Apparatus

•Probe to Central Nervous System effects and/or other interactions between cosmic radiation and human body

Different mechanisms proposed

1. Cherenkov light
2. Direct retinal ionization
3. Knock-on protons

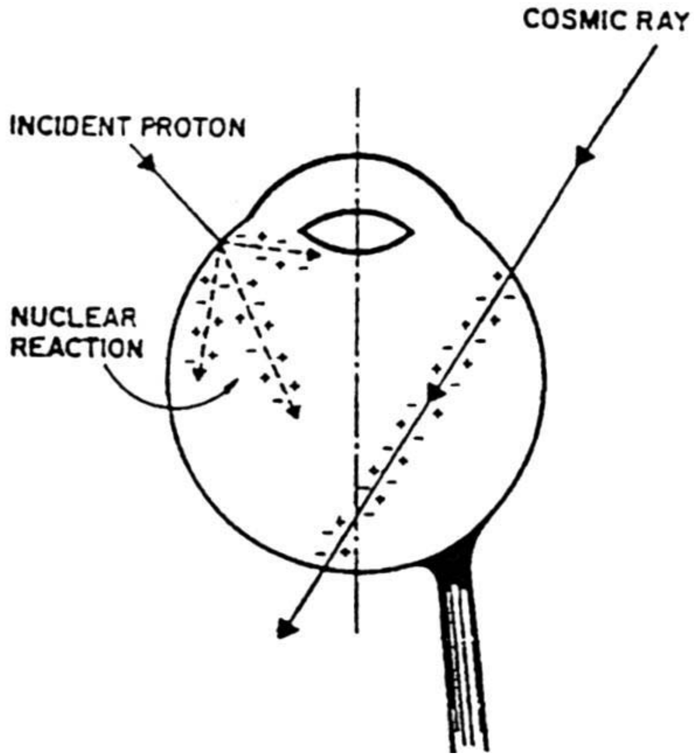

SilEye-1 (1995), SilEye-2 (1997) SilEye-3 (200

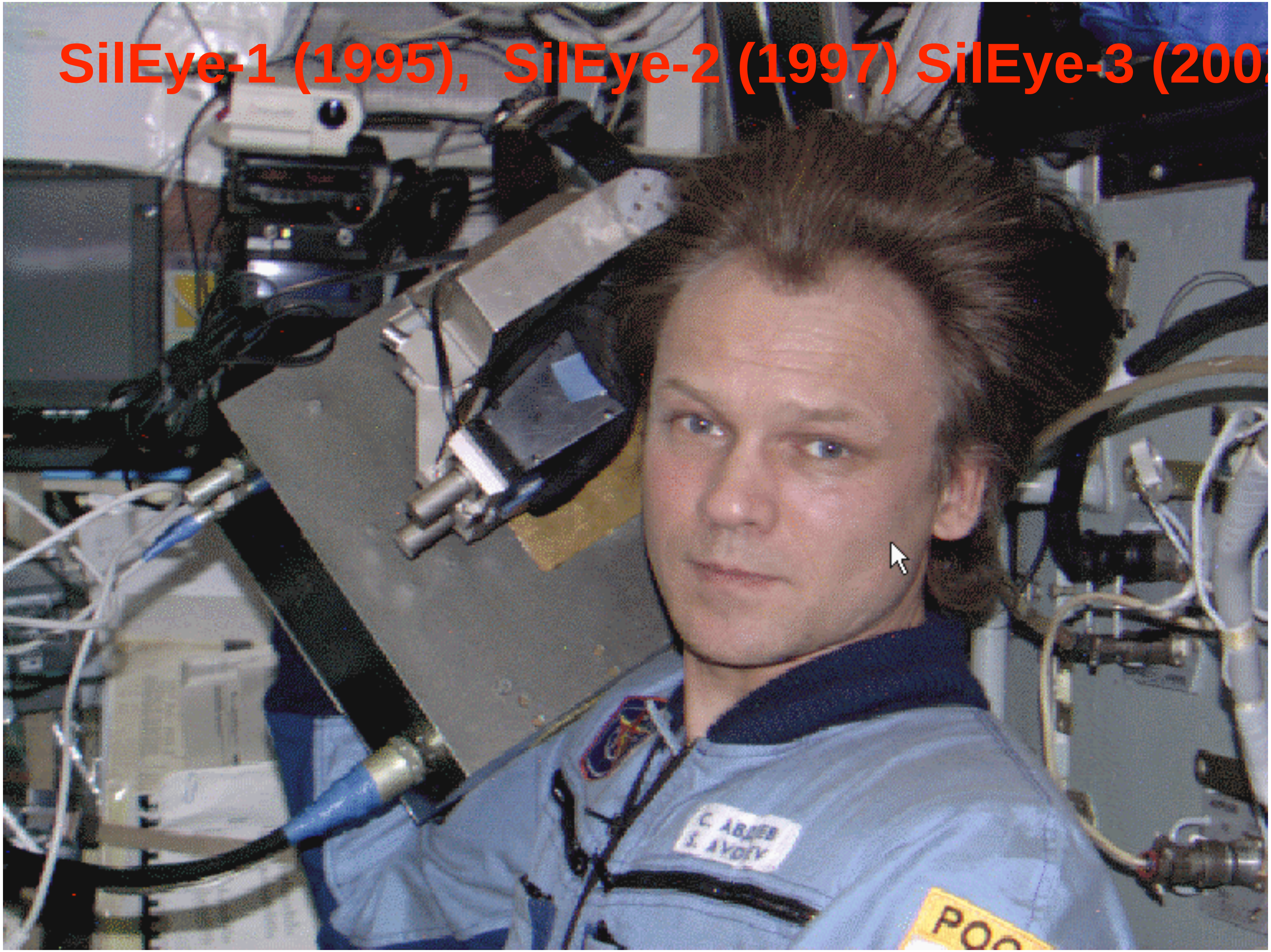

Sileye-1 & -2 on MIR: LF observed locations

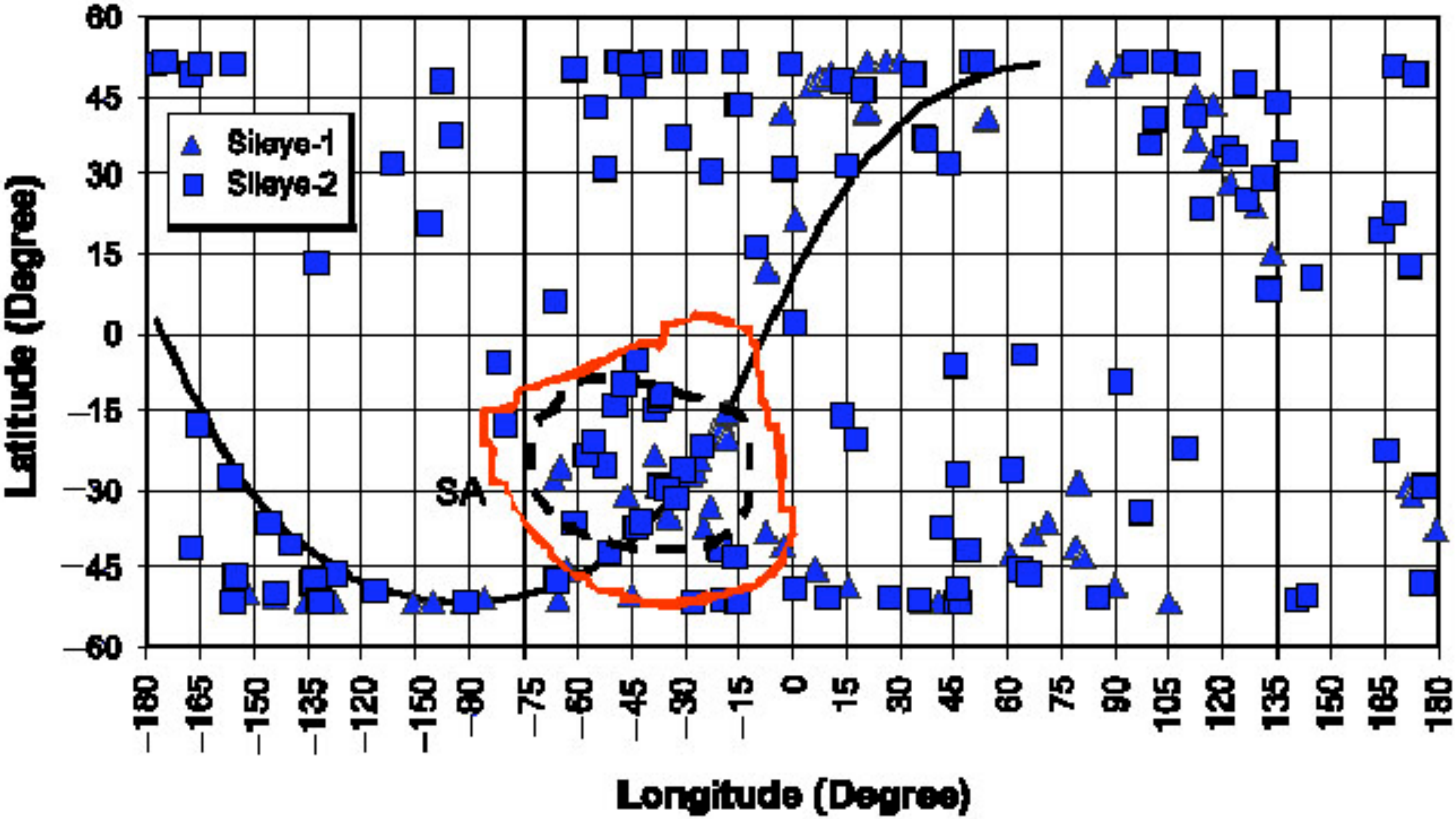

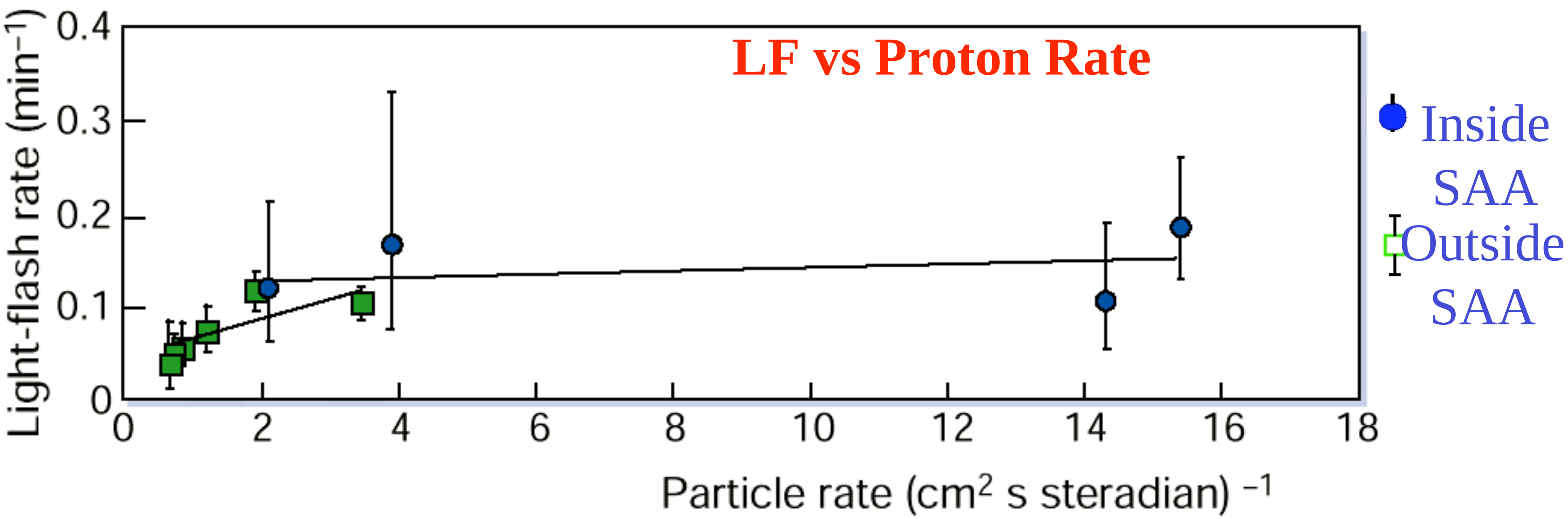

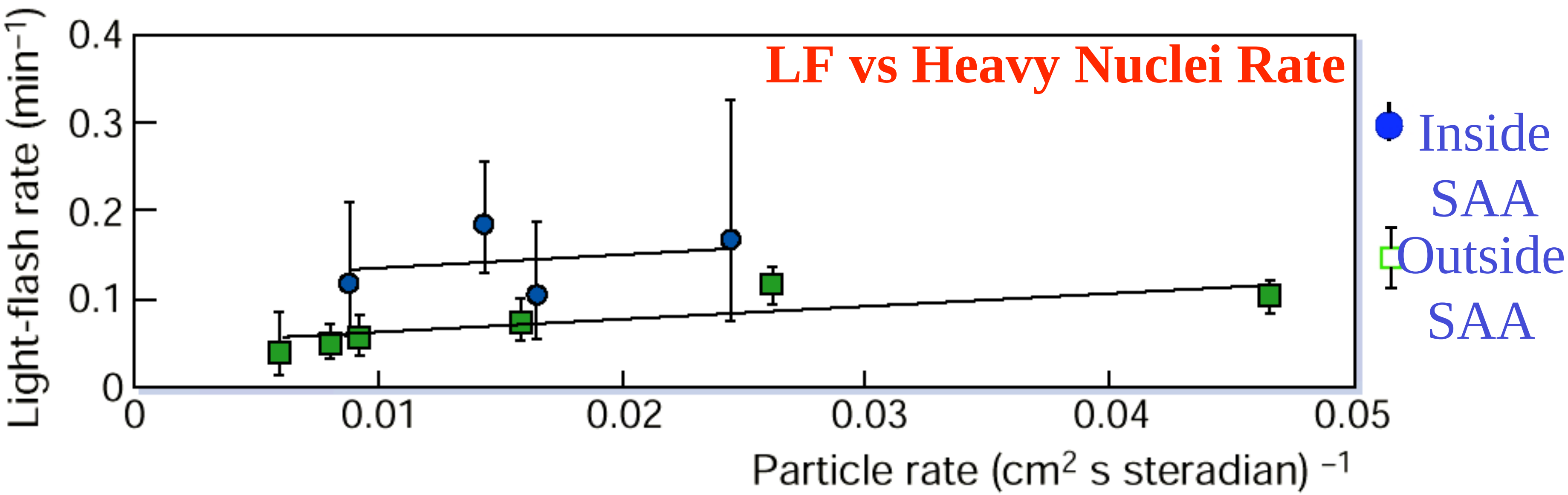

Casolino et al, Nature, 422, 680 (2003)

Avdeev et al, Acta Astr. 50

SILEYE-3 ALTEINO:

The *detector array* is composed of:

Two scintillators, which give the trigger and define the geometry of the system. They are located on top and bottom of the device and are used in coincidence to trigger the acquisition when the device is crossed by a cosmic ray.

- 8 silicon strip detector planes.
There are 4 planes with strips oriented in the X direction and 4 planes oriented in the Y direction to provide a stereoscopic view of the track.

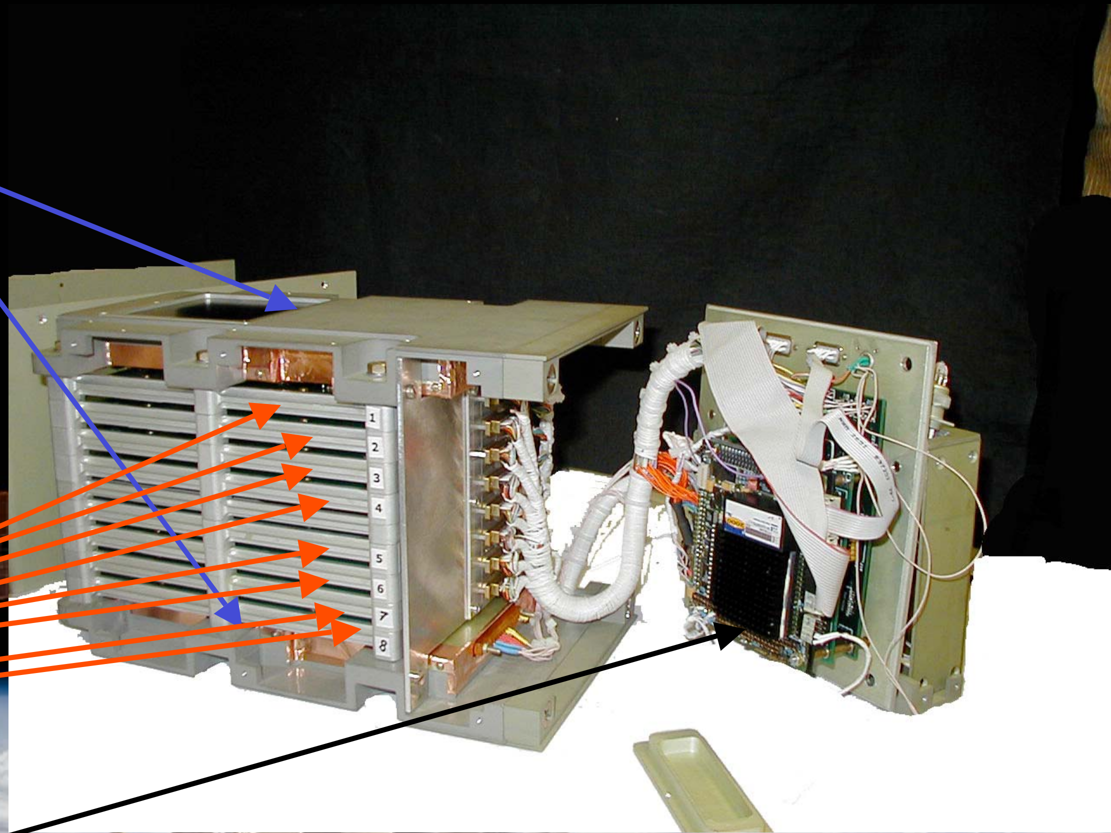

The *acquisition* system consists of a PC-104 based 486 CPU with a PCMCIA interface for data storage and download, coupled with an Analog Devices DSP for the acquisition for the silicon planes.

Silicon detector

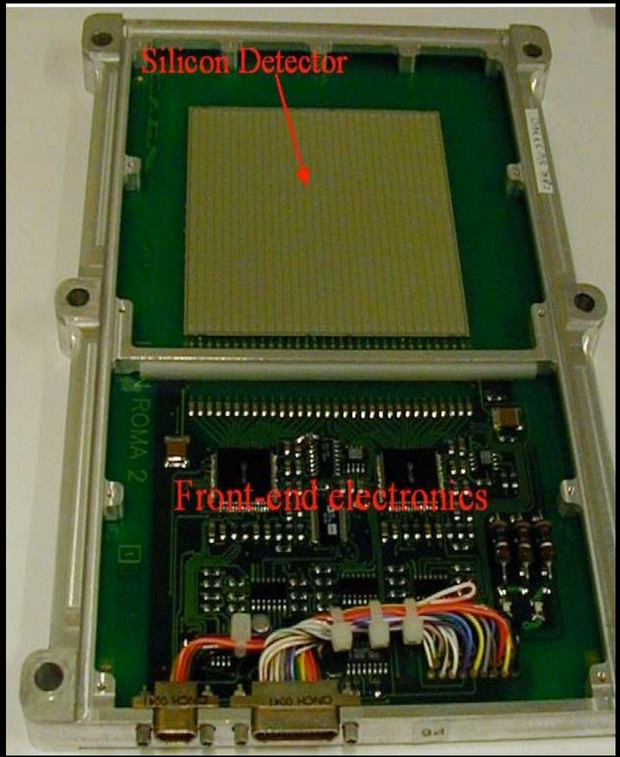

Left: AST detector tower open (without readout electronics): it is possible to see the stack of silicon detectors and the top scintillator (the detector is upside down). The bottom scintillator has been removed for clarity. Rigth: One of the 8 silicon detector boards (X view). It is possible to see the segmentation of the 32 strips of the detector. (Photos taken during assembly in the clean room facilities of Tor Vergata.)

Gem. Factor 42 cm^2 sr

Each sensitive layer contains a

- 8 sensitive layers
- 32 strips/layer; strip pitch 2.5 mm, x 8 cm^2, thickness 380 μm
- 256 Independent channels
- The front-end is a developed version of two 16 channels CR1 chip with a peaking time of 2 μs; a sensitivity of 5 mV/MIP and a maximum counting rate of 30 kHz.
- Detectors and electronics has been developed for the Si-W calorimeter of the PAMELA experiment

ISS008E05896

SILEYE-3 ALTEINO:2002 Italian Soyuz Mission

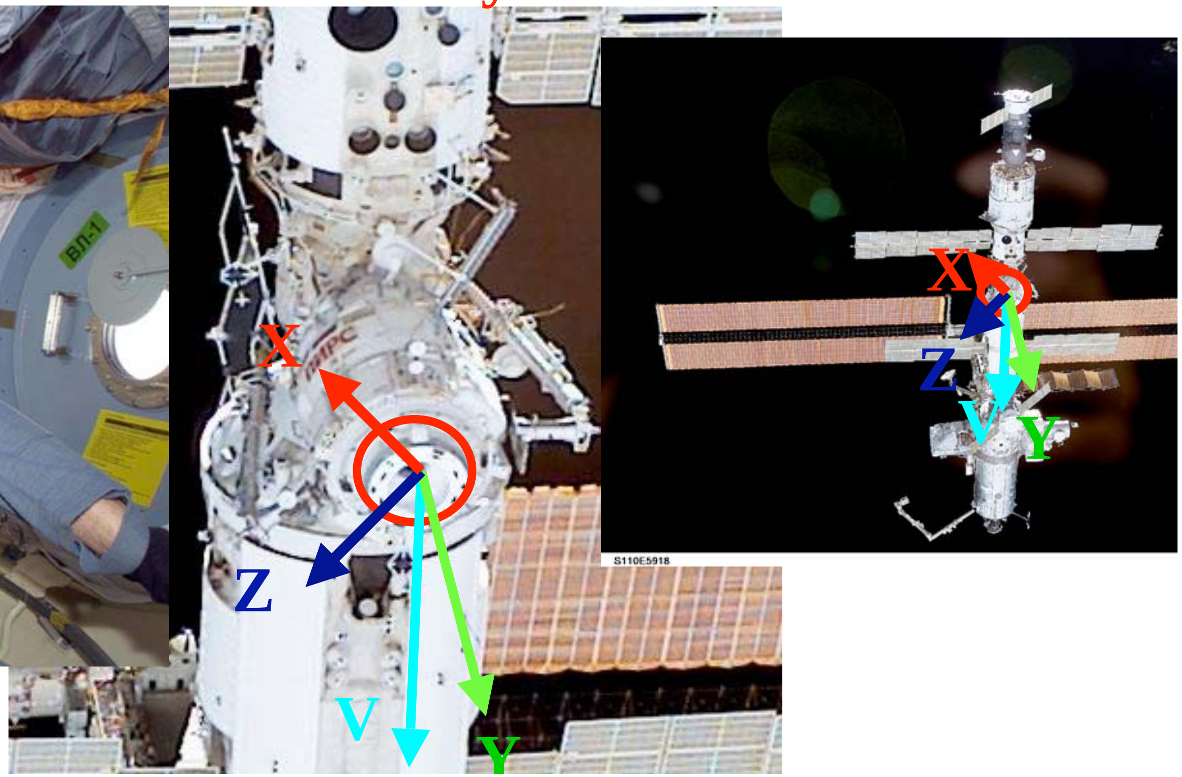

S110E5918

ISS Attitude during flight:

+ZLV +XVV TEA

Yaw: 350

Pitch:350.79

Roll:0

yland)

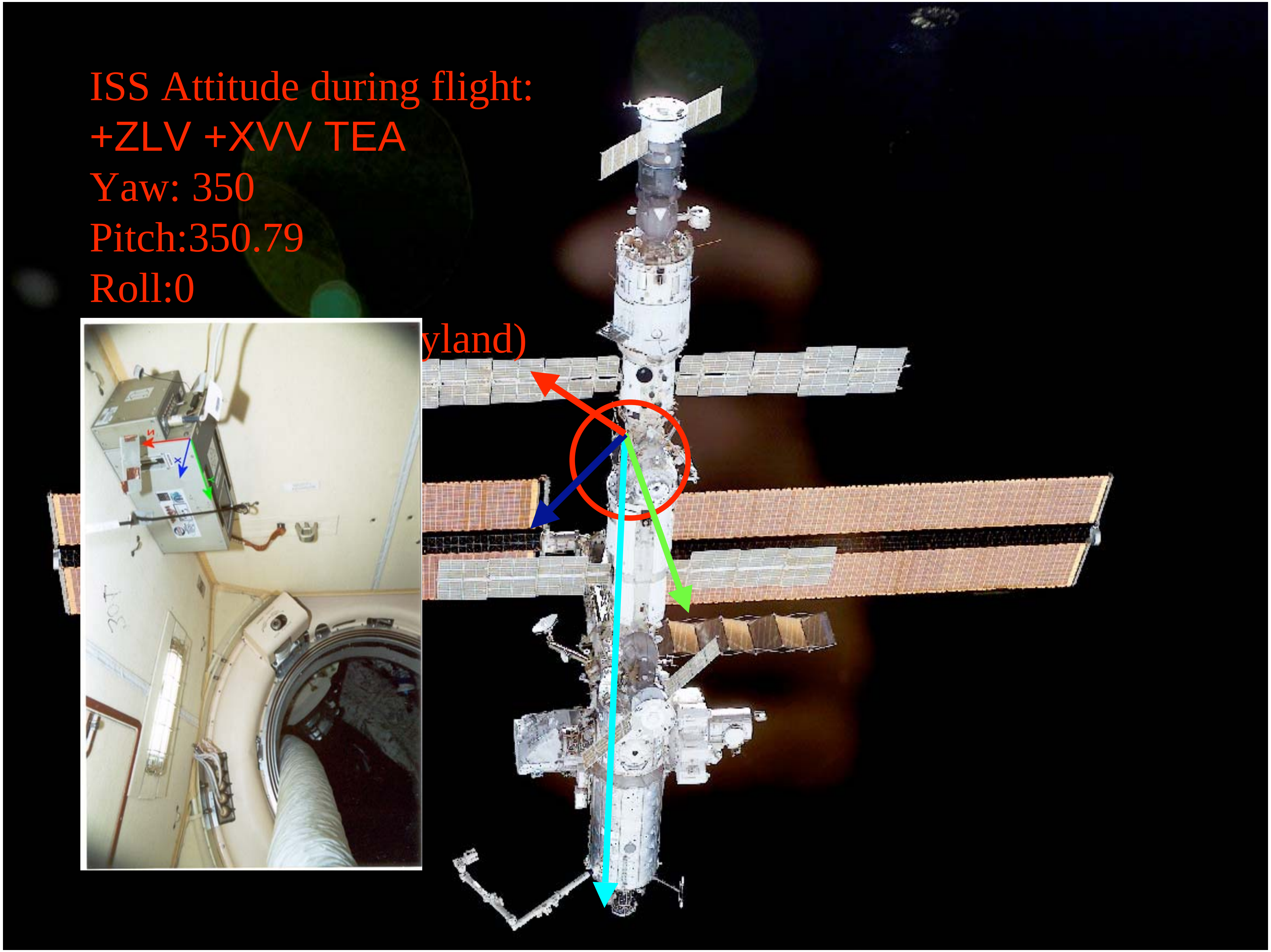

LAZIO - Sirad experiment

Technological demonstrator → science

- New "Lazio" detector

- Light Flash observations
- Alteino + shielding material
- User centre in Tor Vergata → Altea

Lazio-Sirad

- 28 kg payload.
- 6 different experiments/detectors linked together involving:
  - ➢Technology demonstration (SI-PM, Magnetometer)
  - ➢Life science
  - ➢Radiation environment
  - ➢Relationship between seismic phenomena and radiation belts.

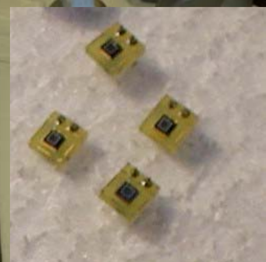

Lazio-MEB

Silicon-Scintillator Tracking Calorime

•Study of nuclear (>40MeV/n) and elec
components inside ISS.
•Study of spatial, angular dependence a
(in long term) of magnetic perturbations
40cm^2 sr
3 scintillators
4 double sided microstrip detectors 16*7 cm
16 Silicon Photomultiplies Tiles

One-axis magnetometer (EGLE)

PC-104 acquisition with PCMCIA cards


To ISS
2005: Alteino & Lazio detectors inside PIRS module of ISS
To Soyuz
РОССИЯ
LAZIO SIRAD
402

Altcriss Scientific Objectives

- **Long term measurements of cosmic ray and radiation environment on ISS (p-Fe >50-100MeV/n)**
- **Effectiveness of different shielding material. Effect on nuclear abundances**
- **Passive dosimeters (JAXA, DLR, Fed II)**
- **Joint measurements with Pamela & Altea**
- **Solar Particle Events**

ALTCRISS collaboration

Dr. Francis Cucinotta, NASA
Prof. Marco Durante, University of Napoli
Dr. Christer Fuglesang, EAC
Dr. Cesare Lobascio, Aleniaspazio
Dr. Aiko Nagamatsu (JAXA)
Prof. Livio Narici, University of Roma Tor Vergata
Prof. Piergiorgio Picozza, University of Roma Tor Vergata
Dr. Guenther Reitz (DLR)
Prof. Lembit Sihver,University of Chalmers (SE)
Prof. Piero Spillantini, University of Florence
Dr. V. Bengin (IBMP)

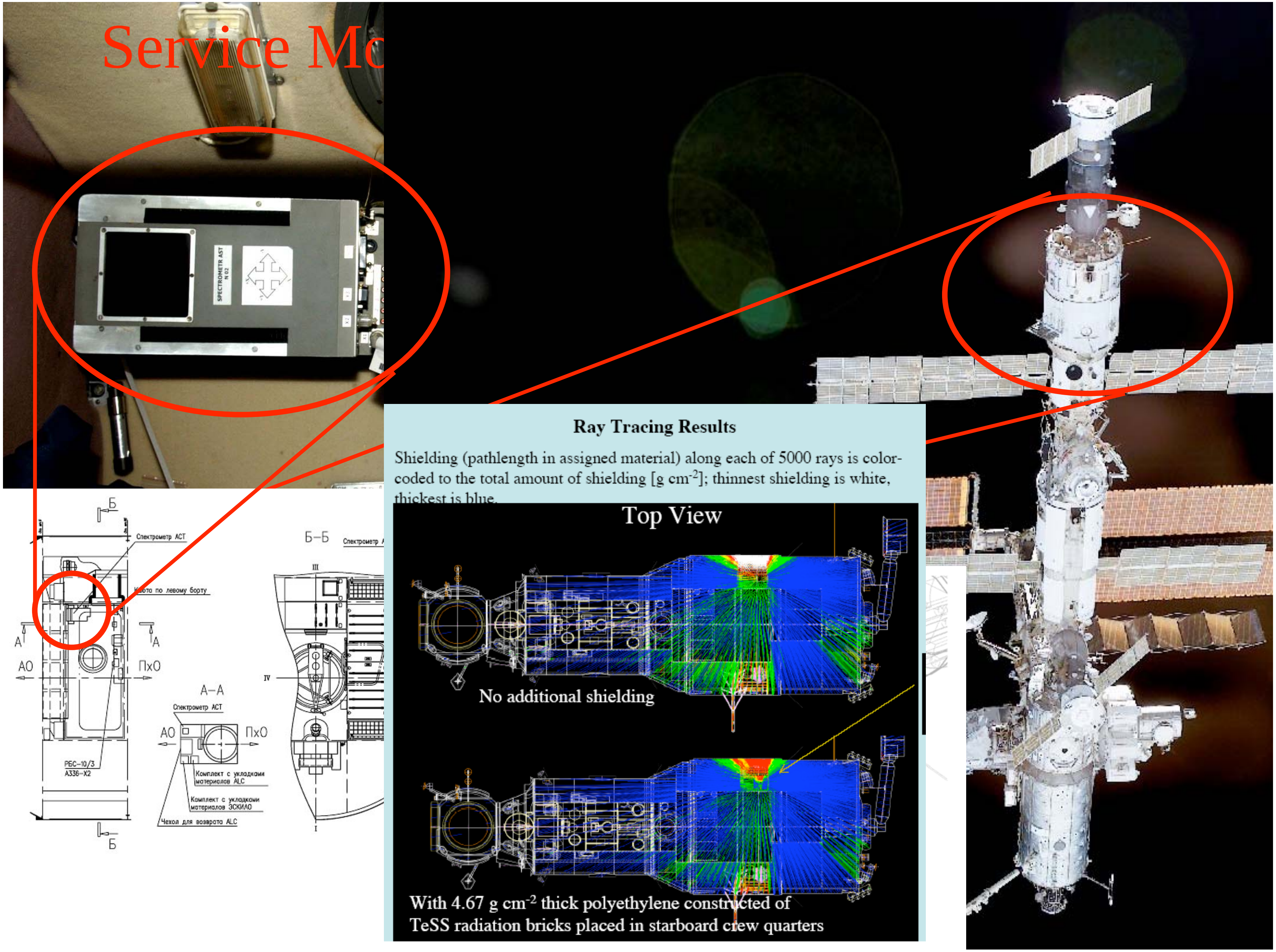

Service Mc
SPECTROMETR AST N 02
Спектрометр АСТ
Б–Б
А–А
АО
ПхО
Комплект с укладками материалов ALC
Чехол для возврата ALC
Ray Tracing Results
Shielding (pathlength in assigned material) along each of 5000 rays is color-coded to the total amount of shielding [g cm-2]; thinnest shielding is white, thickest is blue.
Top View
No additional shielding
With 4.67 g cm-2 thick polyethylene constructed of TeSS radiation bricks placed in starboard crew quarters

Acquisition Rate during mission

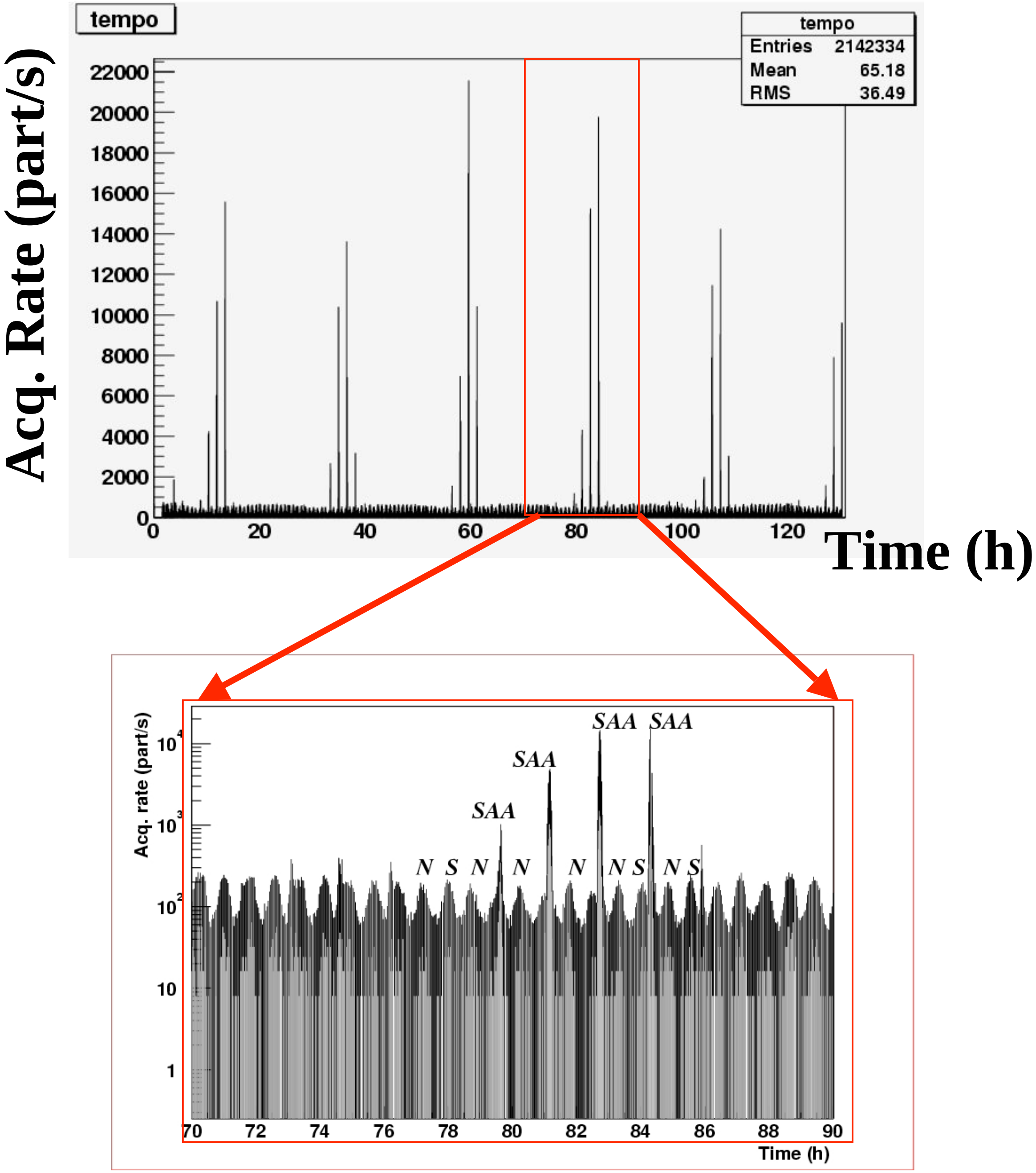

Particle Flux

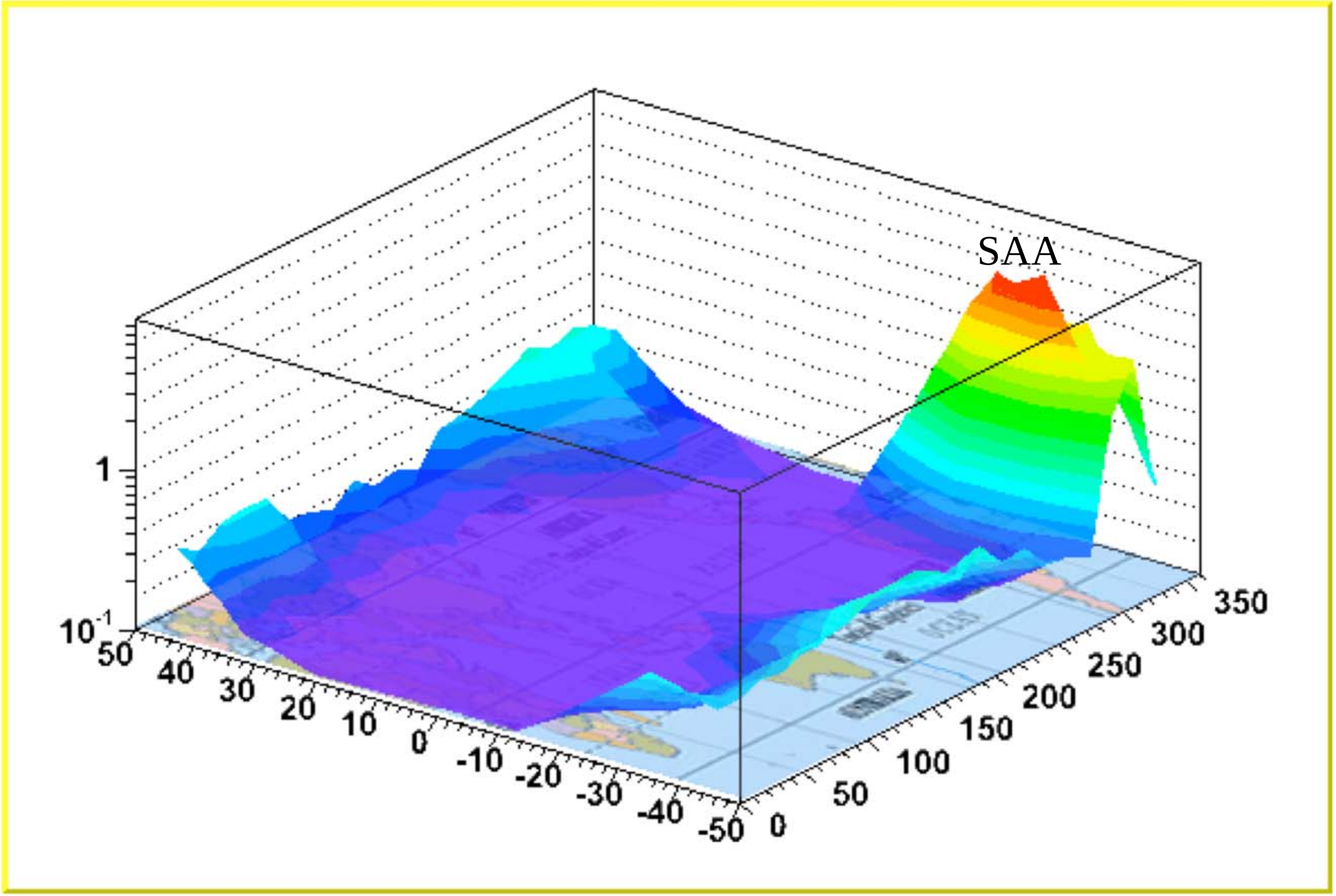

Effect of shielding on nuclear abundances

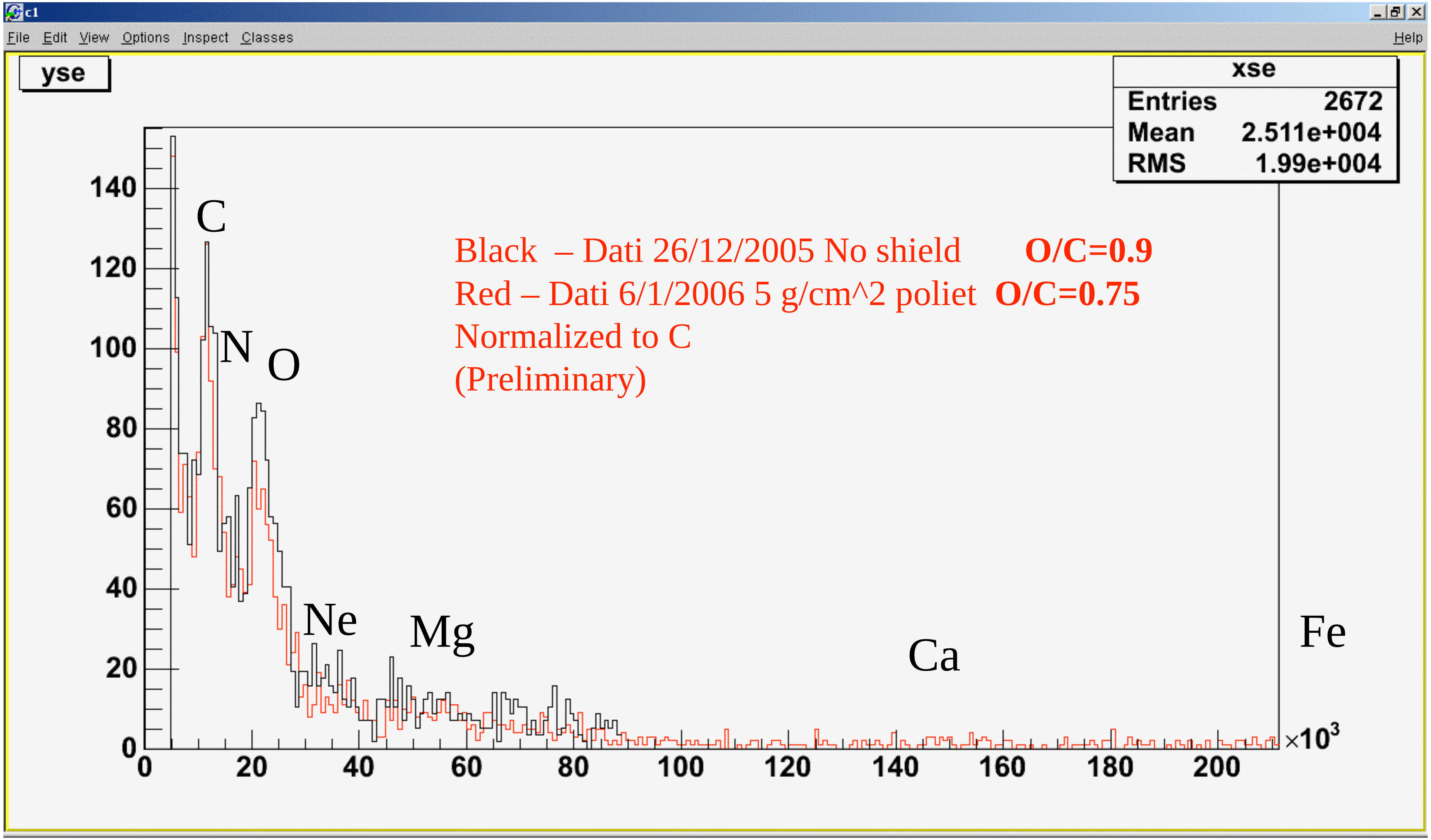

Nuclear Abundances (2002) – Pirs module

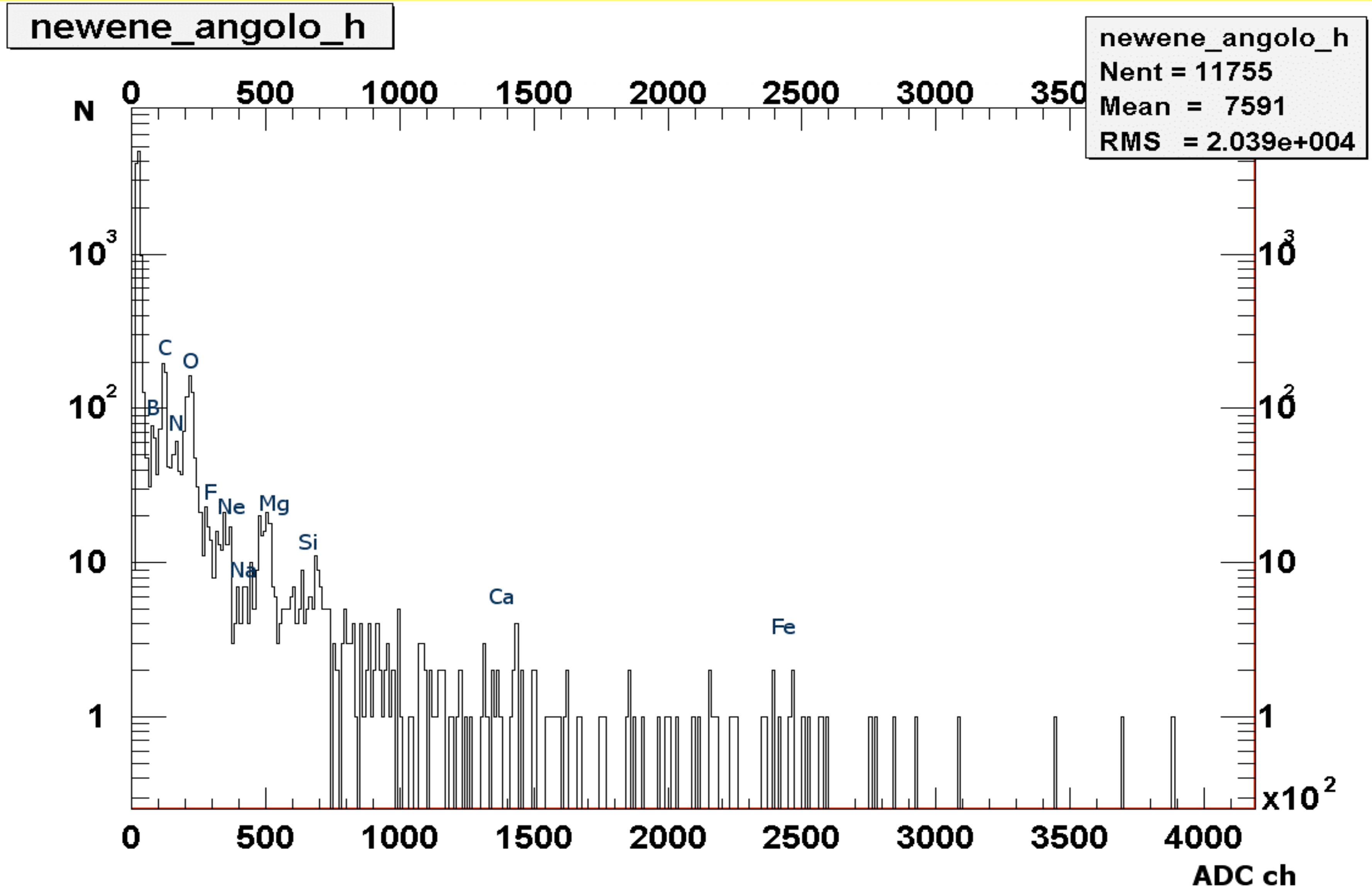

Difference PIRS – Service Module

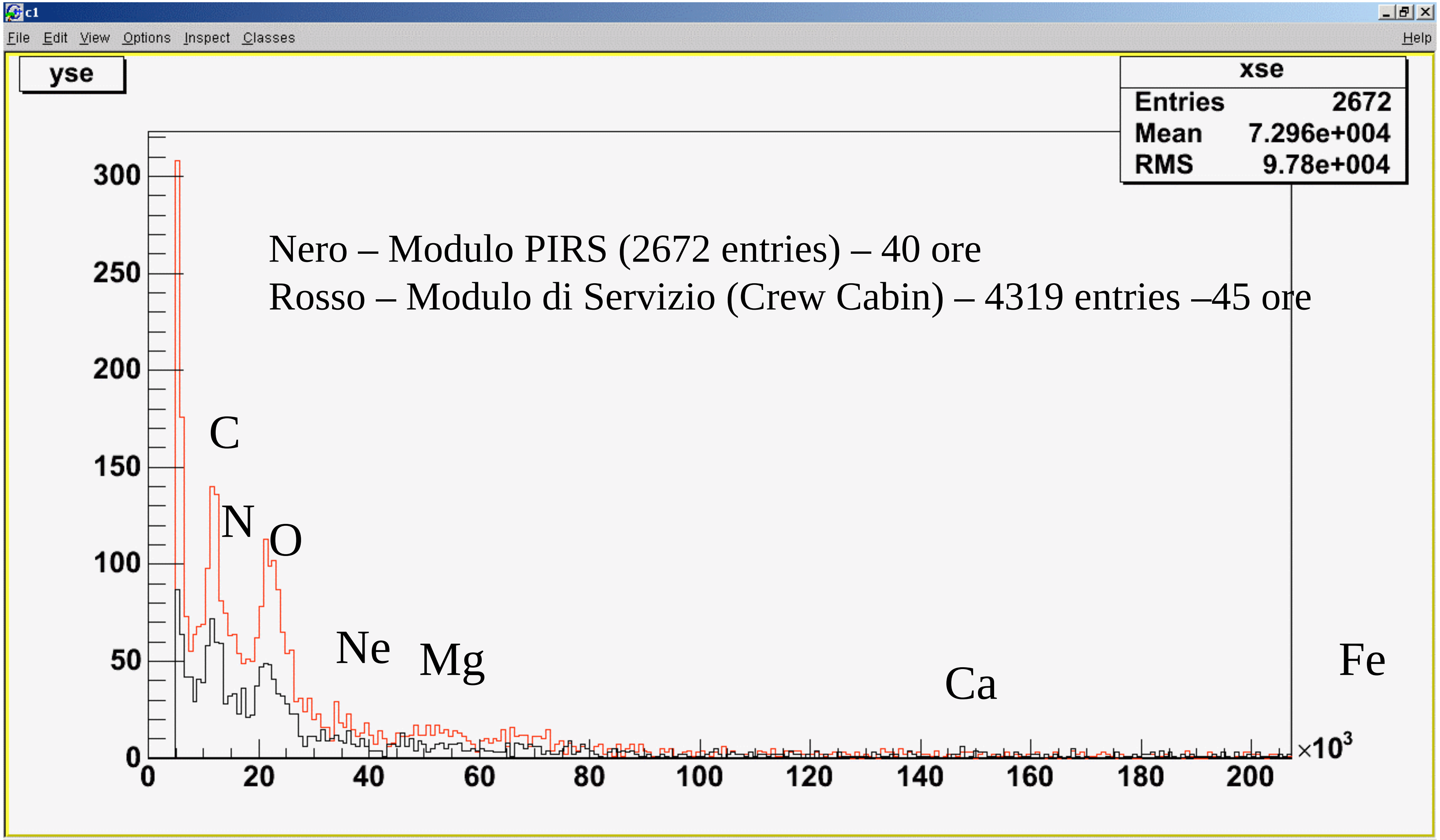

ALTEA

•Currently at JSC
•12 times Sileye-3
•Scheduled for next Shuttle launch…
•6 Light Flash Sessions with astronauts

•Standalone mode: three axis detector

•Shielding studies

ALTEA - space

Experimental protocols

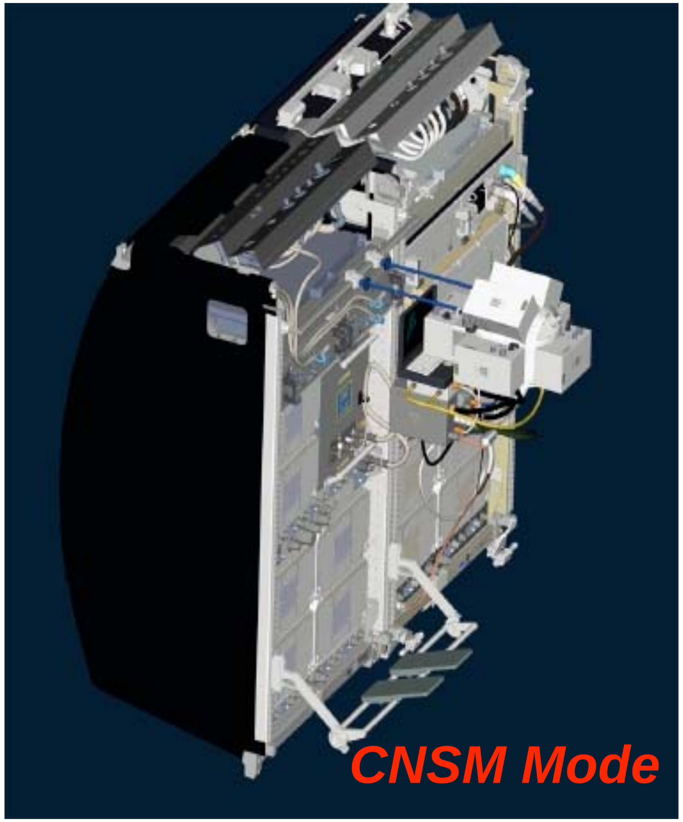

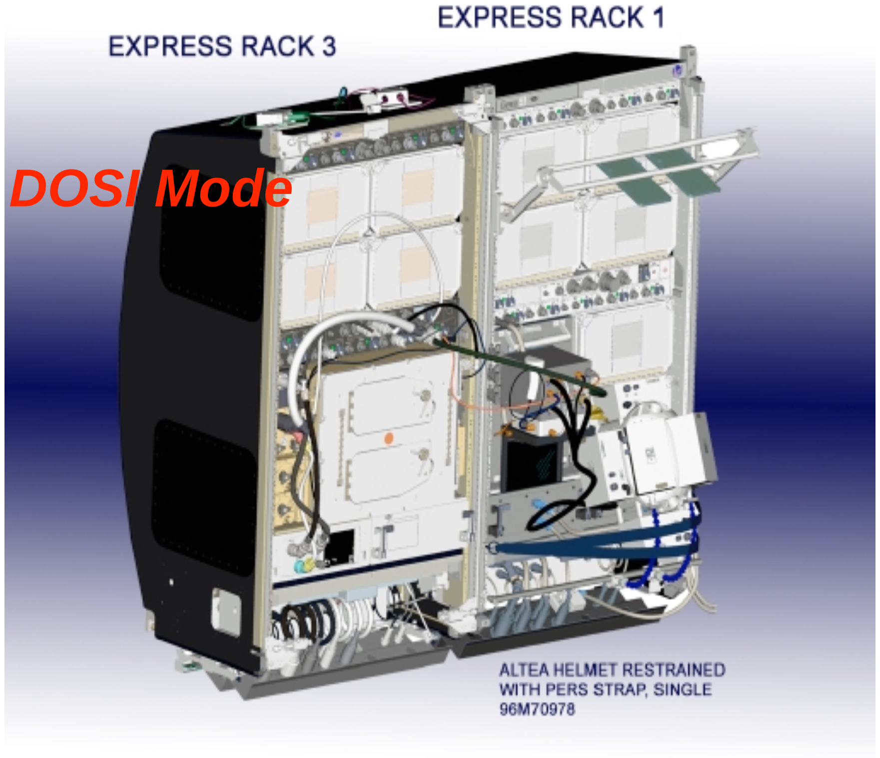

Manned: 6 sessions

the astronaut's electrophysiological activity is measured concurrently with the particles passing through her/his retina/cortex (energy released, trajectory, Z)

Unmanned:

The detectors are tilted 90° downwards to minimize protrusion.

The detectors are 'on' continuously.

Data is downlinked in real time

高エネルギー加速器研究機構 KEK
HIGH ENERGY ACCELERATOR RESEARCH ORGANIZATION

www.kek.jp

KEK – つくば - 27-2-2006

The PAMELA experiment for cosmic ray research in space: Status and Perspectives

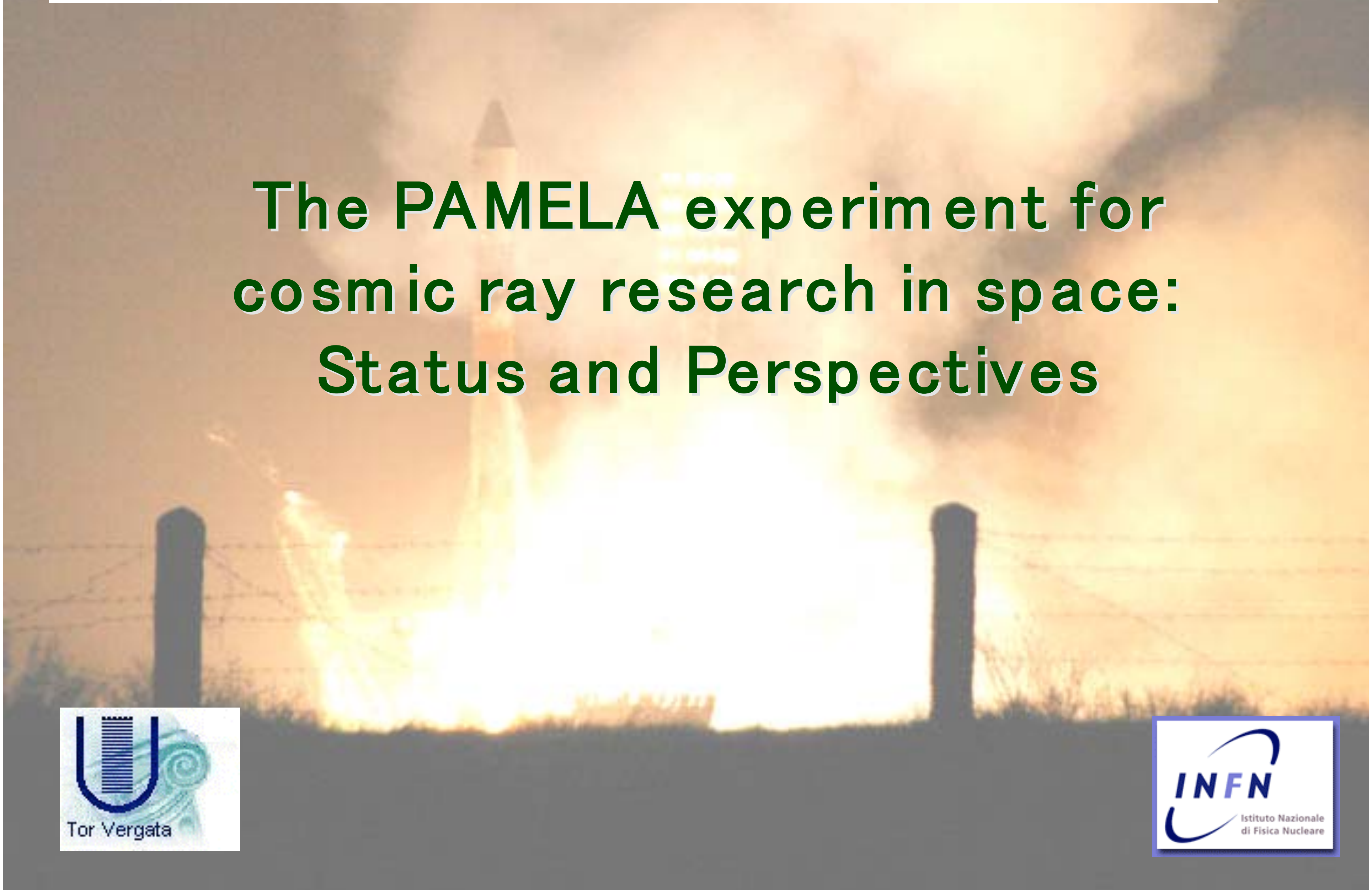

Tor Vergata

INFN Istituto Nazionale di Fisica Nucleare

PAMELA Collaboration

Italy:
- Bari
- Florence
- Frascati
- Naples
- Rome (Tor Vergata)
- Trieste
- CNR, Florence

Russia:
- Moscow
- St. Petersburg

USA:
- GSFC
- NMSU

India:
- Mumbai (TIFR)

Germany:
- Siegen

Sweden:
- KTH, Stockholm

Pamela Detector

Time of Flight
(three scintillators, 6 planes, 48 phototubes)

Magnetic (0.46T) Spectrometer Microstrip detector
(6 double sided microstrip planes)

Silicon Tungsten Tracking Calorimeter
(44 planes of 96 strip)

Shower Catcher Scintillator

Neutron Detector

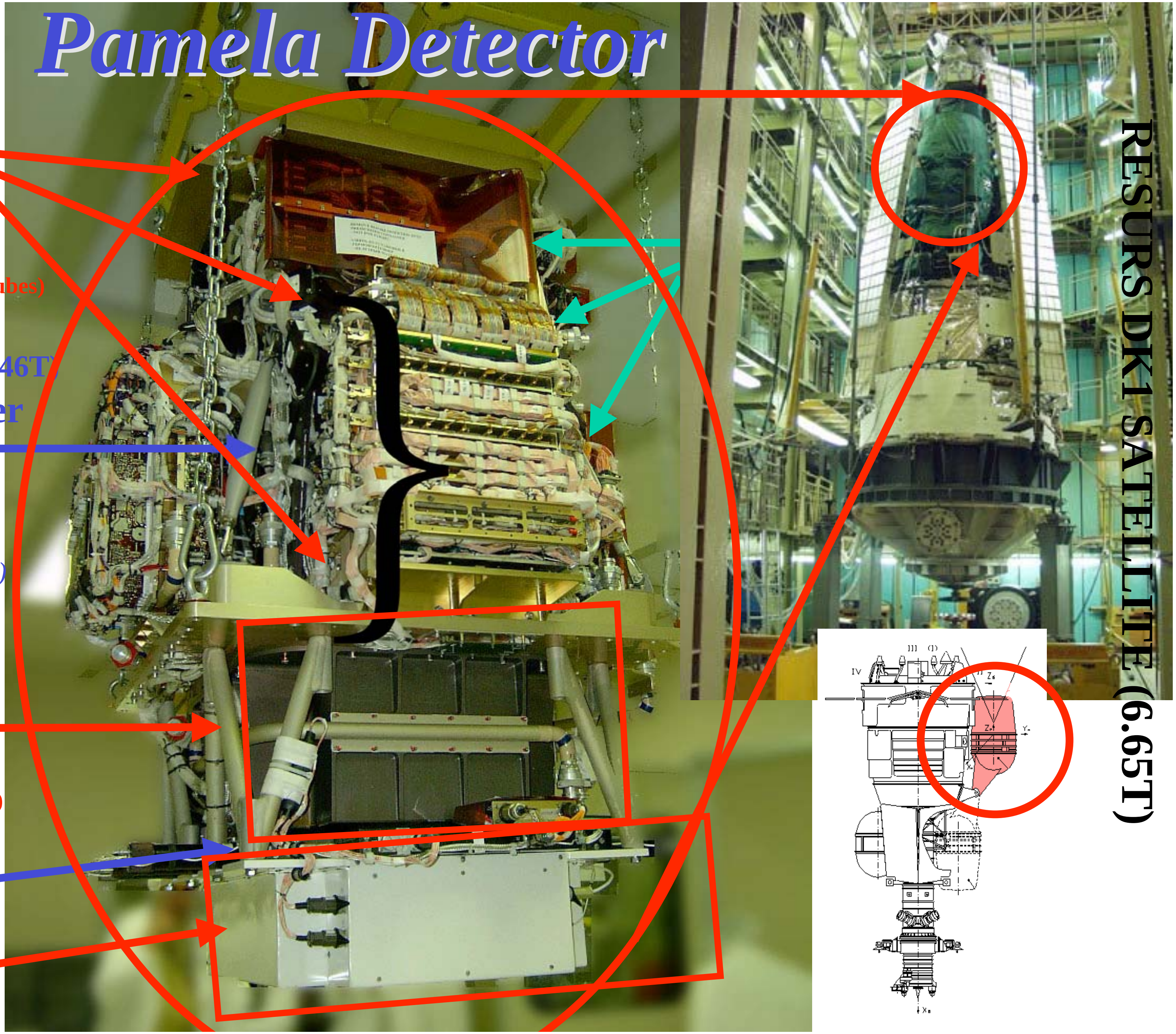

The PAMELA apparatus

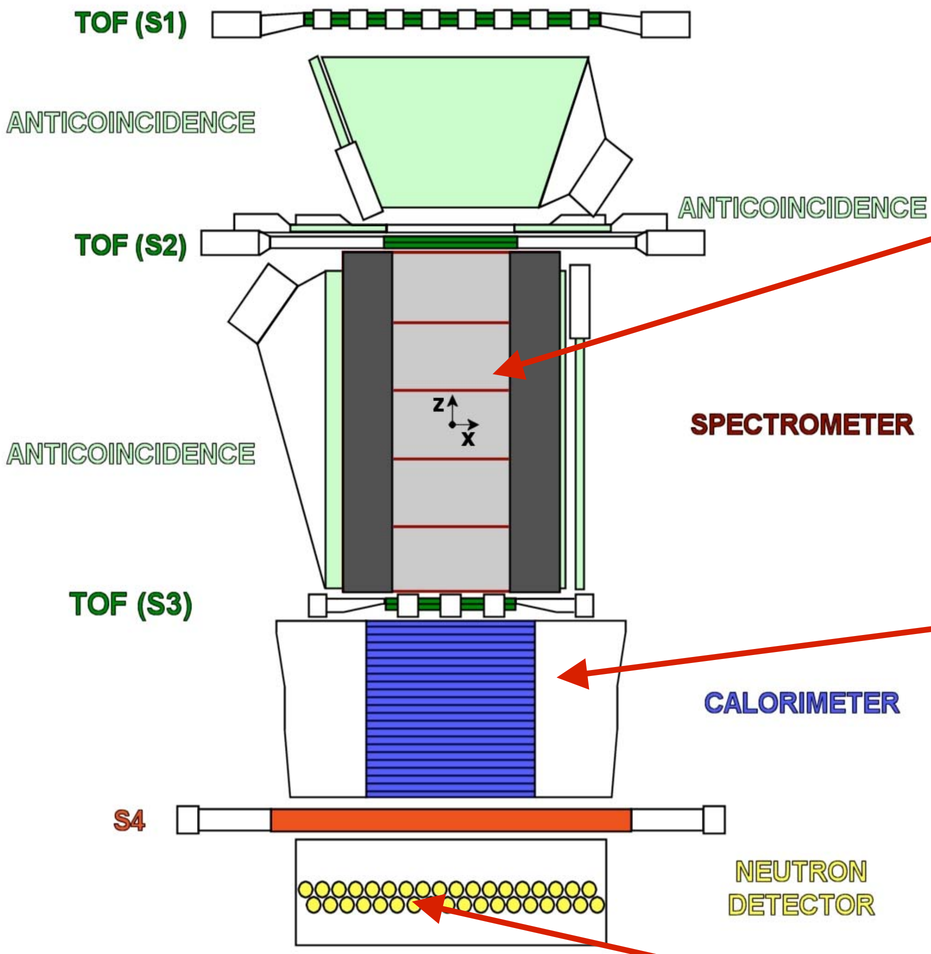

Spatial Resolution
- ≅ 2.8 μm bending view
- ≅ 13.1 μm non-bending view

MDR from test beam data ≅ 1 TV

Calorimeter Performances:
- $\bar{p}/e^+$ selection eff. ~ 90%
- p rejection factor ~ 10^5
- e^- rejection factor > 10^4

ND p/e separation capabilities >10 above 10 GeV/c, increasing with energy

GF ~20.5 cm^{2}sr
Mass: 470 kg
Size: 120x40x45 cm^3
Power Budget: 360 W

Time of Flight / Scintillator

- 6 x-y layers arranged on 3 planes;
- 48 channels.
- Albedo rejection
- Part ident. Up to 1 GeV with 150ps resolution
- Nuclear identification up to Oxygen

DIMENSIONS

S11	8	330 x 51 mm^2	7 mm	357 mm^2
S12	6	408 x 55 mm^2	7 mm	385 mm^2
S21	2	180 x 75 mm^2	5 mm	375 mm^2
S22	2	150 x 90 mm^2	5 mm	450 mm^2
S31	3	150 x 60 mm^2	7 mm	420 mm^2
S32	3	180 x 50 mm^2	7 mm	350 mm^2

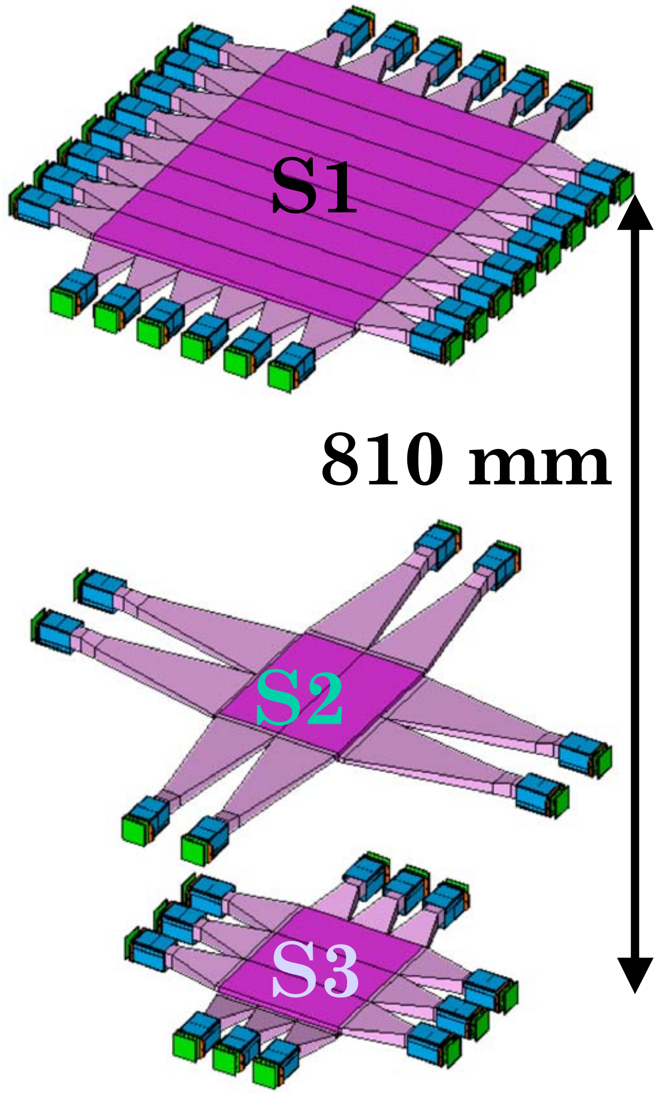

The permanent magnet

- 5 magnetic modules
- Permanent magnet (Nd-Fe-B alloy) assembled in an aluminum mechanics
- Magnetic cavity sizes (132 x 162) mm^2 x 445 mm
- Geometric Factor: **20.5 cm^{2}sr**
- Black IR absorbing painting
- Magnetic shields

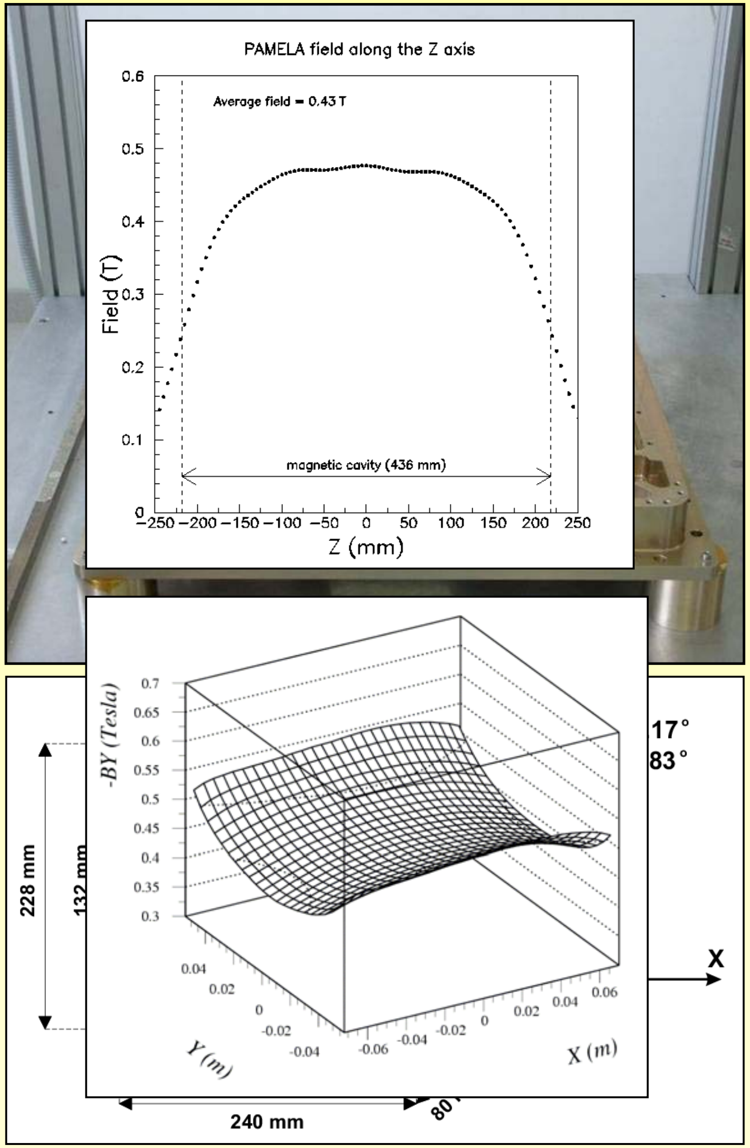

MAGNETIC FIELD MEASUREMENTS

- Gaussmeter (F.W. Bell) equipped with 3-axis probe mounted on a motorized positioning device (0.1mm precision)
- Measurement of the three components in 67367 points 5mm apart from each other
- Field inside the cavity 0.48 T at the center
- Average field along the central axis of the magnetic cavity : **0.43 T**
- Good uniformity
- Measurement of external magnetic field – magnetic momentum < 90 Am^2

The tracking system

6 detector planes composed by 3 "ladders"

- Mechanical assembly
  - no material above/below the plane (1 plane = 0.3% X_0)
  - carbon fibers stiffeners glued laterally to the ladders
- ladder : - 2 microstrip silicon sensors
  - 1 "hybrid" with front-end electronics
- silicon sensors (Hamamatsu):
  - 300 mm, Double Sided - x & y view
  - Double Metal - No Kapton Fanout
  - AC Coupled - No external chips
- FE electronics: VA1 chip
  - Low noise charge preamplifier -
  - Operating point set for optimal compromise:
    - total FE dissipation: 37 W on 36864 channels
    - Dynamic range up to 10 MIP
- DAQ: 12 DSPs
  - data compression (>95%)
  - on-line calibration (PED,SIG,BAD)

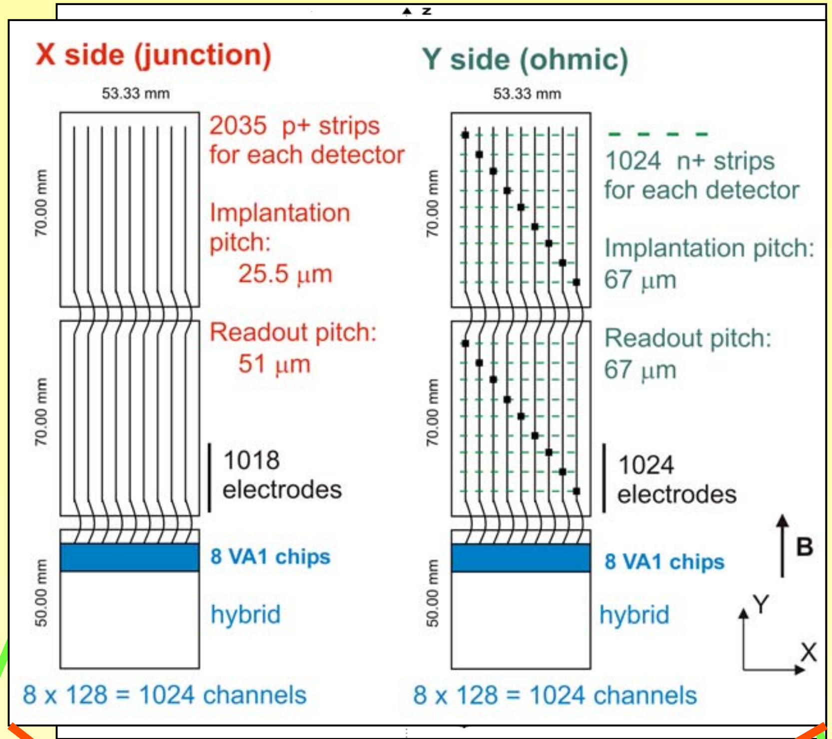

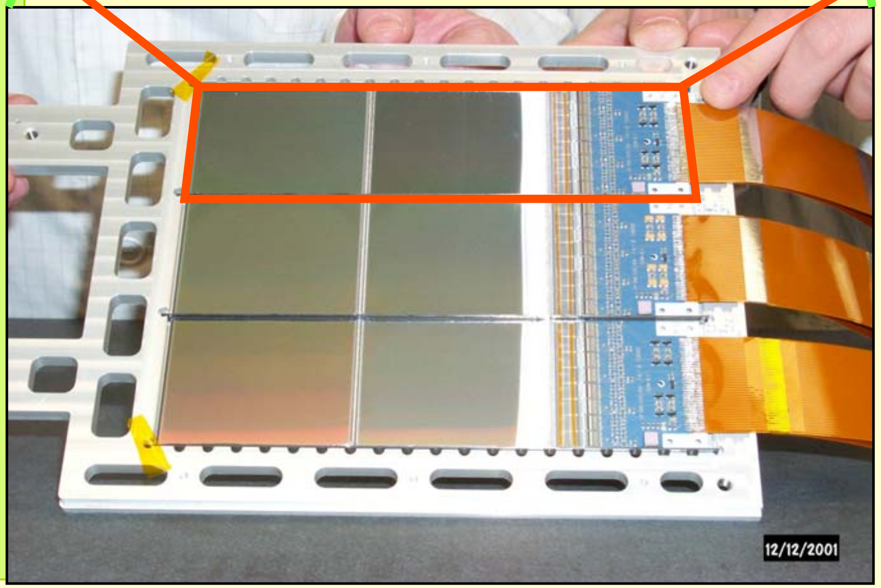

Spatial resolution

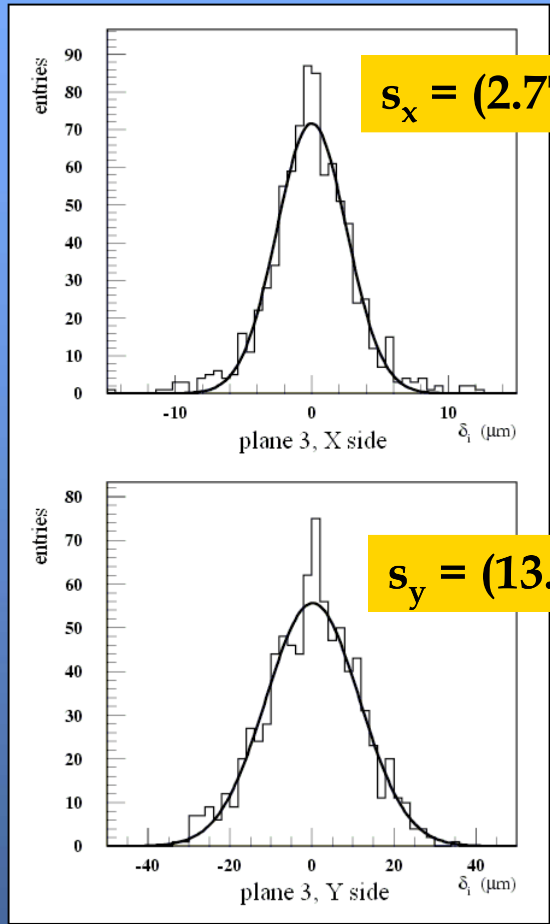

s_x = (2.77 ± 0.04) µm

s_y = (13.1 ± 0.2) µm

40-100 GeV pions (CERN-SPS 2000) beam-test of a small tracking-system prototype

Calorimeter

- 22 planes each with a tungsten layer 2.6 mm thick and 2 silicon detector layers (thickness 380 μ m)
- Each W layer is 0.26 cm (0.74X_o)
- 16 radiation lengths (0.6 interaction length) deep
- 96 strips 2.4 mm wide per silicon layer
- Strips along orthogonal directions between the 2 layers of each plane
- Total number of channels 4224
- Wide dynamic range ≅ 1 - 1200 mip (proton – above iron)

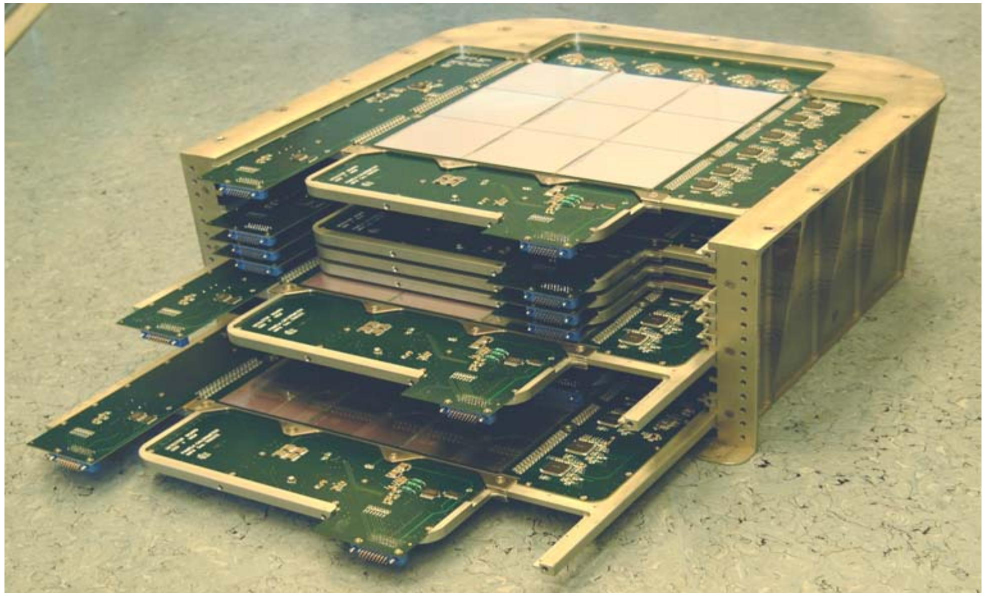

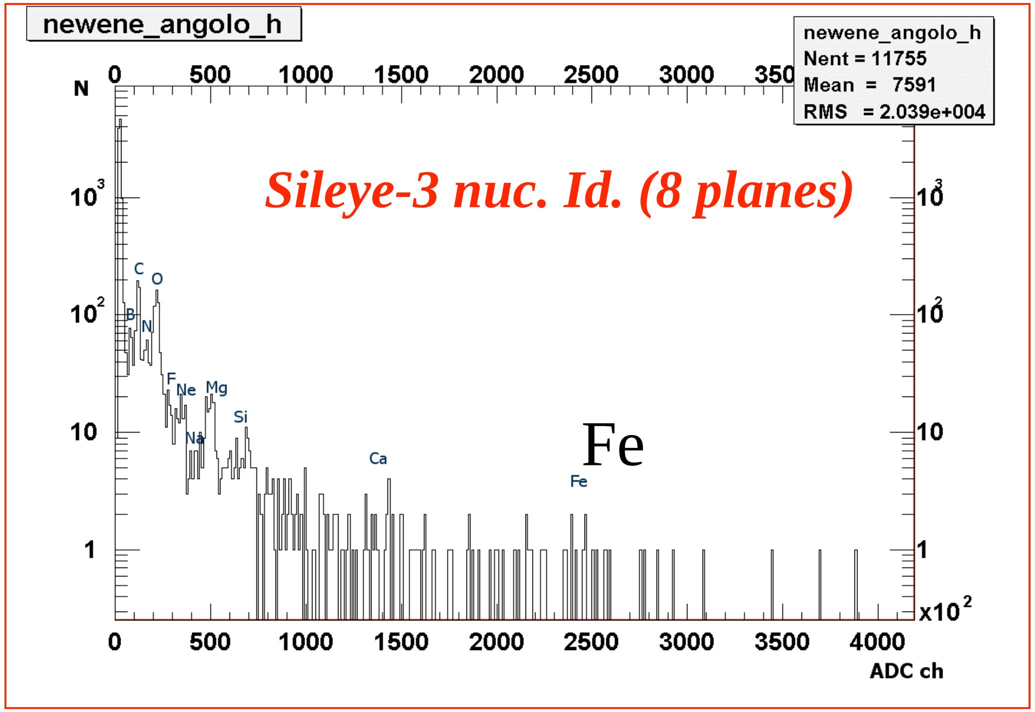

Neutron Detector

Lebedev Physical Institute Academy of Science, Russia

- 36 ^{3}He containers (2 planes)
- 9.5 cm polyethilene moderator enveloped in thin cadmium layer.
- 60x55x15 cm^{3}, 30 kg, 10 W

- **(10% eff for E<1MeV n)**
- Triggered counts
- Background counting

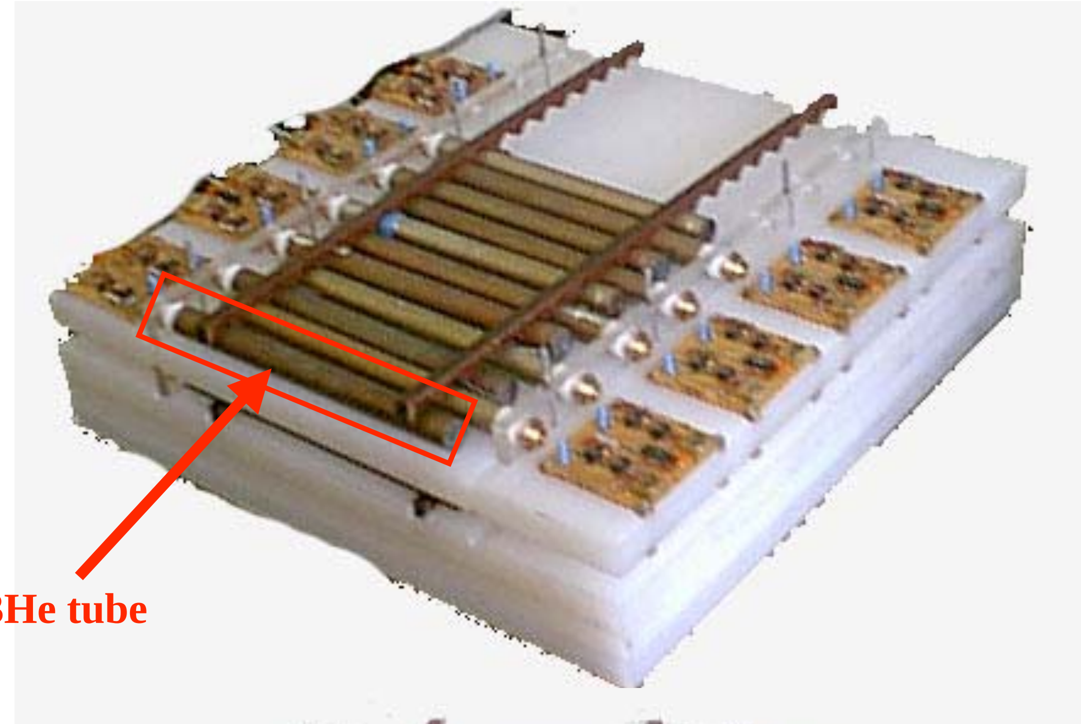

3He tube

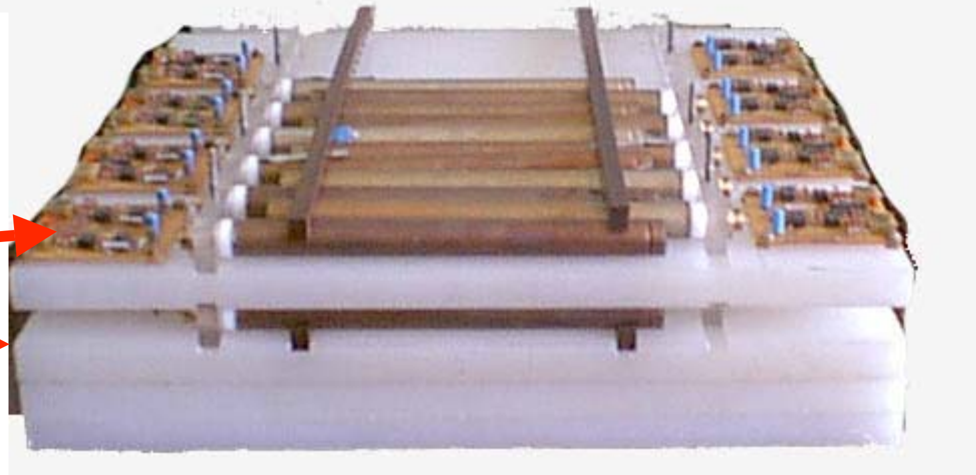

Plane 1

Plane 2

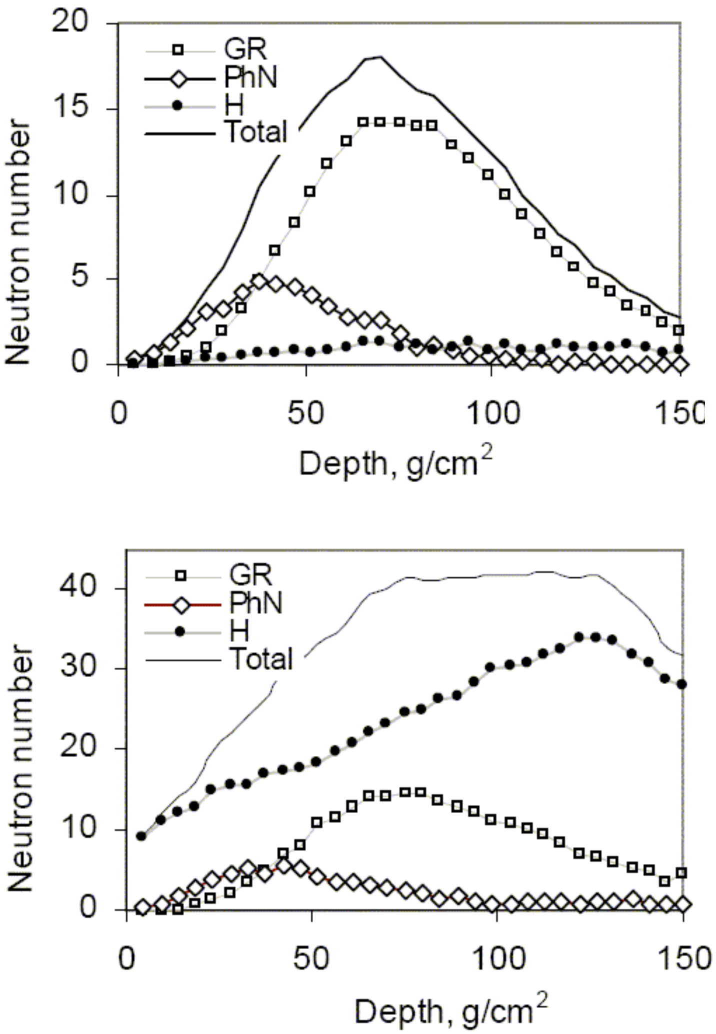

Fig. 2. Upper panel: number of neutrons generated by a primary electron with E=5x10^{11} eV (and its secondaries) at different levels of the calorimeter due to hadron (H), photonuclear (PhN) interactions (without a giant resonance), and a giant resonance (GR). Lower panel: the same as at the upper panel but for a primary proton of the same energy.

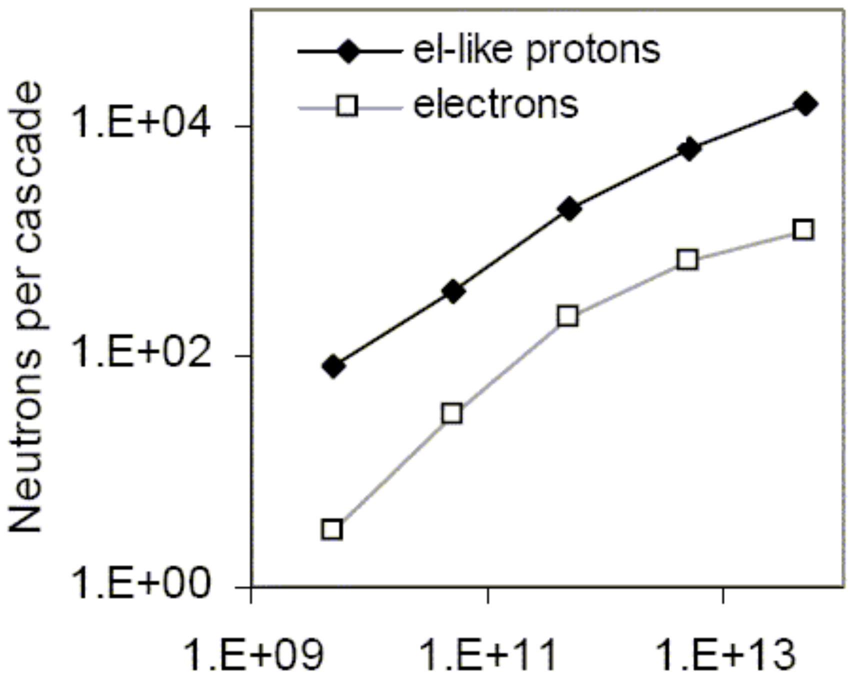

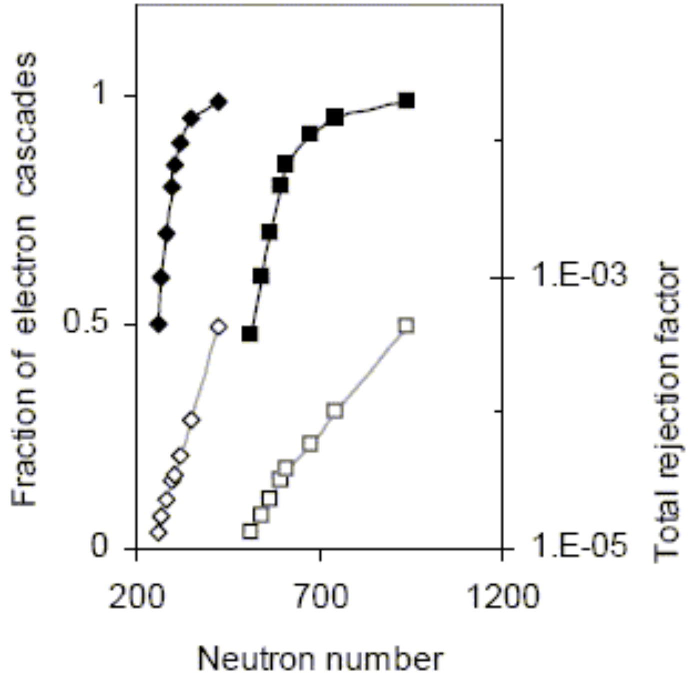

Galper et al, ICRC 2001

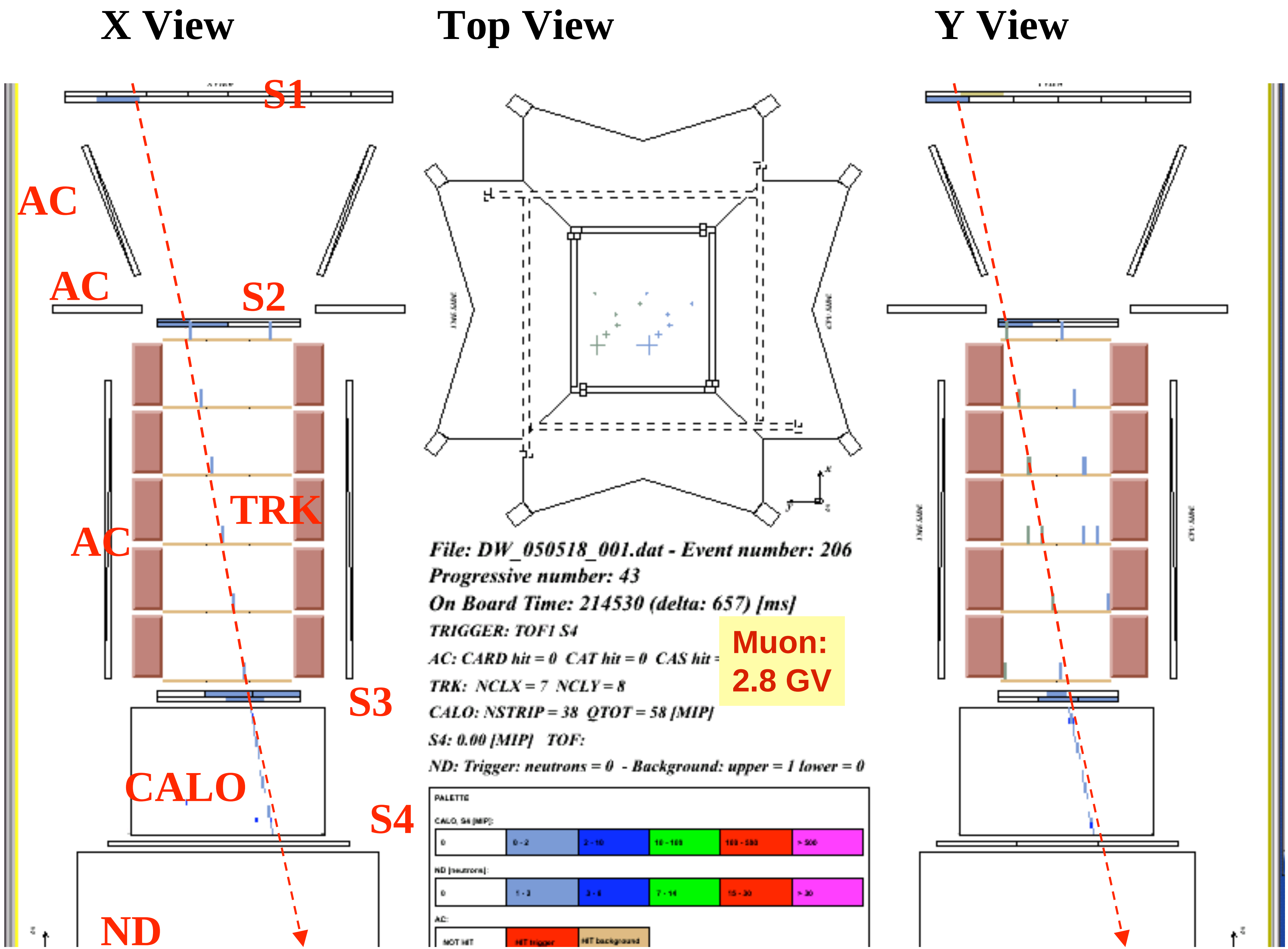
X View
Top View
Y View
S1
AC
AC
S2
TRK
AC
S3
CALO
S4
ND
File: DW_050518_001.dat - Event number: 206
Progressive number: 43
On Board Time: 214530 (delta: 657) [ms]
TRIGGER: TOF1 S4
AC: CARD hit = 0 CAT hit = 0 CAS hit =
TRK: NCLX = 7 NCLY = 8
CALO: NSTRIP = 38 QTOT = 58 [MIP]
S4: 0.00 [MIP] TOF:
ND: Trigger: neutrons = 0 - Background: upper = 1 lower = 0
Muon:
2.8 GV
PALETTE
0
0 - 2
2 - 10
0
7 - 14
15 - 30
> 30
AC:
NOT HIT
HIT trigger
HIT background

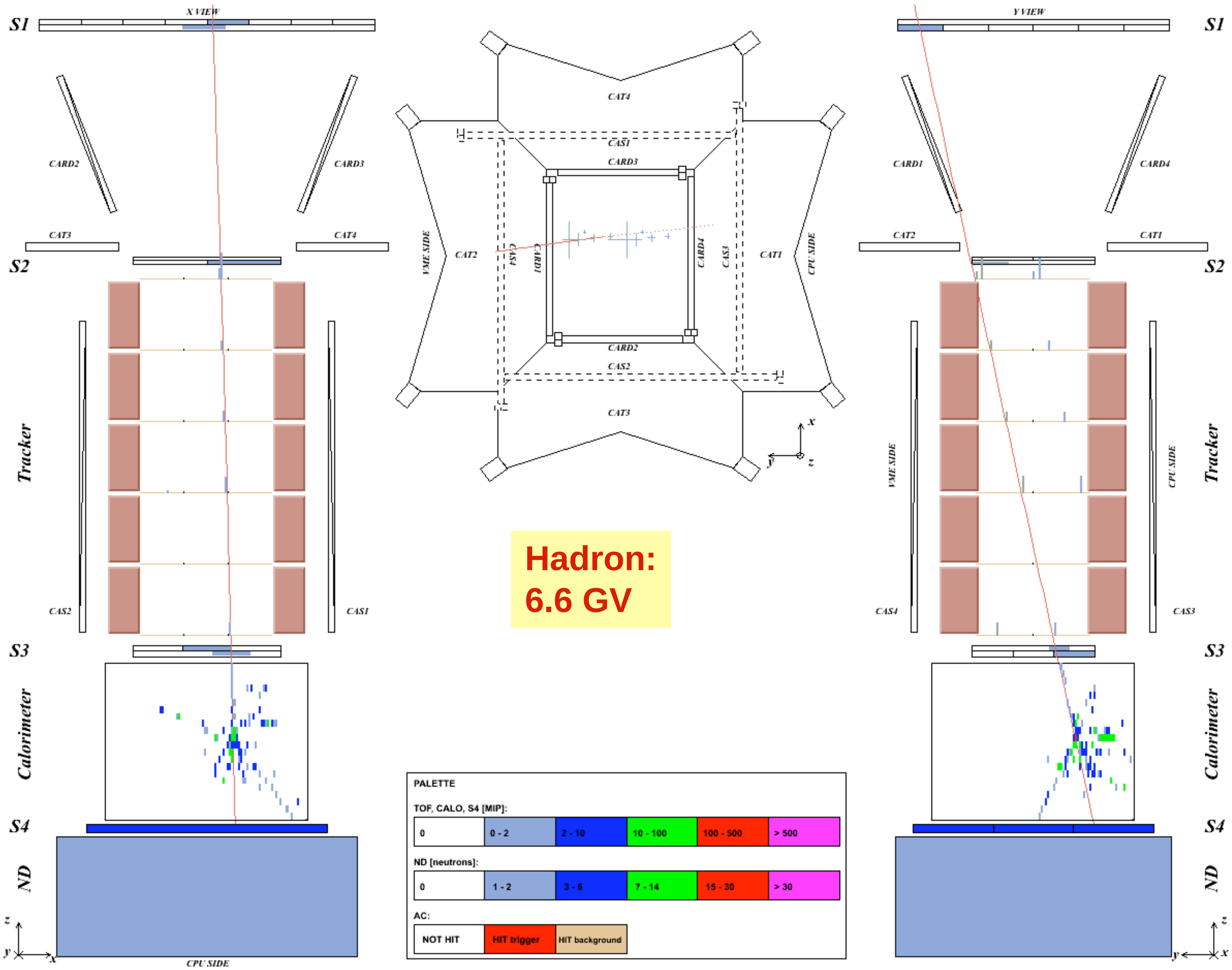

X VIEW
Y VIEW
S1
S2
S3
S4
ND
Tracker
Calorimeter
CARD1
CARD2
CARD3
CARD4
CAT1
CAT2
CAT3
CAT4
CAS1
CAS2
CAS3
CAS4
VME SIDE
CPU SIDE
Hadron:
6.6 GV
PALETTE
TOF, CALO, S4 [MIP]:
0
0 - 2
2 - 10
10 - 100
100 - 500
> 500
ND [neutrons]:
0
1 - 2
3 - 6
7 - 14
15 - 30
> 30
AC:
NOT HIT
HIT trigger
HIT background

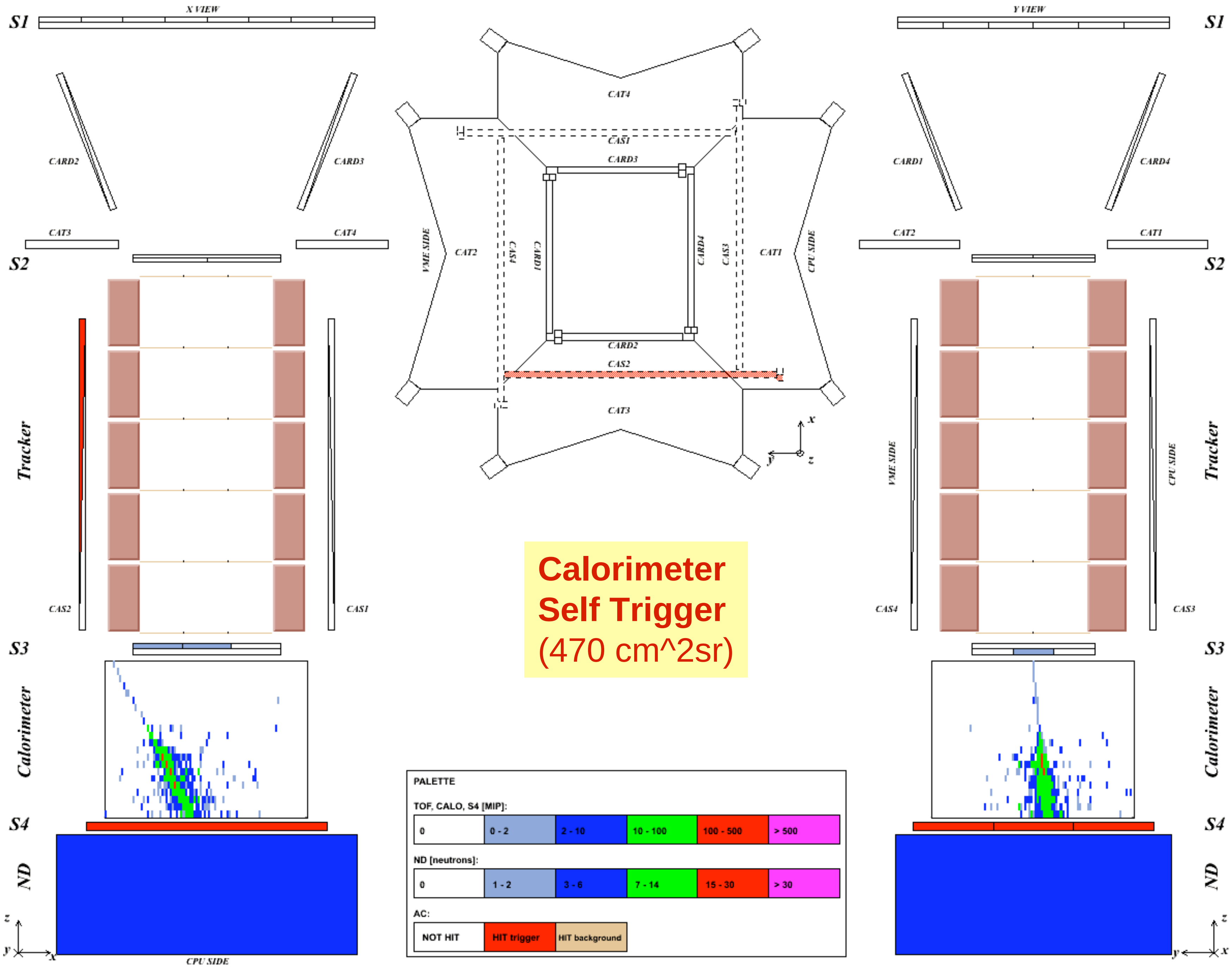

Calorimeter Self Trigger

(470 cm^2sr)

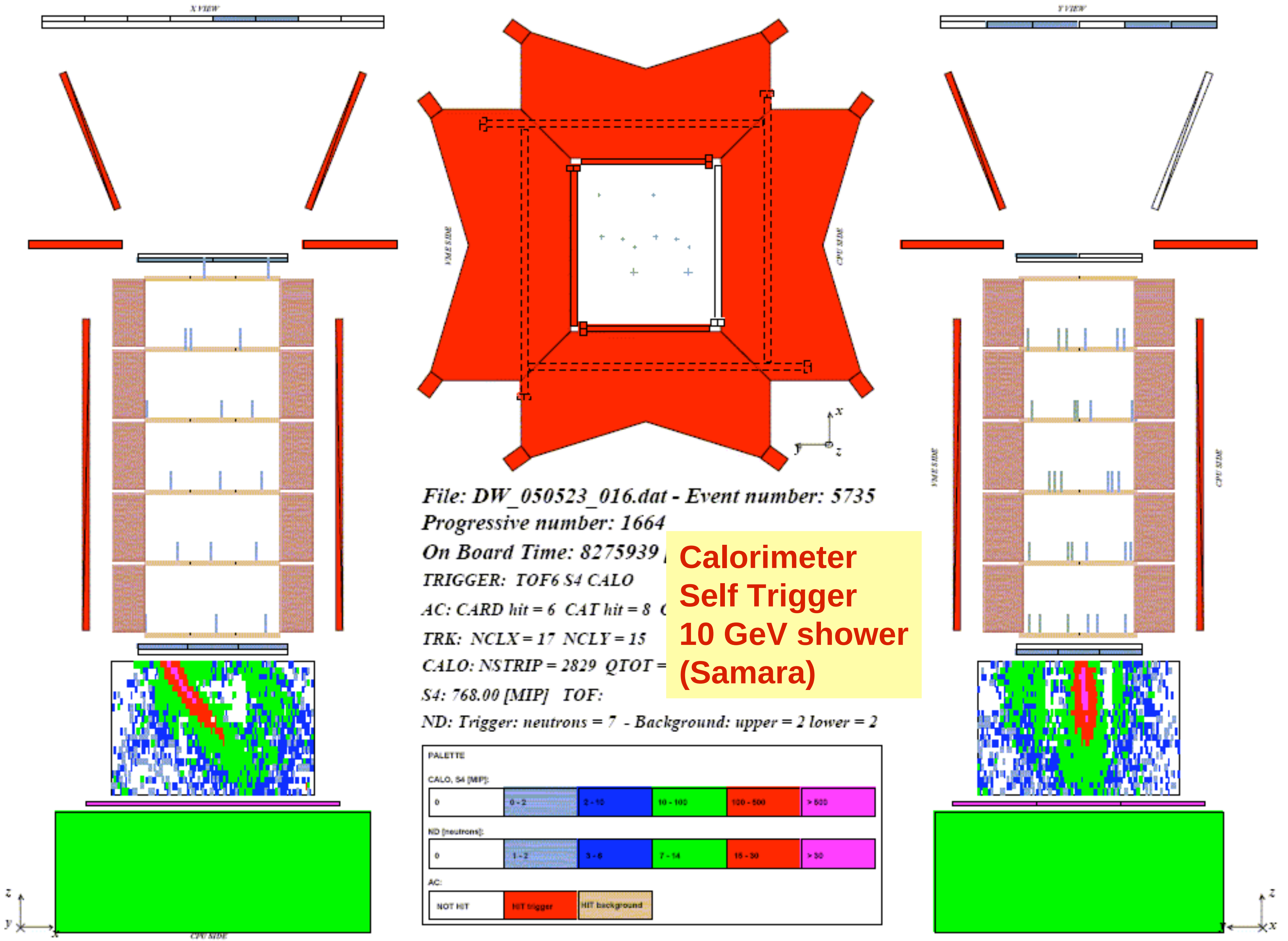

Calorimeter Self Trigger 10 GeV shower (Samara)

Pamela as a Space observatory at 1AU

High Inclination Orbit 70.4°

Galactic cosmic ray
Matter / Antimatter
/ Dark Matter

Solar Energetic particles

Jovian electrons

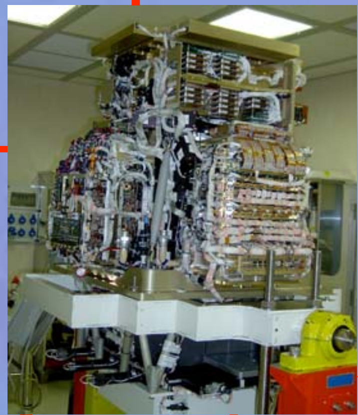

Solar Modulation

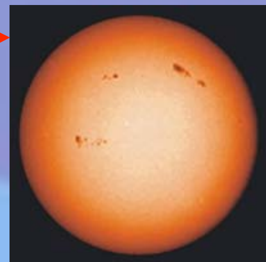

Interplanetary Physics,
Solar Wind Termination Shock

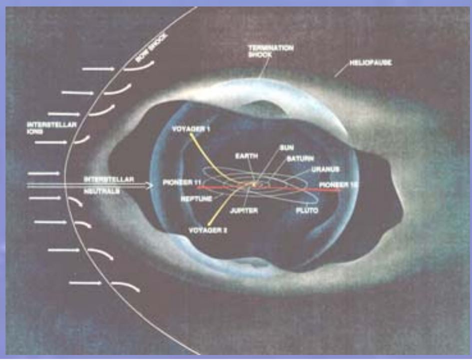

SAA, Albedo,
secondary particle

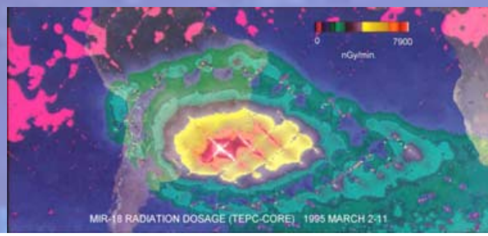

Magnetospheric physics

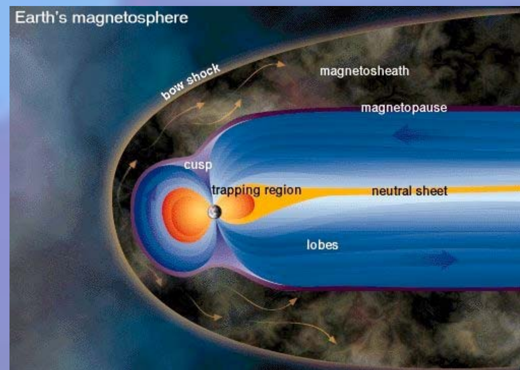

Cosmic ray energy ranges

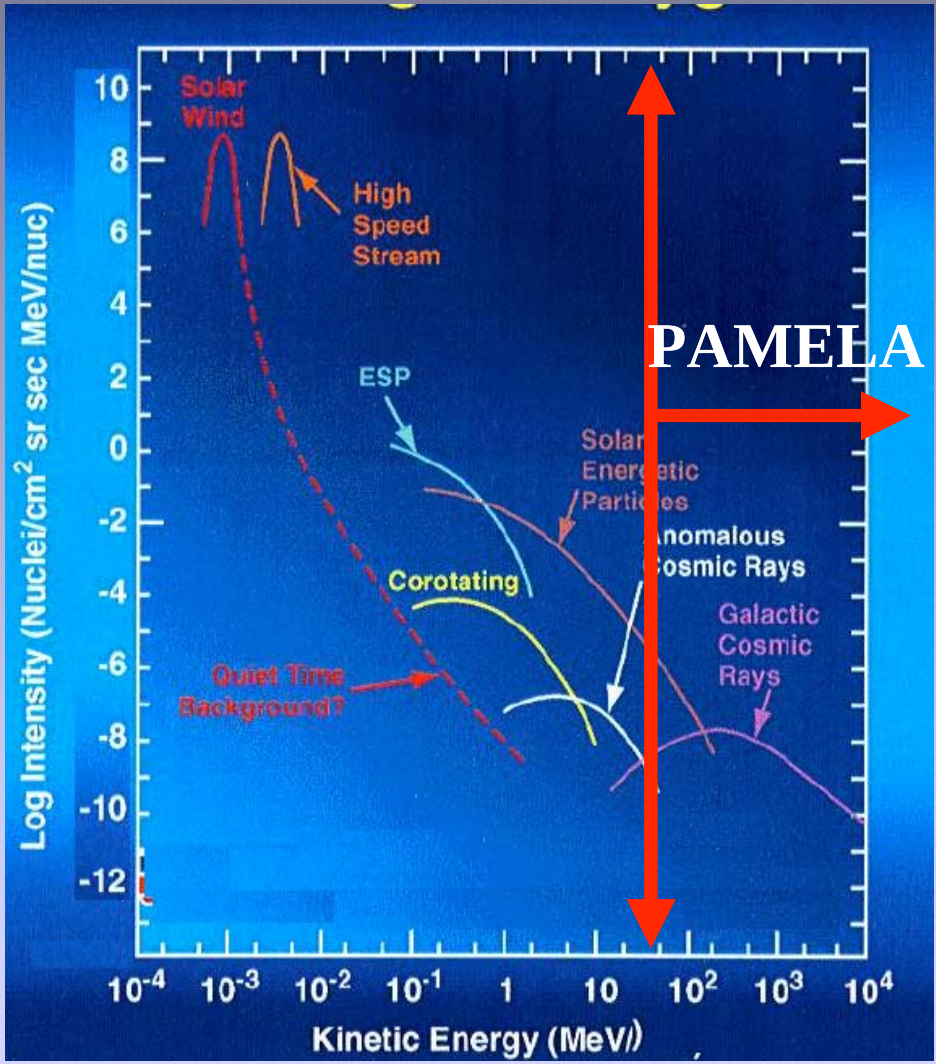

- Solar Modulation effects
- High energy component of Solar Proton Events (from 80 MeV to 10 GeV)
- High energy component of electrons and positrons in Solar Proton Events (from 50 MeV)
- Nuclear composition of Gradual and Impulsive events
- ^3He and ^4He isotopic composition
- Electrons of jovian origin

Pamela main objectives:

Study of antimatter component in cosmic rays:

- Antiprotons (80MeV -190 GeV)
- Positrons (50MeV - 270 GeV)
- Search for Antihelium (some parts 10^{-8})

Study of galactic cosmic ray spectrum

- Protons (80MeV - 700 GeV)
- Electrons (50MeV – 400 GeV)
- Electron+positron (up to 2TeV)
- Nuclei (up to Oxygen)

Search of dark matter

- High energy positron signature
- Low energy antiproton increase…

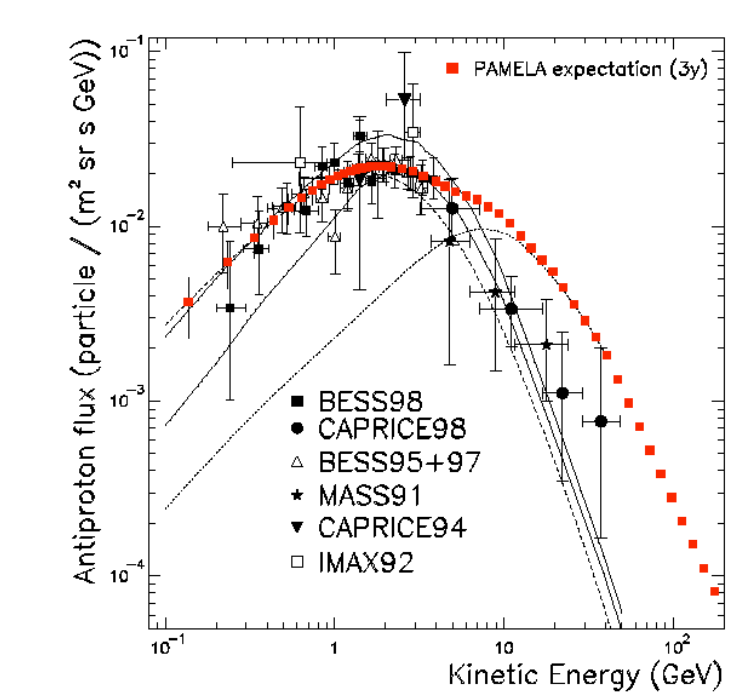

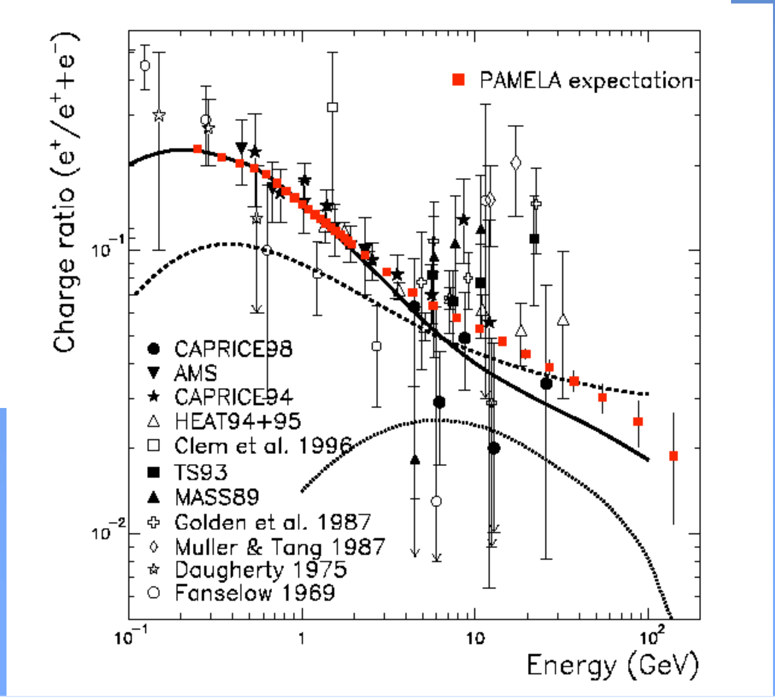

Cosmic-ray antiparticle measurements: antiprotons

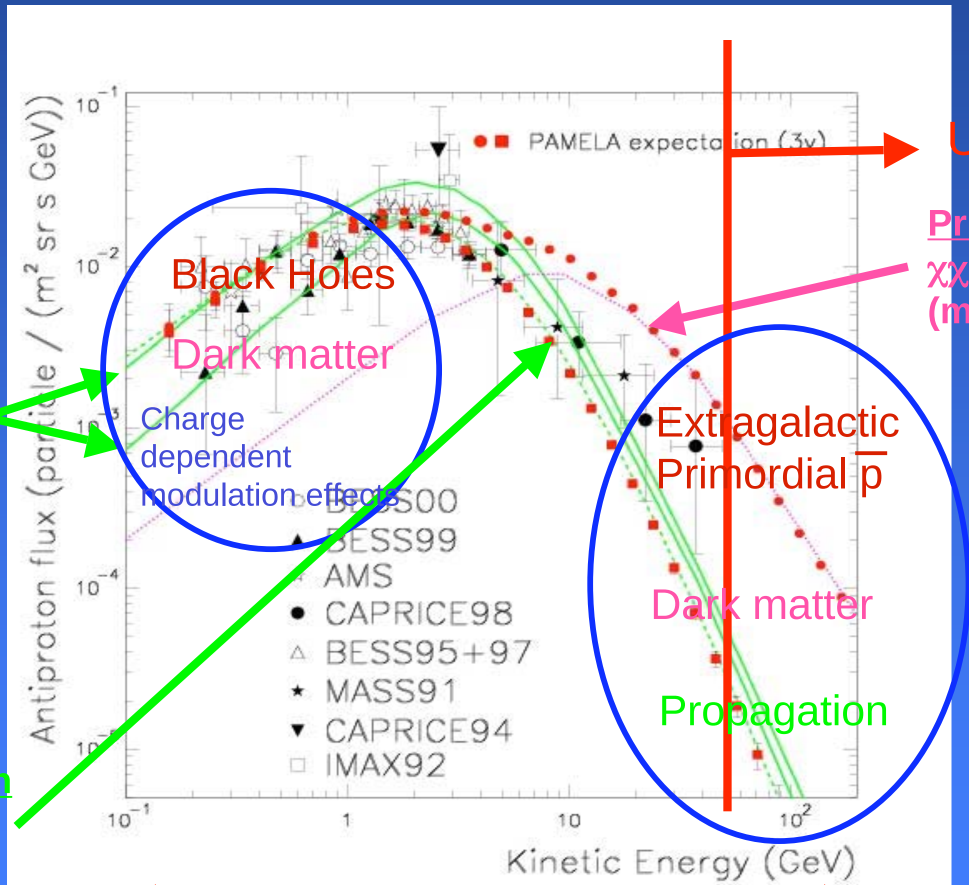

Unexplored Region

Primary production from $\chi\chi$ annihilation ($m(\chi)$ = 964 GeV)

Secondary production (upper and lower limits) Simon et al.

Secondary production (CAPRICE94-based) Bergström et al.

PAMELA energy range

From M. Boezio, ICRC 2005 Pune

Cosmic-ray antiparticle measurements: positrons

Secondary production
'Moskalenko + Strong model' (1998) without reacceleration

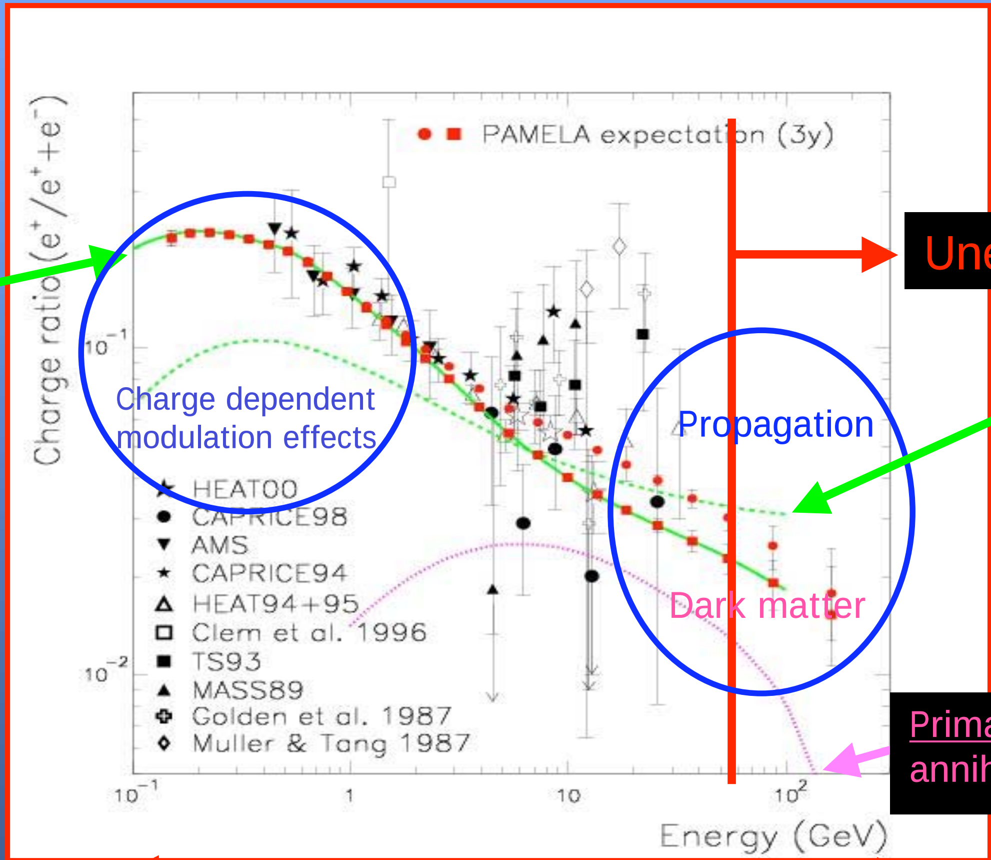

Unexplored Region

Secondary production
'Leaky box model' (Protheroe 1982)

Primary production from $\chi\chi$ annihilation ($m(\chi)$ = 336 GeV)

PAMELA energy range

Cosmic-ray Antimatter Search

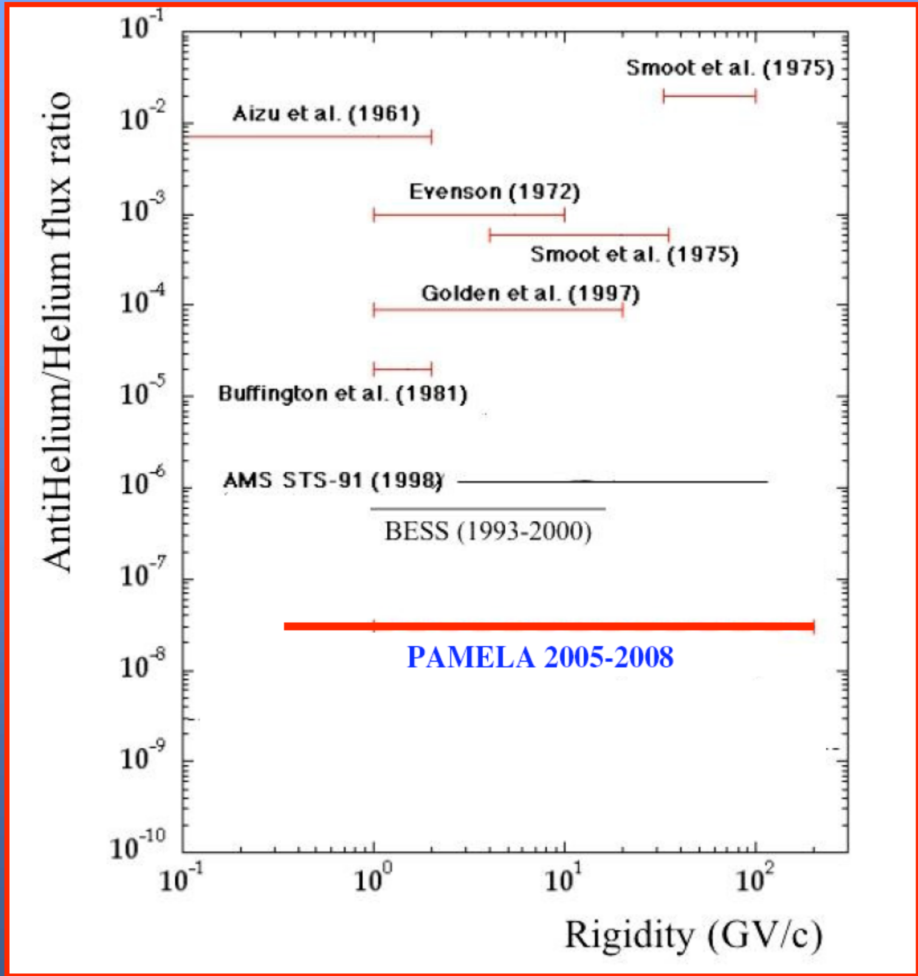

Nuclear abundances: Secondary to primary ratios

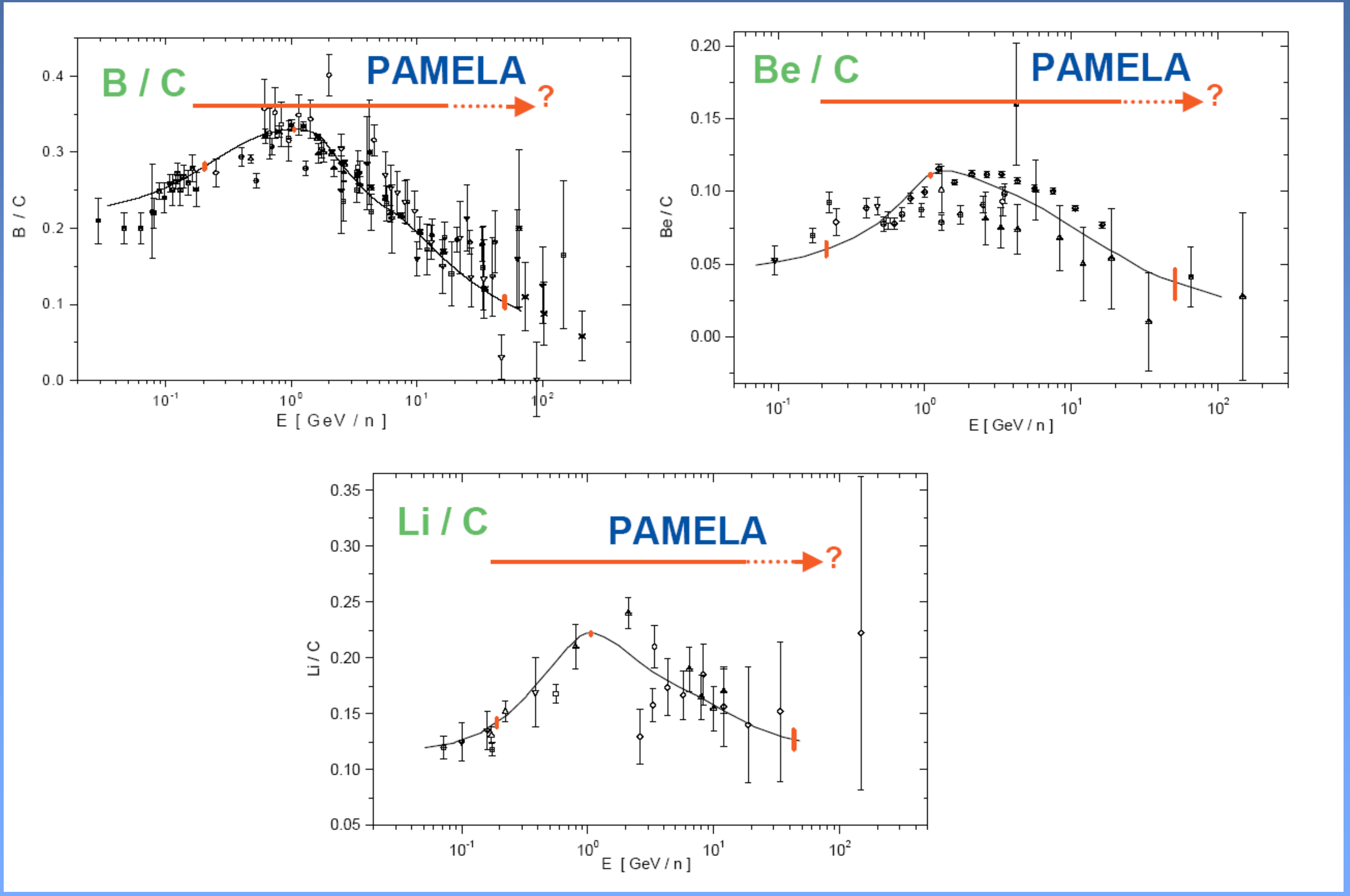

Isotopic abundances

The current situation of the ^3He / ^4He ratio

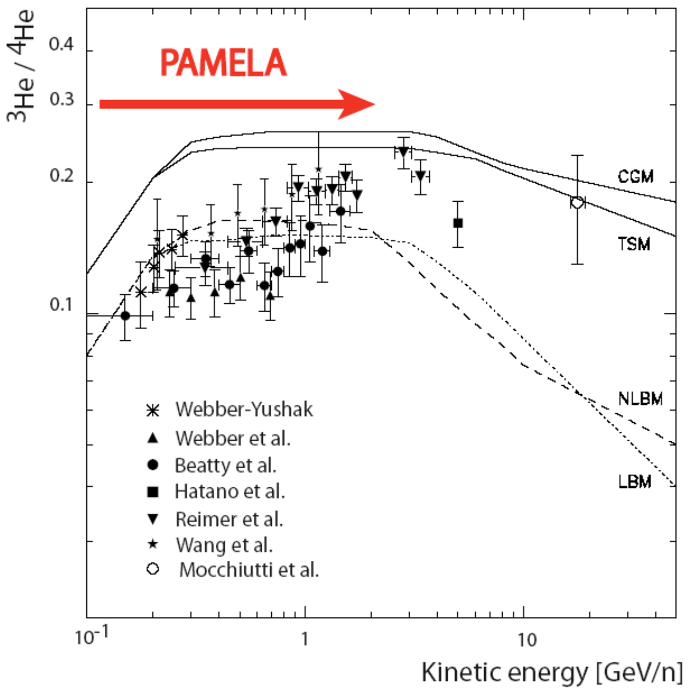

The current situation of the d / He ratio

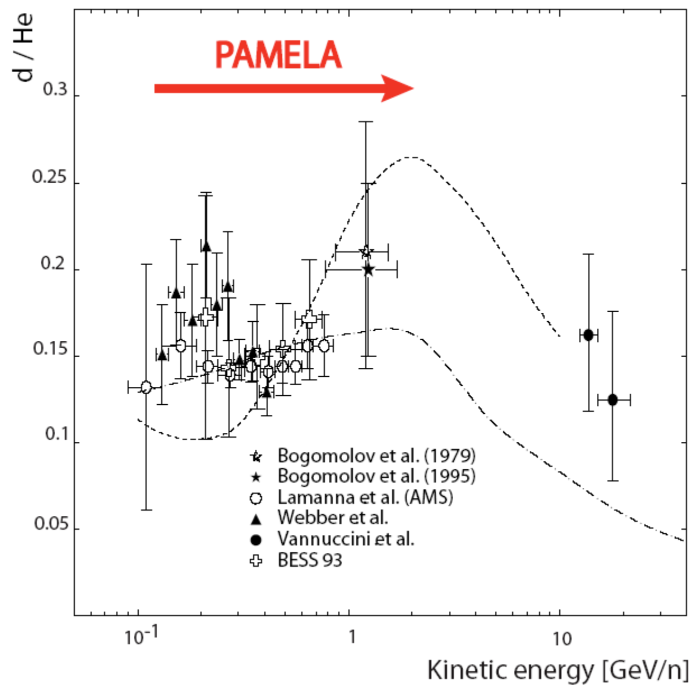

Contemporary measurements on high energy c.r. and antimatter component

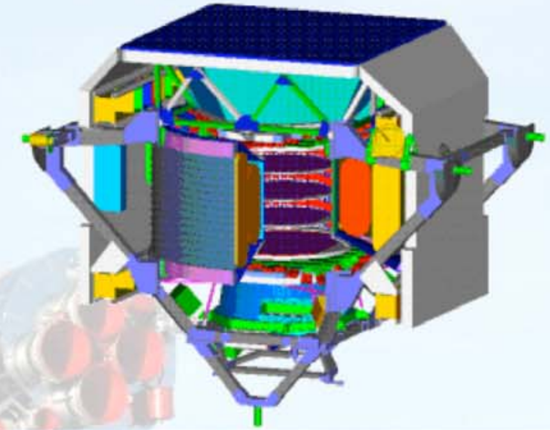

PAMELA + BESS
PAMELA + AMS
A unique chance to:

1. **Reduce systematics among measurements**
2. **Get data at the same time in different cutoff regions (compare south pole region – 70.4^o)**
3. **Possibility to observe time dependent phenomena (SEP, perturbations at low energy)**

(Cast in alphabetical order)

Permanence time:
between

60 and 70.4^o: 13%
65 and 70.4^o: 9%
70 and 70.4^o: 1.8%

Good Proton – Electron Statistics

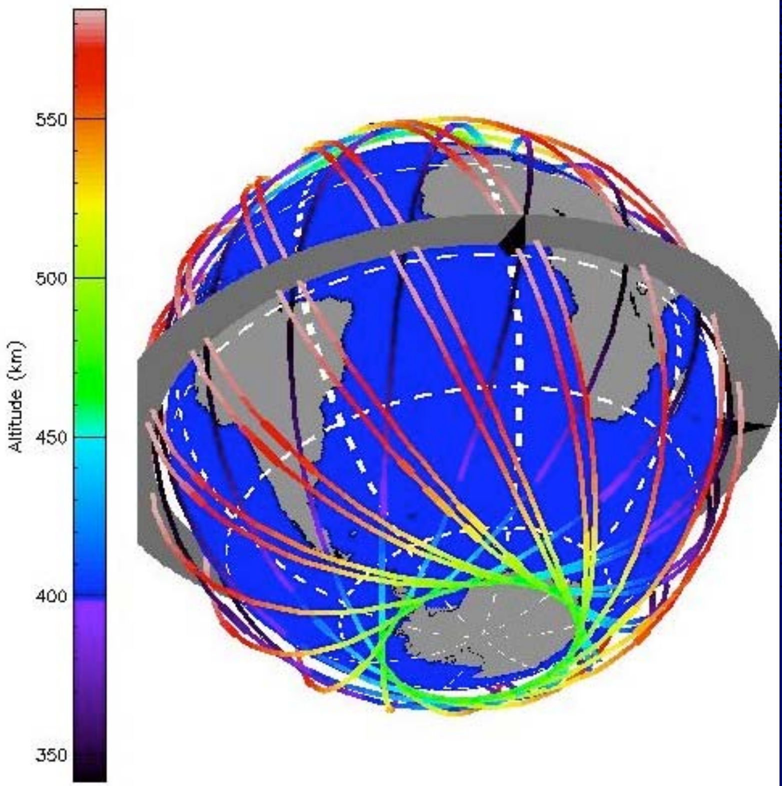

Height varies with time, Cutoff to be estimated

Bess path from S. Haino

Long term solar modulation at 1 AU

- Long term behavior of proton and nuclear abundances
- Charge dependent solar modulation (e+/e- p/p-)
- Correlation with other detectors

Energy range (>80 MeV)

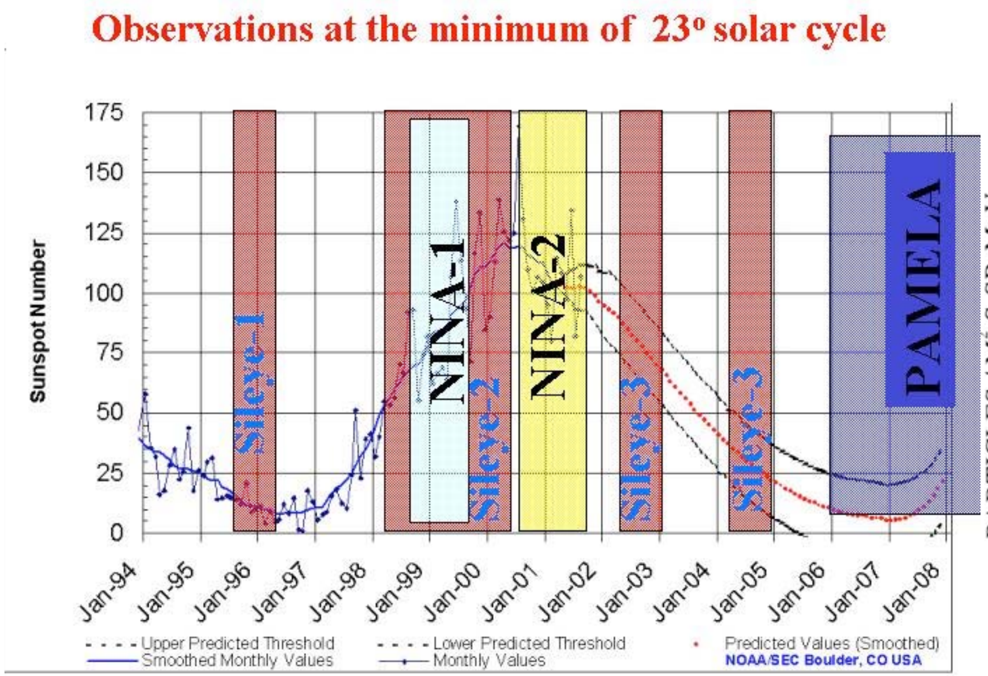

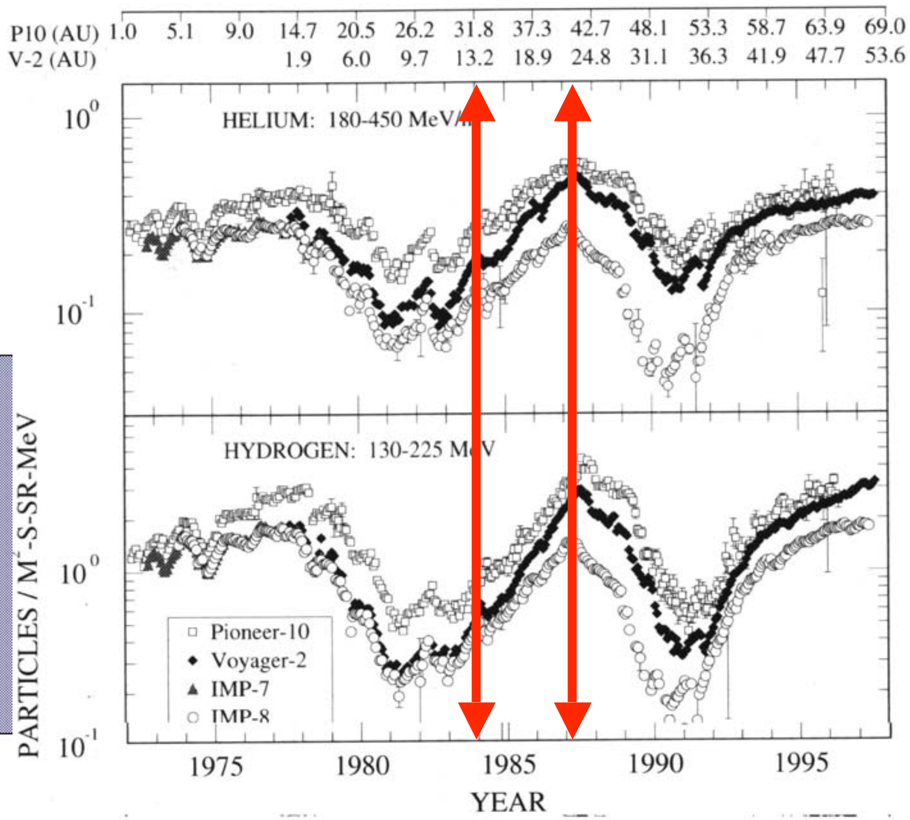

Solar particle events

Multi-GeV event measurement in space:

energy spectrum cutoff

Acceleration

Propagation

H, He Isotopic ratios

Nuclear component up to O

Meteor

Goes

Balloon

Neutron Monitor

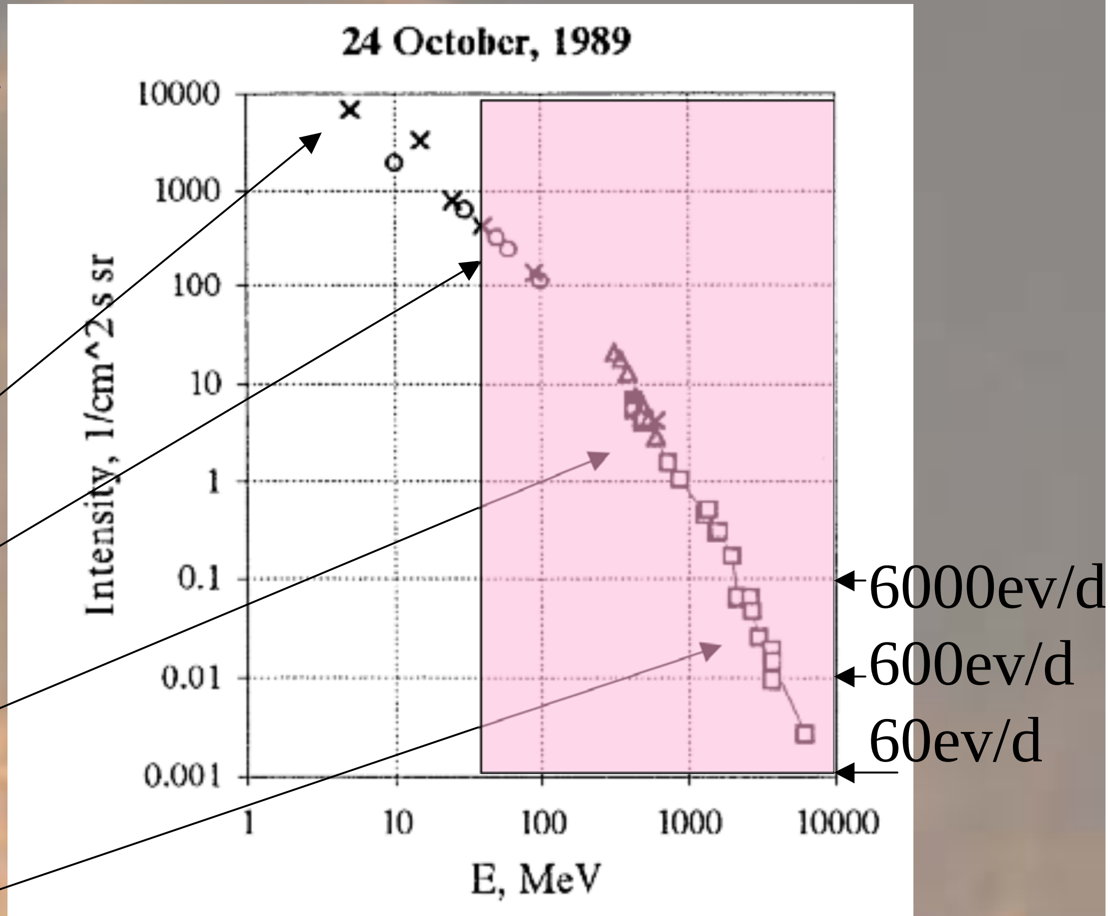

From:
G. A. BAZILEVSKAYA and A. K. SVIRZHEVSKAYA
Space Science Reviews **85**: 431-521, 1998.

Pamela energy range

Solar cycle and Solar particle events

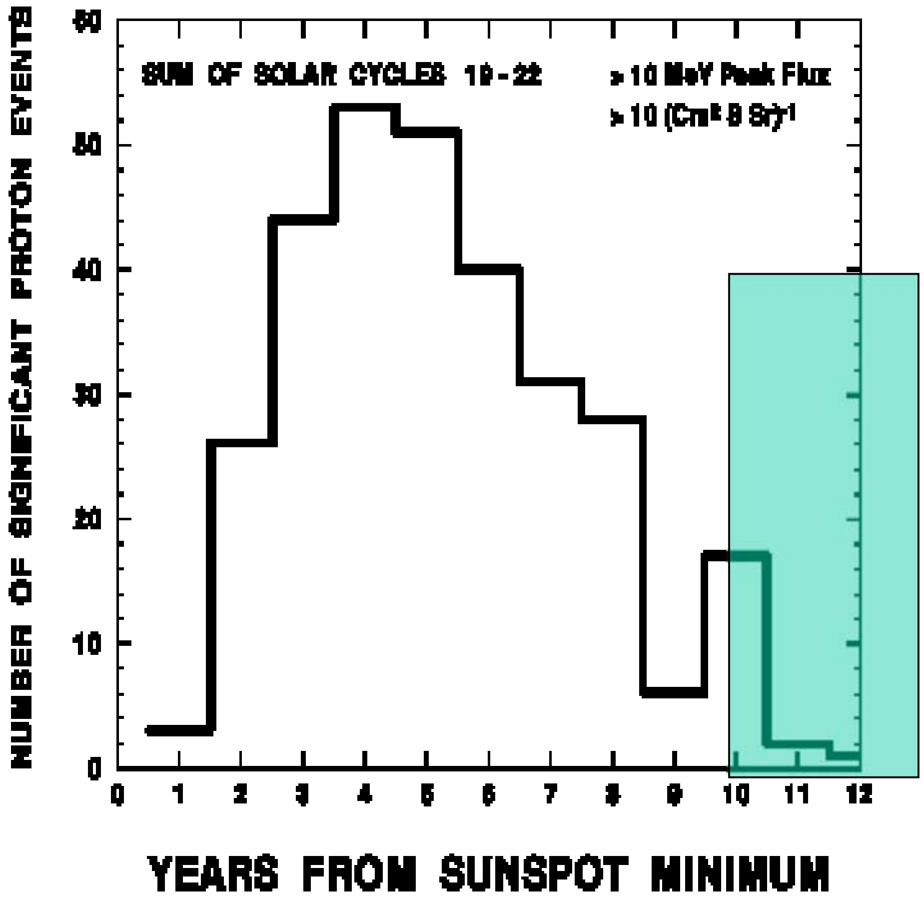

Fig. 2. The summation of significant discrete solar proton events for solar cycles 19-22.

Using Shea and Smart data (ICRC 2001)
we estimate about 20 events with >10 MeV Peak flux >10 part/(cm^2 sr) in three years of operation

Electrons from Solar events

High energy component e^- in SEPs (gradual/impulsive) >6000 e-/day (with 20% orbital live time)

•First measurement of high energy spectral indexes and breakdowns

•First direct measurement of positrons (very high energy ions impact the Sun producing both high energy (GeV) neutrons and pions with the pions decaying directly into photons or into secondary high energy positrons and electrons that in turn radiate).

•Propagation and acceleration effects (shock vs flare question)

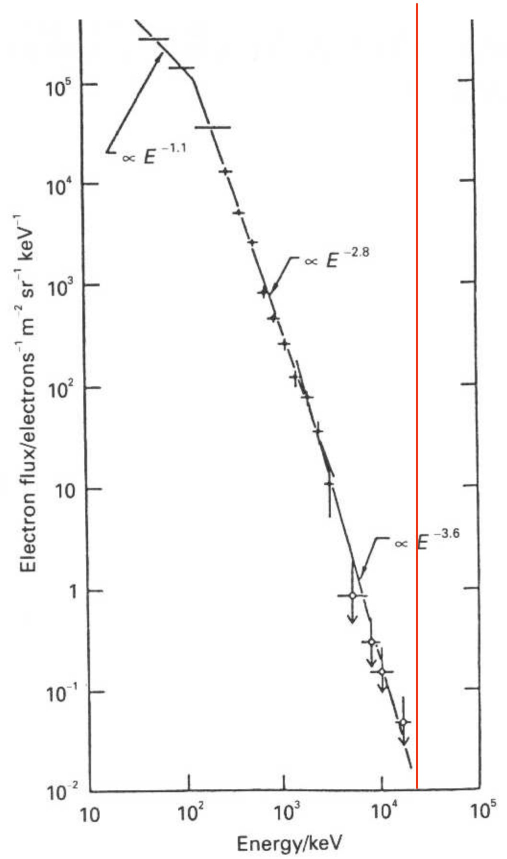

Figure 12.16. The energy spectrum of high energy electrons from the flare of 7 September 1973 as observed by the IMP 6/7 satellites. There is a change in slope of the spectrum at about 100 keV, the index being $\gamma \approx 1.1$ at low energies and about 2.8 at higher energies. (From Guzik, T. G. (1988). *Solar Physics*, **118**, 185.)

Neutrons from Solar Events

- **Produced in nuclear reactions at the flare site, high energy component can reach Earth before decaying.**

- **On the occurrence of solar events, neutrons are expected to reach Earth before protons as they have no charge (neutron/proton dispute on primaries during solar flares, see J. Ryan, rapp. Talk ICRC 2005).**

- **Neutron Detector: 36 ^{3}He counters arranged in two layers, surrounded by polyethilene (9.5 cm)moderator enveloped in thin cadmium layer. Dimesions: 60*55*15cm (10% eff for E<1MeV n)**

- **<u>Background counting</u>**

ところで。。。

BESS is an optimal instrument to detect neutrons from Solar Flares and Solar Particle events:

•Launch campaign is in Antartic Summer
→ always looking at Sun
•Need line of sight, not Parker Spiral
•Detect increase of protons coming from neutron decay
•Possibile also on ground (more difficult… high energy component)

Not so high probability but probably worth looking

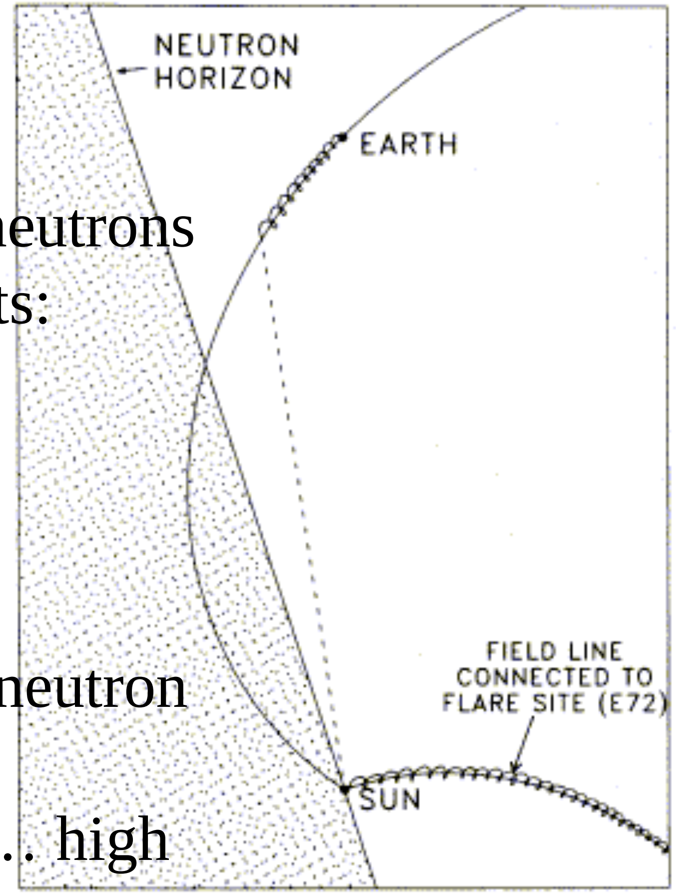

FIG. 2.—Solar system geometry at the time of the 1982 June 3 solar flare in a view perpendicular to the ecliptic plane. Protons from the flare are initially confined to field lines far from the Earth, while neutrons cross the field freely until they decay.

Evenson, Meyer and Pyle, ApJ 274, 875 1983

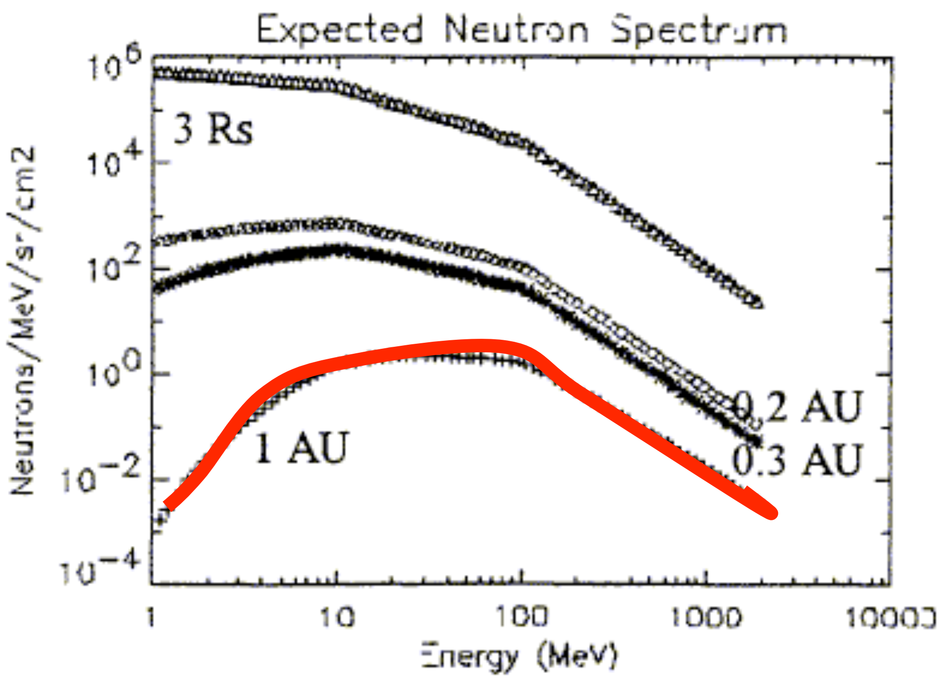

Figure 4: Expected neutron spectra for a 3 June like event at different distances from the solar surface. See text for details.

Vilmer, Maksimovic, Lin and Trotter, Proc of "Solar Encounter: the First Solar Orbiter Workshop", Tenerife, 14-18 may 2001 ESA SP-493

Trapped, albedo and secondary particles

The polar orbit of Pamela will be particularly useful to study:

- **Trapped particle population in the SAA**
- **(different altitudes: 300 – 600 km)**
- **Trapped electrons**
- **Geomagnetic cutoff shifts due to solar events**
- **Albedo particles**
- **Secondary particles produced in the atmosphere…**

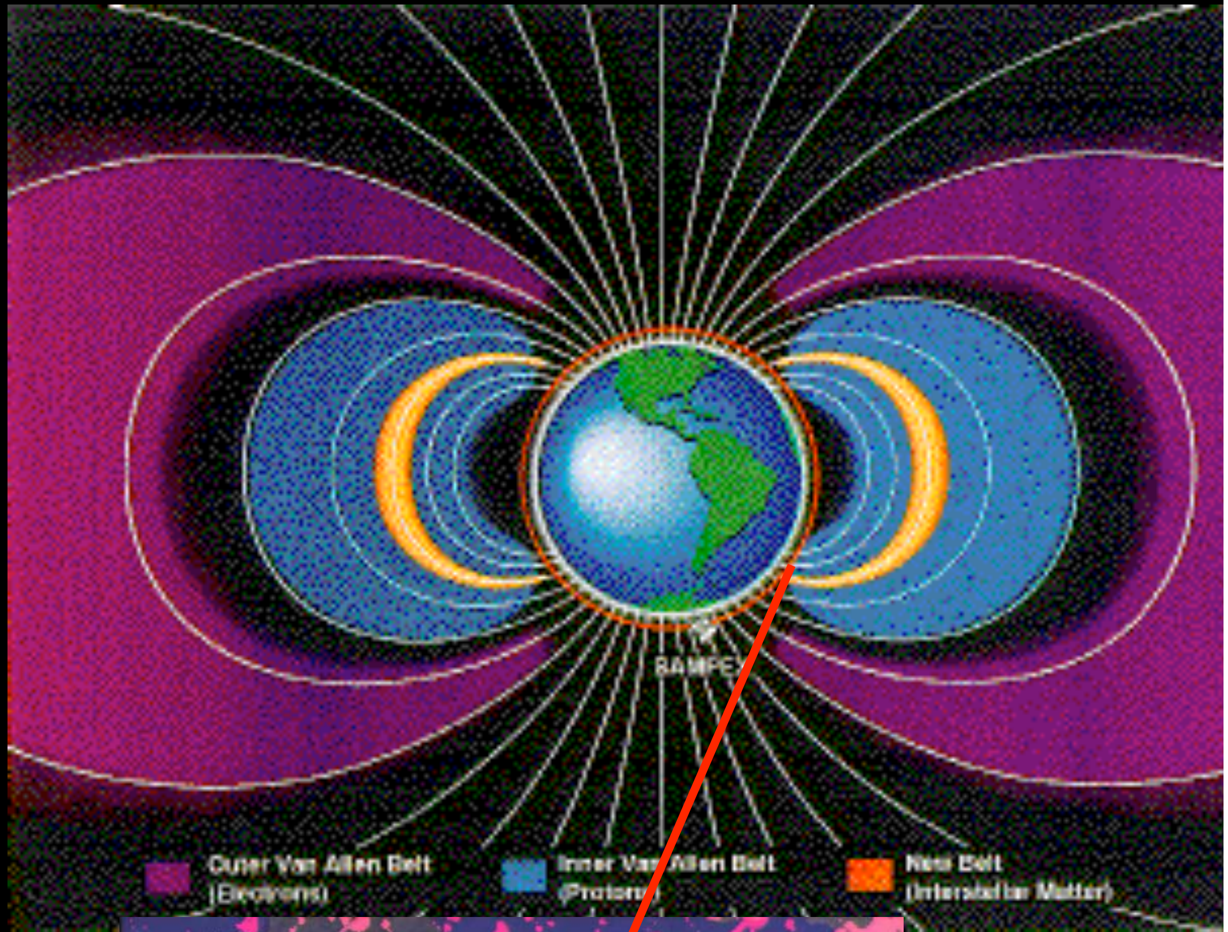

Electrons of Jovian origin:

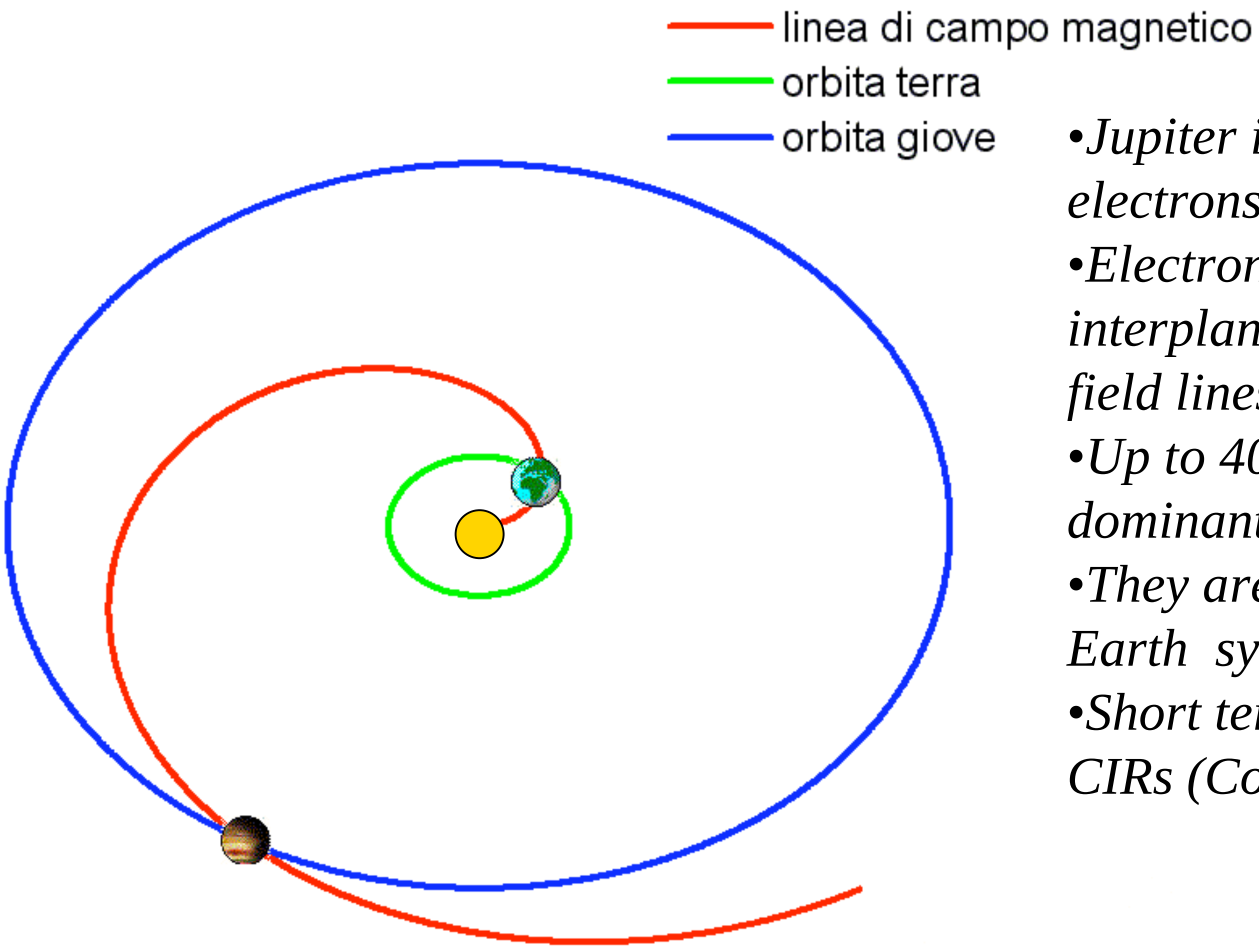

- *Jupiter is a source of high energy electrons*
- *Electrons propagate in interplanetary space following local field lines of the solar wind.*
- *Up to 40 MeV jovian electron are dominant population*
- *They are modulated by Jupiter-Earth synodic period (13 months)*
- *Short term (27 day) modulation by CIRs (Coronal Interaction Regions)*

Observation of Jovian Electrons: Pioneer, Voyager, Ulysses..

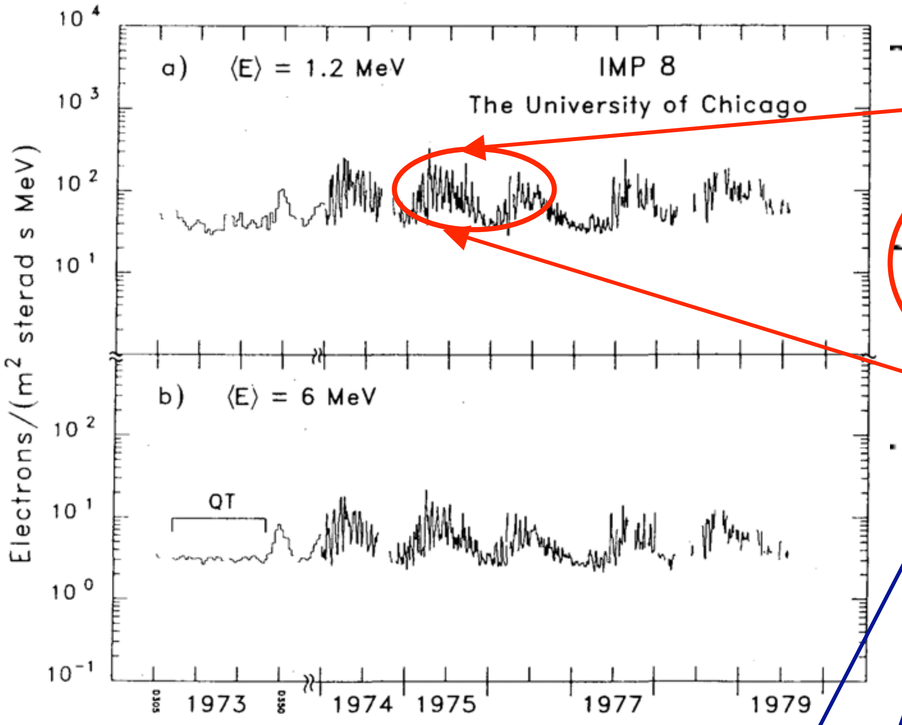

FIG. 8.—The University of Chicago *IMP 8* electron differential fluxes for mean energies of (*a*) 1.2 MeV and (*b*) 6 MeV. Solar flares events and geomagnetospheric bursts have been deleted. The fluxes in 1973, with an extended quiet-time (QT) interval, were averaged in 1 day intervals and are shown on an expanded time scale. After 1973 the fluxes were averaged in 3 day intervals.

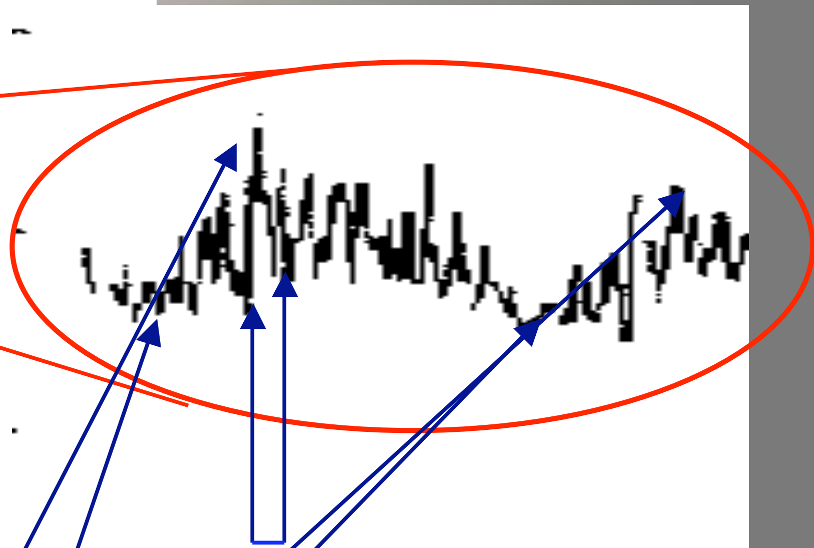

27 day solar (CIR) modulation

13 month Jupiter -Earth sinodic period

(Opposed field line)

(Same field line)

Total flux (Jovian + galactic e^-)

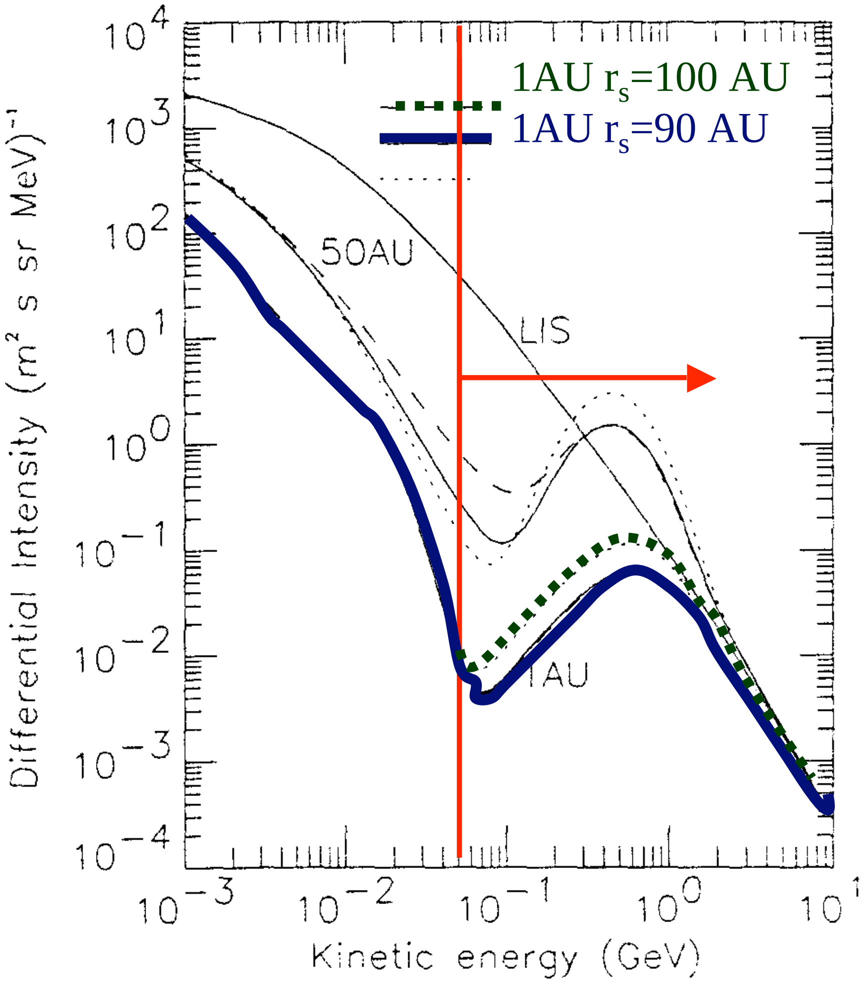

Figure 3. Modulated spectra for combined galactic and Jovian electrons at 1 AU and 50 AU in the equatorial plane in comparison with the assumed LIS at 120 AU. The effects of moving the TS from 80 AU to 100 AU are pronounced at 50 AU where the modulated spectra exceed the LIS between $\sim$200 MeV and $\sim$2 GeV, with the effect dissipating at $E < \sim 20$ MeV. At 1 AU these effects are

- Jovian electrons dominate at low energies
- They are reaccelerated by the Termination Shock
- Very sensitive to Shock Position
- Short (27d) and long (399d) term modulation
- Electron – Positron measurement

allows separation of the two populations

- <u>*Pamela e^- ≅ 50000/month*</u>
- *Jovian component≅ 1% (600/month)*
- *First high energy (>50 MeV) measurement of primary Jovian component*

Poitgieter & Ferrera JGR 107, A7 10.1029/2001JA009040, 2002

PAMELA STATUS

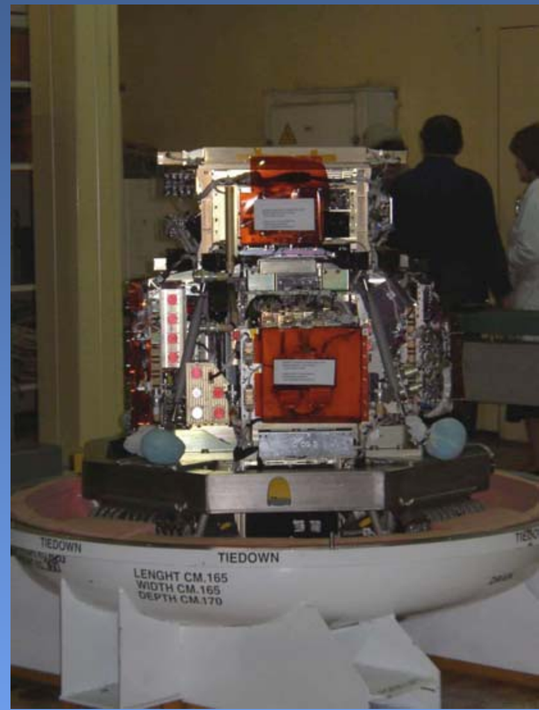

Mass & Thermal Model

- Integrated with Resurs
- Cooling loop
- Mechanical support

Technological Model

- Integrated with resurs
- Electrical, electronical
- Logic & acquisition tests

Flight Model

- Integrated in Tor Vergata
- Integrated with Resurs
- All tests passed
- To be shipped to Baikonur b plane

Ground data sessions

We had so far two main sessions of cosmic ray acquisitions on ground:

- **Rome** – Tor Vergata University clean room: February/March 2005

- **Samara** – Progress clean area: May 2005

- Number of files downlinked in Rome:

  311 *in about* **480 hours** *of data taking*

- Number of files downlinked in Samara:

  113 *in about* **140 hours** *of data taking*

TOF and CALO event identification

TOF - Rome Data

CALO - SPS data

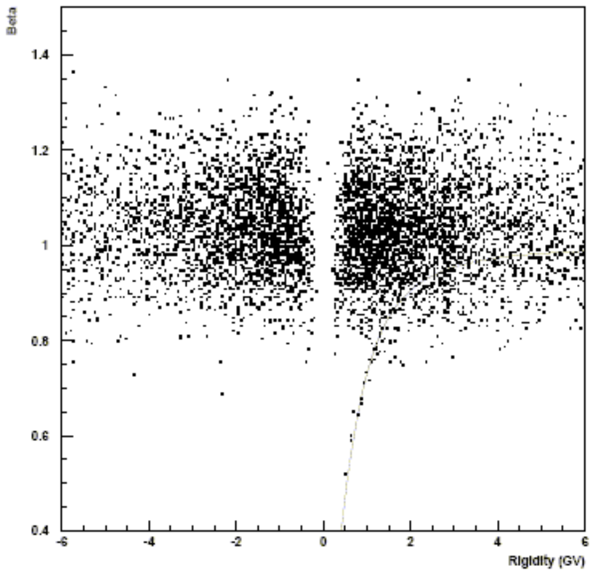

Discrimination capability of the time-of-flight system. The measured velocity $\beta = L/c \cdot 1/t$ (where L is the distance between the TOF planes employed in the measurement, and t is the flight time) is plotted against the particle rigidity R as measured by the spectrometer for a sample of cosmic rays at ground level. While most of the detected particles are muons, few protons can be identified as the point lying near the plotted curve, which shows their expected $\beta(R)$ relation.

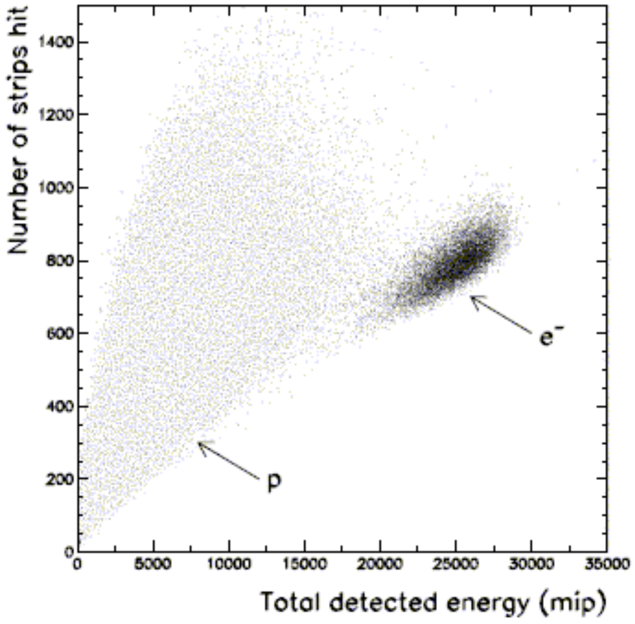

Discrimination capability of the calorimeter between protons and electrons, on the basis of the number of strips involved in the shower and of the total energy released. Data refer to particles with a momentum of 200 GeV/c acquired on a beam test at the CERN SPS facility in 2002.

TRK deflection distribution – Rome Data

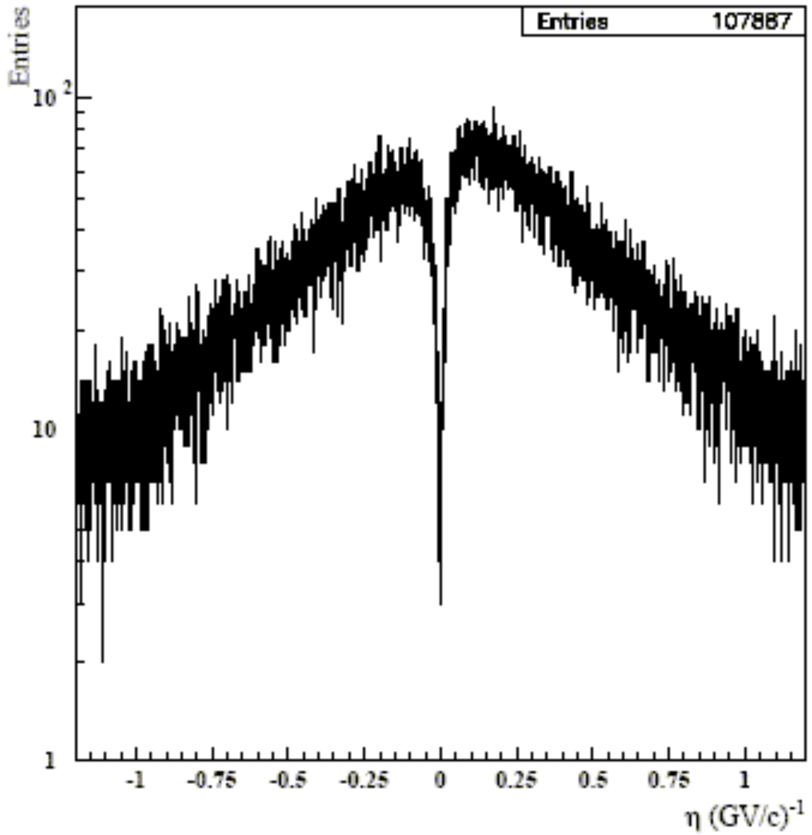

Deflection distribution of cosmic rays at ground level, after the whole-tracker alignment has been applied. The larger abundance of positive particles can be noticed.

Ground muon results – Rome & Samara runs

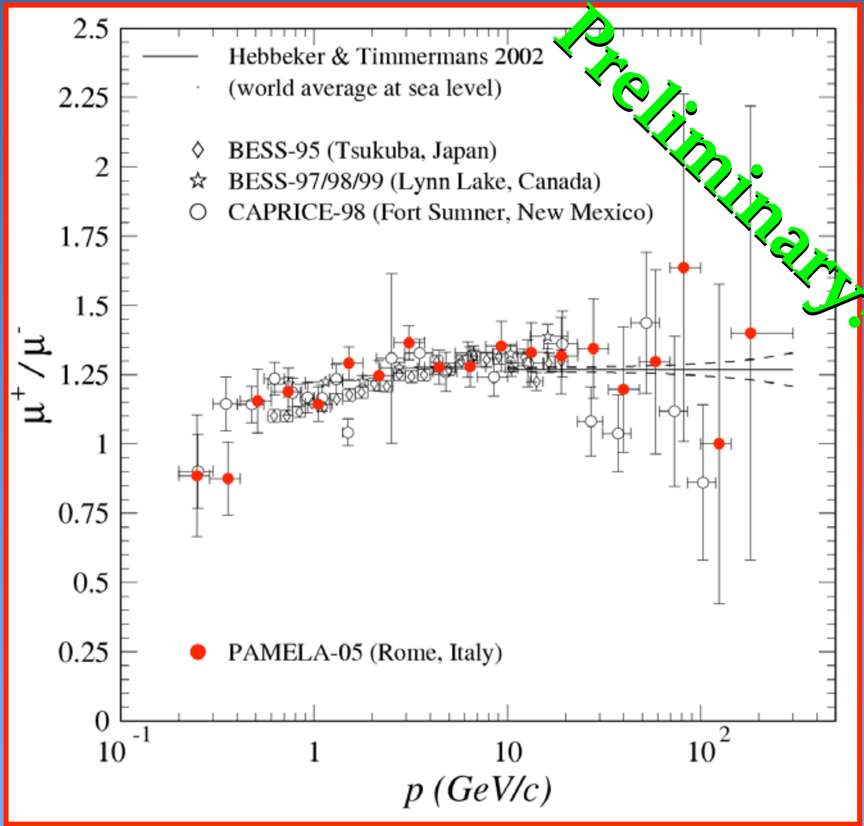

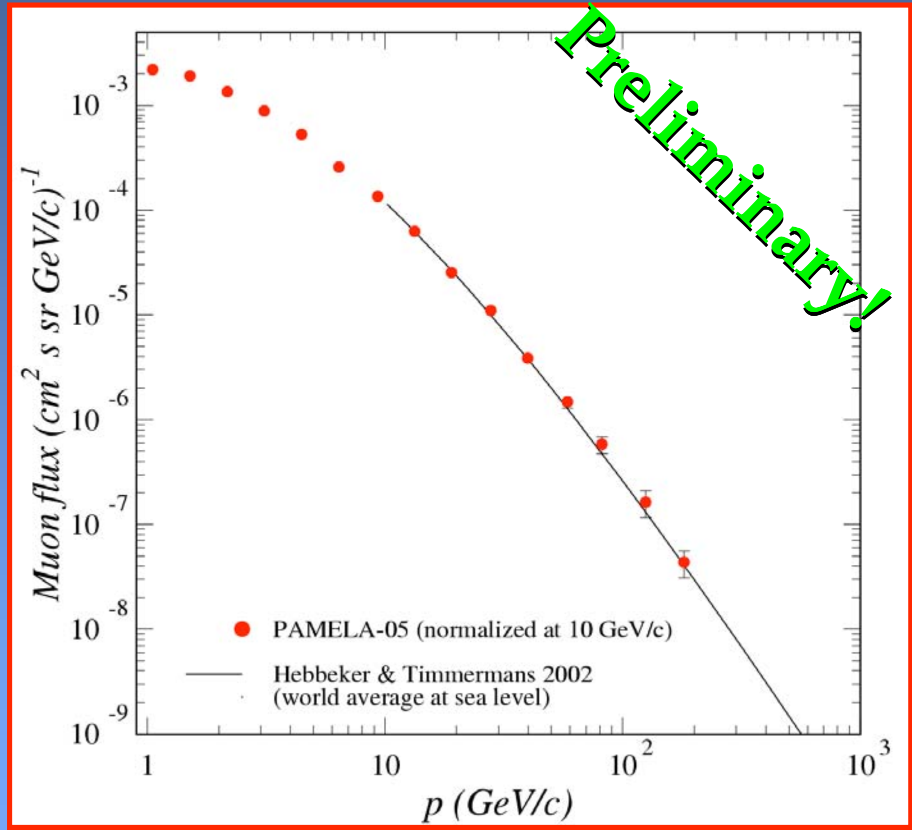

+ LAST WEEK tests in GSI with heavy nuclei to calibrate nuclear & isotopic identification capabilities

Current Status

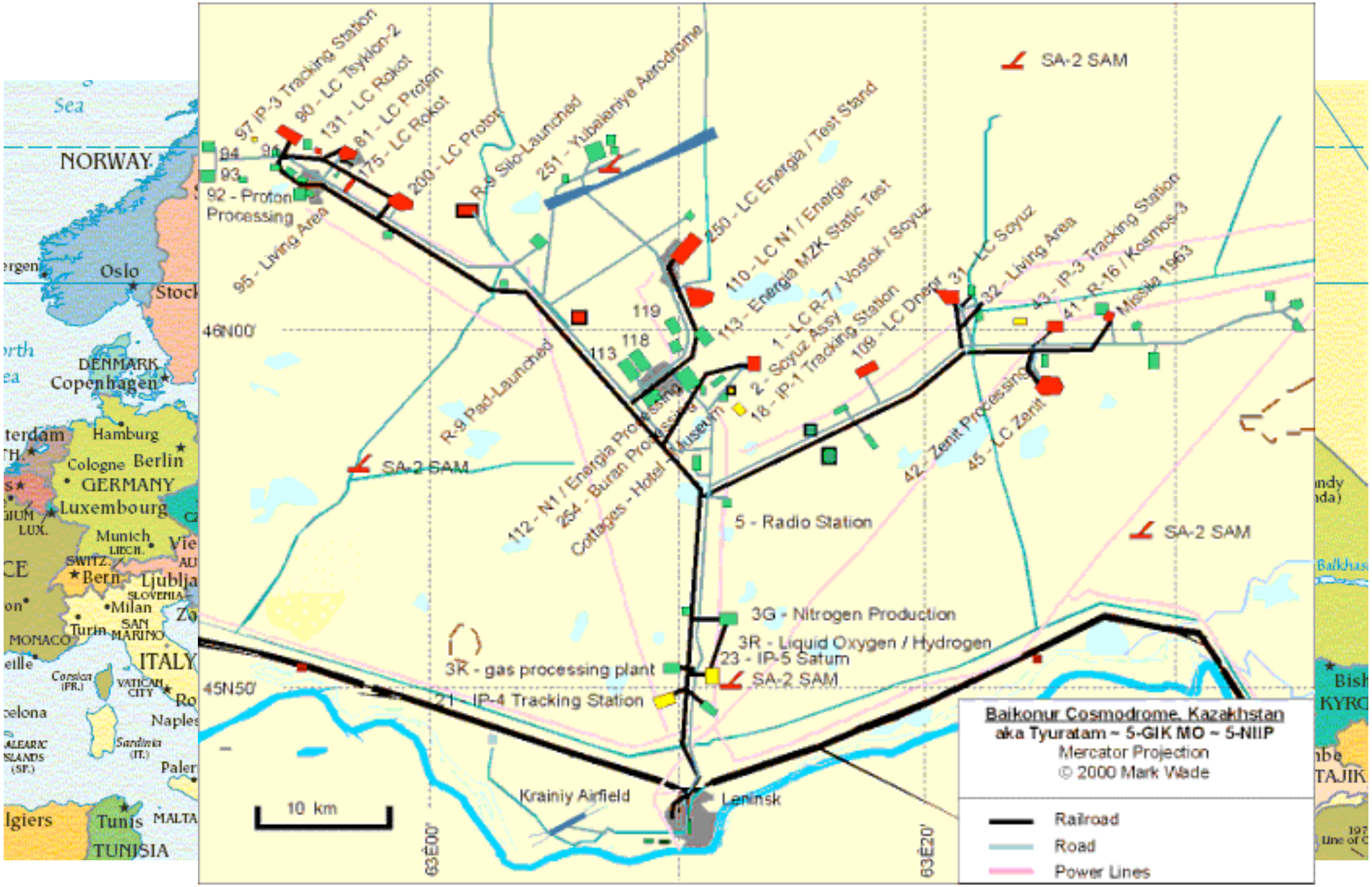

Integration & Launch in Baikonur cosmodr
Spring 2006

広告

Availability of PhD positions (post-graduate) in Roma Tor Vergata University:

http://www.uniroma2.it/postgrad/inglese/applicazioni/instruction.htm

And/or contact casolino@roma2.infn.it or picozza@roma2.infn.it